OPEN ACCESS

University of BRISTOL

This electronic thesis or dissertation has been downloaded from Explore Bristol Research, http://research-information.bristol.ac.uk

Author:
Hernandez Fajardo, Oscar

Title:
Mechanistic and Reactivity Studies of First-Row Complexes as Catalysts in Cross-Coupling Reactions.

General rights
Access to the thesis is subject to the Creative Commons Attribution - NonCommercial-No Derivatives 4.0 International Public License. A copy of this may be found at https://creativecommons.org/licenses/by-nc-nd/4.0/legalcode This license sets out your rights and the restrictions that apply to your access to the thesis so it is important you read this before proceeding.

Take down policy
Some pages of this thesis may have been removed for copyright restrictions prior to having it been deposited in Explore Bristol Research. However, if you have discovered material within the thesis that you consider to be unlawful e.g. breaches of copyright (either yours or that of a third party) or any other law, including but not limited to those relating to patent, trademark, confidentiality, data protection, obscenity, defamation, libel, then please contact collections-metadata@bristol.ac.uk and include the following information in your message:

• Your contact details
• Bibliographic details for the item, including a URL
• An outline nature of the complaint

Your claim will be investigated and, where appropriate, the item in question will be removed from public view as soon as possible.

Mechanistic and Reactivity Studies of First-Row Complexes as Catalysts in Cross-Coupling Reactions.

Oscar Hernández Fajardo

A thesis submitted to the University of Bristol in accordance with the requirements of the degree of Doctor of Philosophy in the School of Chemistry, Faculty of Science.

November 2018

Abstract

Iron(II) complexes show activity in Negishi cross-coupling reactions. A series of mechanistic studies were conducted using spectroscopic techniques in order to improve the understanding of this reaction. It has been observed that Fe(II) is reduced to Fe(I) species when it interacts with the nucleophilic reagent in the reaction mixture. These reduced species show excellent catalytic activity. A kinetic study was conducted using UV-vis spectroscopy which demonstrates that the presence of Lewis acids and Lewis bases influence the speed of reaction. A free-energy relationship using the Hammett equation suggests a free radical mechanism. Activation parameters provided evidence for an associative transition step. The data obtained revealed a complex system of reactions. With the experimental results obtained in these studies, mechanisms for the iron(I) catalysed cross-coupling reaction were proposed.

An X-ray absorbance spectroscopy study was conducted in iron complexes in order to illuminate the role of iron of the species. Reaction mixtures of typical cross-coupling reactions were examined at the end of the reaction in order to detect iron complexes and characterise them. A reaction time-dependent study was undertaken to determine the iron complexes in the reaction mixture. A kinetic study on the Negishi cross-coupling using iron(II) was conducted. The experimental results from the kinetic study on iron(I) and the kinetic study on iron(II) were used to propose a mechanism of reaction for the iron catalysed Negishi cross-coupling.

The development of a new cross-coupling system using manganese as pre-catalyst was explored. The use of different ligands, additives and conditions of the reaction was tested.

Acknowledgements

A massive thanks to my supervisor Professor Robin Bedford for giving the opportunity to work with him and for the help provided. I will always admire your enthusiasm and creativity.

Thanks to all my friends in the Bedford group: Starting with Michelle, Paul, Johnny and Dom who introduced me to everything in the laboratory and to the life in the UK. Thanks to Sanita, Stephen, Harry, Mattia and Soneela for all the good chats, for enjoying my great taste in music and making a fun work environment in the lab.

I thank the postdocs in the Bedford group: Antonis, David, Peter and Carolina, who were always helpful and taught me a lot. I appreciate the willingness to share your expertise.

I thank all my friends in Bristol, particularly to the Mexican community in Bristol which gave a little piece of my country abroad.

I am so grateful to my parents, who have always been rooting for me and cheering me up. A massive thanks to my brother, who is always someone I could talk without judgment. I am grateful to my grandfather, who helps me and cares about me.

Thanks to the Consejo Nacional de Ciencia y Tecnología (CONACyT) for its financial support throughout my doctoral studies.

I declare that the work in this dissertation was carried out in accordance with the requirements of the University's Regulations and Code of Practice for Research Degree Programmes and that it has not been submitted for any other academic award. Except where indicated by specific reference in the text, the work is the candidate's own work. Work done in collaboration with, or with the assistance of, others, is indicated as such. Any views expressed in the dissertation are those of the author.

SIGNED: ..... DATE:.....

Abbreviations

Ac	Acetyl
acac	Acetylacetonate
Ar	Aryl
B(Arf)4	Tetrakis[3,5-bis(trifluoromethyl)phenyl]borate
Bn	Benzyl
cat.	Catalyst
COD	Cyclooctadiene
Cy	Tricyclohexylphosphine
DABCO	1,4-diazabicyclo[2.2.2]octane
dba	Dibenzylideneacetone
dbm	Dibenzoylmethane
depe	Diethylenephosphine
DFT	Density functional theory
DIBAL	Diisobutylaluminum hydride
DMA	Dimethylacetamide
DME	Dimethoxyethane
dpbz	1,2-bis(diphenylphosphino)benzene
dppe	1,2-bis(diphenylphosphino)ethane
dppm	Bis(diphenylphosphino)methane
dppp	1,2-bis(diphenylphosphino)propane
EPR	Electron Paramagnetic Resonance
eq	Equivalents
EXAFS	Extended X-ray absorption fine structure
Fe_{act}	Active Iron Catalyst
Fe_{off}	Iron off-cycle species
Fe_{on}	Iron on-cycle species
Fe_{out}	Stable iron species
Fe_{pre}	Iron pre-catalyst
h	Hour
HMPA	Hexamethylphosphoramide
iBu	isobutyl
IMes	1,3-Dimesitylimidazol-2-ylidene, 1,3-bis(2,4,6-trimethylphenyl)-imidazolium
iPr	Isopropyl
M	Metal
Mes	Mesitylene
min	Minutes
NHC	N-heterocyclic
NMP	N-Methyl-2-pyrrolidone
NMR	Nuclear Magnetic Resonance
OA	Oxidative addition
Otf	Triflate
Ots	Tosylate
PEG	Polyethylene glycol
Piv	Pivalate
PPh3	Triphenylphosphine
Py	Pyridine
RE	Reductive elimination
RT	Room Temperature
s	Seconds
SALEN	N,N'-bis(salicylidene)ethylenediamine
sBu	Secbutyl
SET	Single electron transfer
SET	Single electron transfer
T	Temperature
tBu	tertbutyl
Tf	Triflate
TFA	Trifluoroacetic acid
THF	Tetrahydrofuran
TM	Transition metal
TMEDA	N,N,N',N'-tetramethylethylenediamine
TMS	Tetramethylsilane
XANES	X-ray absorption near edge structure
XAS	X-ray absorption spectroscopy

Table of contents

Chapter 1 Introduction 7
1.1 Metal-catalysed cross-coupling reactions 8
1.2 First row transition metal catalysed cross-coupling reactions 9
1.3 Palladium Cross-coupling reactions 11
1.4. Use of softer nucleophiles 13
1.5 Iron as a catalyst 23
Chapter 2. Exploring Fe(I) reactivity in Negishi Cross-Coupling 44
2.1 Introduction 45
2.2 General Considerations 71
2.3 Preliminary UV-Vis studies in Fe catalysed cross-coupling. 72
2.4 Kinetic studies on the oxidation of Fe(I) 76
2.5 Order of reaction 88
2.6 Linear free energy relationship analysis using the Hammett equation. 97
2.7 Activation parameters of the reaction of [FeBr(dpbz)$_2$] and BnBr in the presence of $ZnBr_2$ ... 102
2.8 Mechanism of reaction. 105
2.9 Conclusions and Future Work 109
Chapter 3. Further studies on the iron-catalysed cross-coupling 111
3.1 Introduction 112
3.2 Results and discussion 114
3.3 Monitoring the catalysis using $FeBr_2(dpbz)_2$ 122
Chapter 4. Developing a novel Manganese-catalysed Negishi cross-coupling system. 127
4.1 Introduction 128
4.2 Results and discussion 137
4.3 Conclusions and future work 146
Chapter 5. Experimental 148
5.1. General experimental procedures 149
5.2 Experimental Details for Chapter 2 150
5.3 Experimental Details Chapter 3 155
5.4. Experimental details Chapter 4 155
Chapter 6. References 156

Chapter 1 Introduction

1.1 Metal-catalysed cross-coupling reactions

Homogenous catalysis has revolutionise synthetic chemistry with new methodologies which are characterized by a reduction in the amount of waste produced, have increased selectivity, yields, and are time and energy efficiency. For this reason, catalysis is considered one of the principles of green chemistry, providing economic, sustainable and efficient synthesis.[1]

Carbon-carbon bond-forming reactions are one of the most important techniques developed in modern organic synthesis. These reactions are fundamental for the synthesis of fine chemicals, making this field of chemistry a pillar for the synthesis of natural products, pharmaceuticals and biologically active compounds.[2]

Among a range of carbon-carbon bond forming reactions, cross-coupling reaction stands out as one that has been useful and relevant. Cross-coupling reaction involves the formation of a carbon-carbon bond between a nucleophilic compound and an electrophile with a leaving group. This reaction is facilitated by a transition metal complex like palladium or nickel. Aryl or alkyl groups are the most common organic coupling fragments, and the nucleophile commonly has Mg, Zn, B or Si; leaving groups in the electrophile include Cl, Br, I, OTf or OTs. (Scheme 1. 1).

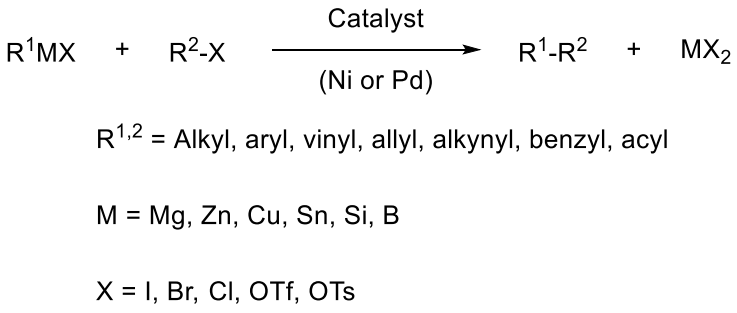

Scheme 1. 1 Cross-coupling catalysed by transition metals

Thanks to the efforts made in this area of organometallic chemistry, the development of new methods for the construction of organic molecules has increased, resulting in a rich assortment of synthetic routes which can be used depending on the nature of the substrate and providing options that can avoid side reactivity.[3]

A challenge for cross-coupling reactions is the presence of competitive side-reactions such as homocoupling, which forms the R^1-R^1 and R^2-R^2 side products from the reaction of two nucleophiles or electrophiles molecules. Throughout the history of transition metal cross-coupling reactions, suppressing the formation of these side-products has been an important goal in order to optimise the yields of the desired products. This goal has been achieved using different ligands, which can provide a different stereo-electronic environment at the metal centre.

1.2 First row transition metal catalysed cross-coupling reactions

By the first decades of the 20th century, a limited number of cross-coupling reactions were known using Grignard Reagents and related organoalkali metals containing Li, Na, K. (Scheme 1. 2) These reactions worked better using sterically less hindered primary and secondary alkyl electrophiles (R^2X). Nevertheless, the scope was limited due to reactivity, for instance, unsaturated electrophiles could not be activated.[4]

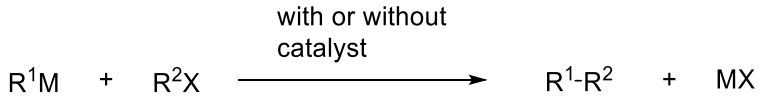

Scheme 1. 2 Primitive system of cross-coupling reaction

In the 1940s, Kharasch reported the use of cobalt(II) chloride, manganese(II) chloride, nickel(II) chloride, chromium(III) chloride and copper(I) chloride for the coupling of aryl Grignards with organic halides. These catalysis did not use any supporting ligands,[5] and this resulted in modest yields of cross-coupling product with high amounts of homo-coupling byproducts.[5]

Kochi and co-workers independently reported the use of Li_2CuCl_4 to catalyse the reaction between alkyl magnesium halides and alkyl electrophiles.[6]

Kumada and Tamao introduced in the 1970s the first modern cross-coupling reaction, where Grignard reagents were used as nucleophiles with sp^2-carbon halides in one of the simplest methods of cross-coupling.[7] This reaction uses complexes of palladium or nickel as pre-catalysts with phosphine ligands to get a highly selective reaction. This reaction was tested using aryl and vinyl chlorides with alkyl and aryl Grignard reagents (Scheme 1.3). Mechanistic studies of this reaction led to suggest a catalytic cycle where the metal was reduced, and then oxidative addition, transmetallation and reductive elimination steps proceeded with the nucleophile and the electrophile. [8,9]

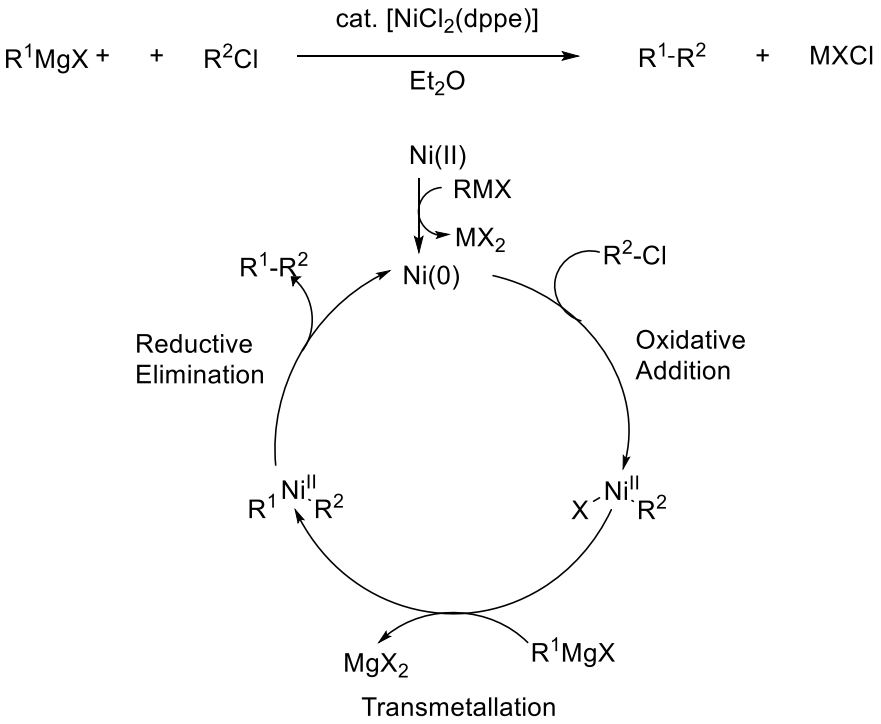

Scheme 1. 3 Nickel-catalysed Kumada coupling and proposed mechanism.

The challenging sp^3-sp^3 coupling of alkyl electrophiles with an alkyl Grignard reagent was reported by Kambe and co-workers[10], who developed in 2002 the coupling of alkyl bromides and chlorides with alkyl Grignard reagents using a mixture of $NiCl_2$ and 1,3-butadiene (Scheme 1.4)[11]. For this reaction, 1,3-butadiene was proposed to have an ancillary role in the reaction,

coordinating to the nickel centre through a bis-π-allyl bond, conferring upon the metal centre the electronic environment necessary for facilitating the coupling. Furthermore, Kambe discovered that palladium was also active for sp^3-sp^3 couplings, showing that alkyl fluorides worked better than the bromides.[12]

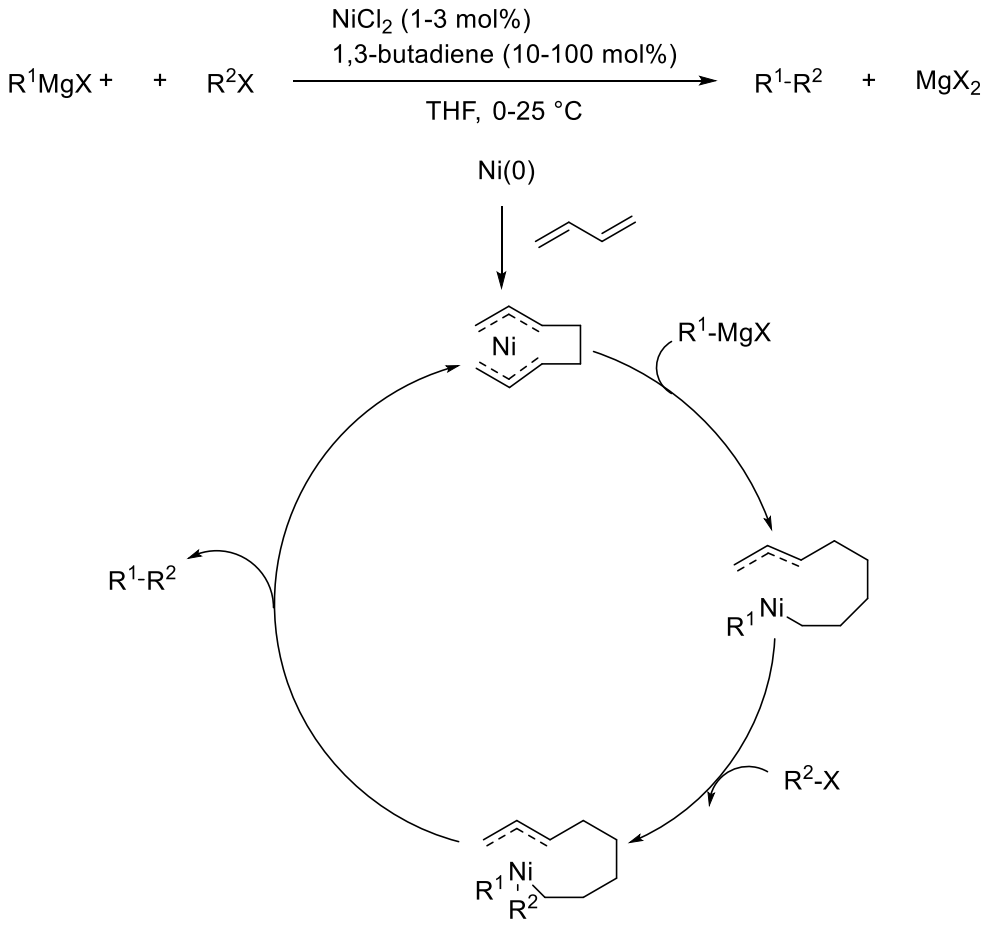

Scheme 1. 4 nickel-catalysed alkyl-alkyl coupling reaction

1.3 Palladium Cross-coupling reactions

Thanks to the novelty of the results that nickel catalysis gave, new efforts in the field were conducted, and eventually, palladium complexes emerged as excellent catalytic candidates. Murahashi and co-workers reported the cross-coupling of vinyl halides with alkyl lithium and alkyl Grignard reagents (Scheme 1.5)[13]. Ishikawa and co-workers discovered the reaction of

aryl halides and aryl Grignard reagents pre-catalysed by a palladium(II) complex.[14] They found that the palladium was reduced to a Pd(0) species in situ which is the active species.

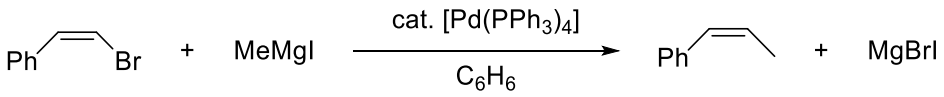

Scheme 1. 5 Palladium-catalysed cross-coupling reaction discovered by Murahashi and co-workers

Palladium complex catalysis resulted in more predictable and flexible reactions compared to nickel catalysts, which is prone to undesired side reactions. Palladium complexes could be applied to a broad range of substrates and reactions. So the focus shifted to the study of palladium and the development of new systems.[14] Palladium is more expensive than nickel, but thanks to its excellent activity and selectivity, it became the core of the field, retaining this place ever since. This relevance was acknowledged with the Nobel prize for chemistry awarded to Heck, Negishi and Suzuki in 2010 for their contributions to palladium-catalysed cross-coupling.[3] The extensive mechanistic studies of Pd catalysis has led to the general mechanism displayed in scheme 1.6.

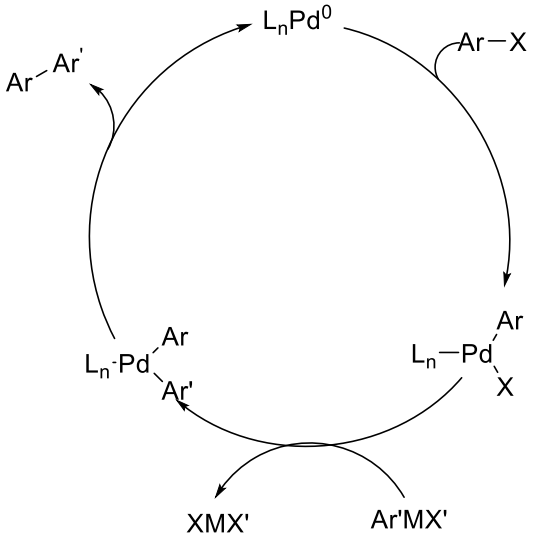

Scheme 1. 6 General mechanisms for Pd-catalysed cross-coupling

An example of the relevance of the Kumada reactions is the synthesis of molecules with biological importance done by Muzler and co-workers using a palladium-catalysed Kumada reaction as a synthetic step in the total synthesis of 15-deoxy-16-(m-tolyl)-17,18,19,20-tetranorisocarbacylin (Scheme 1.7, a).[15] Another example is the synthesis of epothilone B which was archived by Danishefsky using an sp^2-sp^3 Kumada coupling (Scheme 1. 7, b).[16]

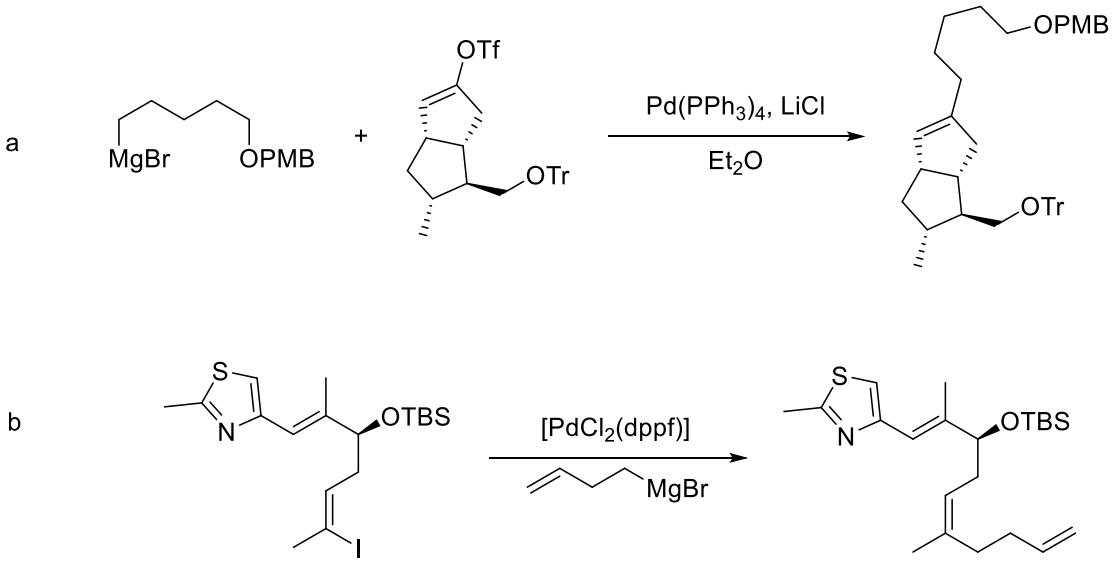

Scheme 1. 7 Palladium-catalysed coupling in the synthesis of molecules with biological importance

1.4. Use of softer nucleophiles

The use of Grignard reagents comes with some drawbacks: the high reactivity of these compounds promotes some undesirable reactions if the organic electrophile has a sensitive functional group, which in turn diminishes the yield of the desired product. The use of less reactive nucleophiles would provide the necessary conditions to avoid side reactions without the need for protecting the functional group, allowing more flexibility for subsequent reactions on the resulting cross-coupled product. Examples of milder nucleophiles were presented by Negishi using organozinc, and organoaluminum.[4] Suzuki and Miyaura developed a reaction using organoboron reagents.[17] Stille worked using organotin reagents[18], and Hiyama used organosilicon species.[19]

1.4.1 Organoaluminium reagents

In 1976 Negishi and co-workers reported on the use of organometallic aluminium reagents in cross-coupling reactions catalysed by Ni or Pd.[20,2121]. Alkenylalane species were used with alkenyl halides in the presence of nickel or palladium complexes (Scheme 1.8).

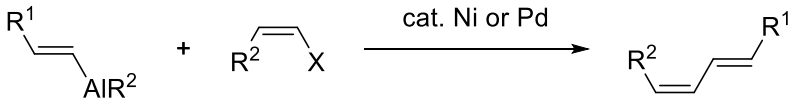

Scheme 1. 8 Pd or Ni-catalysed cross-coupling using aluminium reagents

Other reagents that have been used with success are $AlPh_3$ and $AlEt_3$.[22–24] but these reagents are limited to transferring only one of their organic fragments. This limitation can be circumvented using mixed organoalanes $RAl(^iBu)_2$ (R = aryl, alkenyl and alkynyl) and $Li[RAl(^iBu)_2]$. In both cases, the R group is transferred leaving the alkyl moieties intact.[25,26]. More recently, Knochel and co-workers developed the subsequent palladium-catalysed reaction of aryl halides with aluminium powder which forms in situ the organoalane, which is subsequently coupled with aryl halides (Scheme 1. 9).

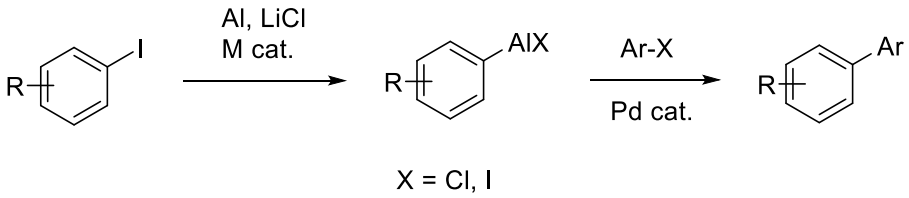

Scheme 1. 9 Alumination of aryl halides and sequential cross-coupling

1.4.2 Organozinc reagents

The characteristic intolerance in some functional groups to Grignard reagents has been addressed by using organozinc reagents instead. These compounds are softer nucleophiles and are compatible with a range of functional groups such as esters and nitriles. The first development of organozinc based cross-couplings was introduced by Negishi and co-workers

when they screened alternative metals in order to find new potential organometallic nucleophiles.[27] Alkynyl zinc halides displayed an excellent performance reacting with 2-iodotoluene, resulting in a 91% yield of the cross-coupled product (Scheme 1.10).

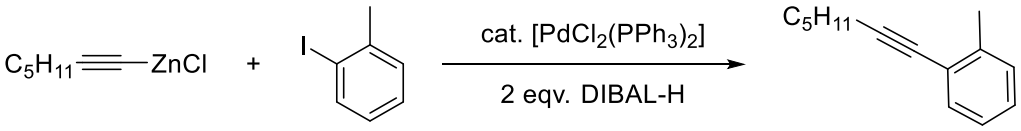

Scheme 1. 10 First palladium-catalysed coupling reaction using an organozinc reagent

Diorganozinc (R_2Zn) reagents showed higher reactivity than their organozinc halide (RZnX) counterparts. Unfortunately, typically only one of the two organic groups transfers during transmetallation reactions.

Organozinc has shown to react quickly with palladium to form the transmetallated intermediate very efficiently; this has provided the Negishi reaction with an advantage over other soft nucleophiles. Nevertheless, a significant disadvantage for these reagents is their high sensitivity towards air and moisture.

Another example of the use of organozinc reagents was reported by Knochel and co-workers where they used solid, salt-stabilised organozinc reagents which are air and moisture resistant. Aryl and heteroaryl bromides alongside benzyl chlorides reacted successfully with magnesium and $Zn(OPivalate)_2{\cdot}LiCl$ forming the RZn(OPiv) reagent. Subsequent reaction of the zinc reagent using palladium as the catalyst was performed using aryl and heteroaryl halides (Scheme 1.11).[28,29]

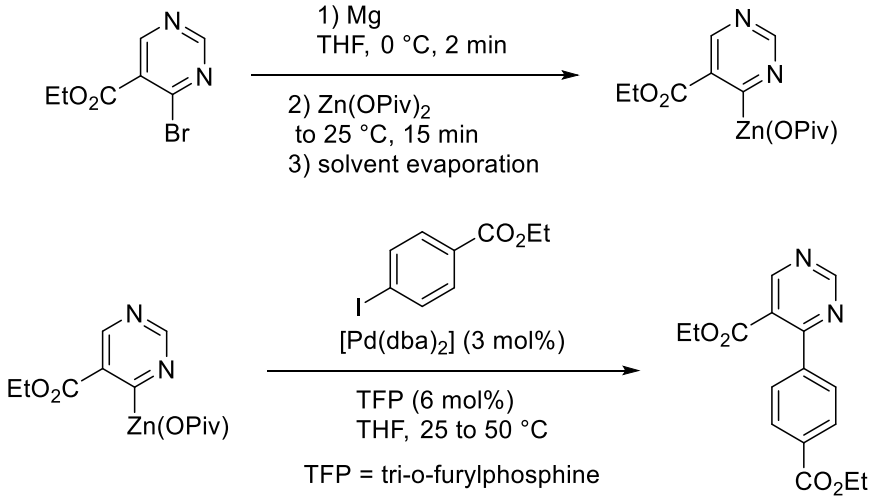

Scheme 1. 11 Use of stable zinc salt as the nucleophile

Nickel pre-catalysts have also been shown to be active in the Negishi cross-coupling. Tucker and co-workers demonstrated that aryl chlorides could be coupled with aryl zinc reagents. This reactivity is of primary importance as these substrates have shown a lower reactivity compared with bromides and iodides in palladium-catalysed cross-coupling (Scheme 1.12).[30]

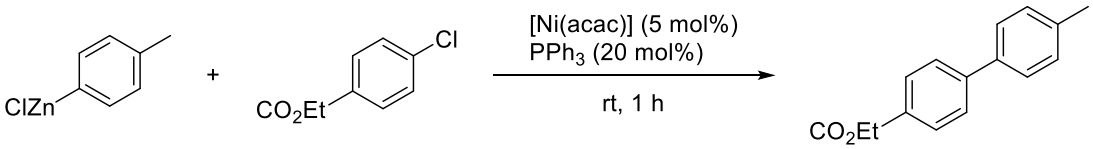

Scheme 1. 12 Cross-coupling of aryl chlorides with nickel as pre-catalyst

A limitation of Pd-catalysed cross-coupling is the generally poor ability to effectively couple alkyl halide electrophiles due to their propensity to undergo β-hydride elimination which has a faster rate compared to the oxidative addition (Scheme 1.13).[1] A solution to this restriction is the use of specific ligands and the use of nickel pre-catalysts.

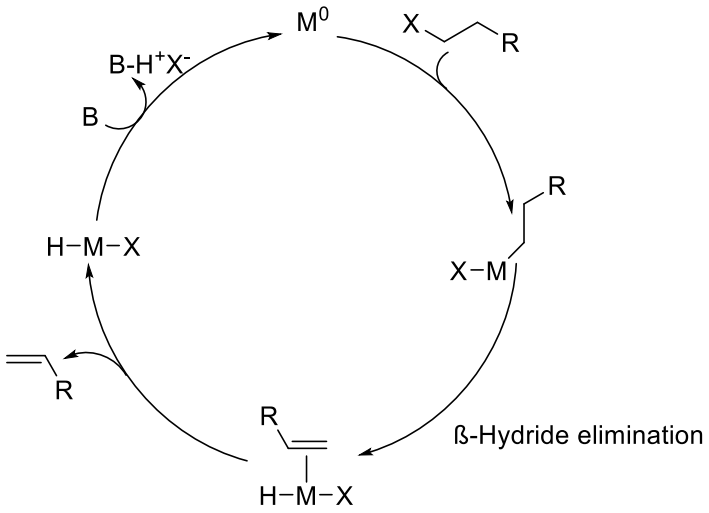

Scheme 1. 13 Postulated mechanism of the β-H elimination as a side reaction.

Knochel and co-workers demonstrated that the coupling of functionalised alkyl iodides with aryl zinc bromides was facilitated by a mixture of [Ni(acac)$_2$] and 4-(trifluoromethyl)styrene.[31] Later reports by the same author used alkyl iodides and dialkylzinc reagents.[32] Fu and co-workers have expanded the work to new pre-catalysts with the reaction of alkyl bromides with alkyl zinc iodides at room temperature using [Ni(COD)$_2$] (COD = cyclooctadiene) and (^{s}Bu)-Pybox as the ligand.[33] Interestingly, this approach has been expanded to the cross-coupling of secondary alkyl species and alkylzinc reagents in regioselective and asymmetric processes (Scheme 1.14).[34]

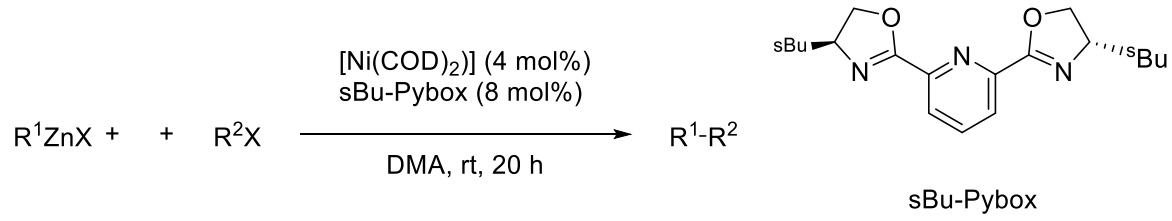

Scheme 1. 14 sp^3-sp^3 Nickel-catalysed Negishi cross-coupling reaction.

Negishi reactions are widely used in total synthesis; for instance, the synthesis of β-carotene was done by Negishi and co-workers in 2001 (Scheme 1.15).[35]

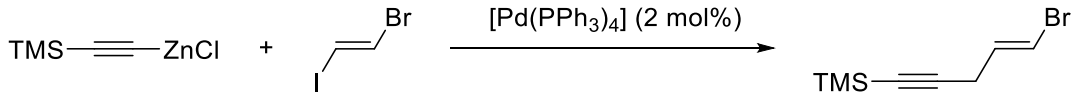

Scheme 1. 15 Negishi coupling used in the total synthesis of β-carotene

1.4.3 Stille Coupling

Organostannane reagents have proved tolerant to a range of functionalities. Their stability and ease of handling characterise them. However, their toxicity is a significant drawback. Stille and Milstein reported in 1978 the first use of organotin in palladium-catalysed reactions (Scheme 1.16).[36]

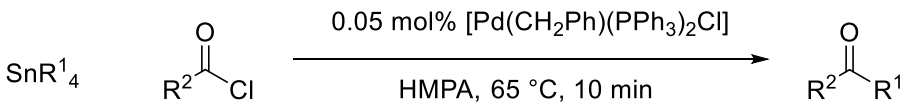

Scheme 1. 16 Stille's cross-coupling of acid chlorides and organostannanes

Stille reported the cross-coupling of a range of acid chlorides and aryl benzoyl chlorides which have different functional groups with tetra-alkyl or arylstannanes using a palladium compound as pre-catalyst. $[Pd(PPh_3)_4]$ and $[Pd(CH_2Ph)(PPh_3)_2Cl]$ are also competent for this reaction.

1.4.4 Organoboron reagents.

Organoboron reagents possess some advantages compared to other nucleophiles: they are air stable, have high functional group tolerance, and they are not toxic. The Suzuki-Miyaura reactions use organoboron reagents as the nucleophile. Organoboron complexes can be obtained from boronic acids and boronic acid pinacol esters which are commercially available, therefore organoboron compounds have become ideal nucleophiles. These boron-based nucleophiles show a lower reactivity compared with organozinc reagents, but the addition of a base activates them and facilitates transmetallation with the metallic centre of the catalyst (Scheme 1.17).

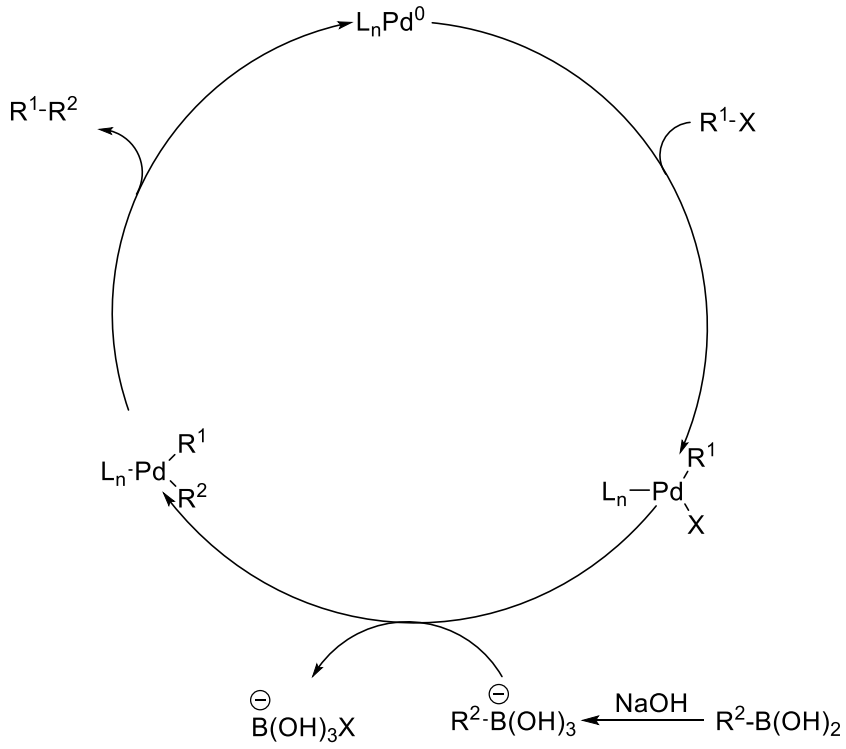

Scheme 1.17 Activation of boronic acids

The first report of a cross-coupling of organoboron reagents and organohalides in the presence of palladium was published by Suzuki and Miyaura in 1979.[37] They successfully coupled 1-alkenylborane with an alkenyl, alkynyl or aryl halide (Scheme 1.18).

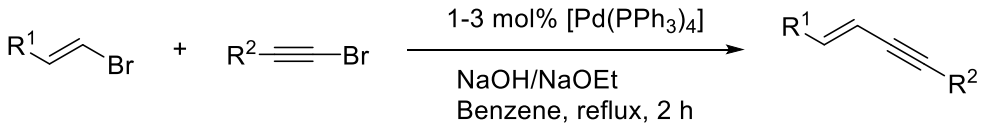

Scheme 1. 18 First report of cross-coupling reaction.

In 1981, an aryl halide was coupled with phenylboronic acid in the presence of Na_2CO_3 (Scheme 1.19).[38] For this reaction, Pd(II) pre-catalysts are employed which, under the reaction conditions are reduced to the active species. This reaction has much versatility as aryl bromides, iodides and triflates could be arylated. On the other hand, aryl chlorides were inert under these conditions.

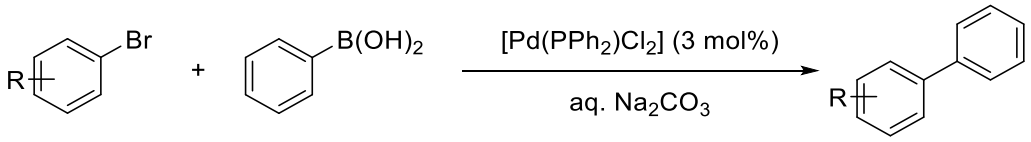

Scheme 1. 19 Aryl-Aryl Suzuki-Miyaura cross-coupling

Suzuki cross-couplings research has had important advances using vinyl or aryl bromides, iodides and triflates, but the chloride analogues have shown to be more challenging. The stronger C-Cl bond is responsible for the inferior reactivity compared to C-Br and C-I bond energy, making it difficult for the chloride to undergo oxidative addition with the palladium catalyst.[39] Gronowitz and co-workers reported coupling of 2,4-dichloropyrimidine with 2-thienylboronic acid. Only the chloride in 4-position would undergo substitution (Scheme 1.20).[40]

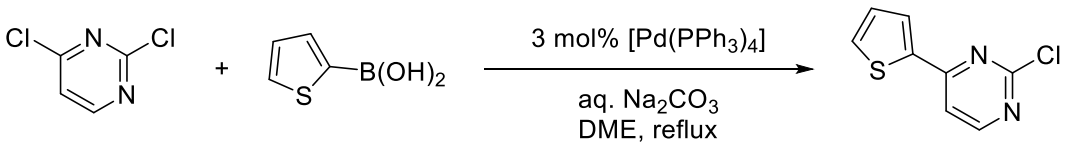

Scheme 1. 20 Cross-coupling of 2,4-dichloropyrimidine with 2-thienylboronic acid.

Hermann and co-workers used a phosphorus-based palladacycle catalyst to couple 4-chloroacetophenone with phenylboronic acid (Scheme 1.21).[41] This system was the first report of a Suzuki cross-coupling of a non-heteroaryl chloride.

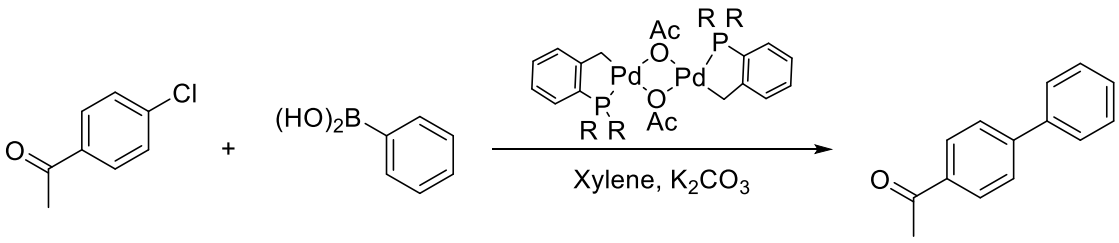

Scheme 1. 21 Cross-coupling of 4-chloroacetophenone and phenylboronic acid.

Buchwald and co-workers combined $Pd(OAc)_2$ and the ligand 2-(dimethylamino)-2'-dicyclohexylphosphinobiphenyl to achieve the successful activation of aryl chlorides (Scheme 1.22).[42] This system was extended to other biphenyl ligands, achieving the room temperature coupling of aryl chlorides using a catalyst load of 0.001 mol%.

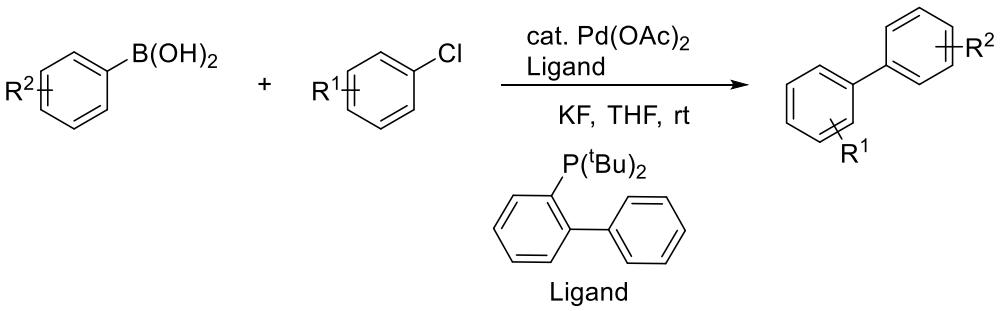

Scheme 1. 22 Cross-coupling of aryl chlorides

Bedford and co-workers prepared palladium tricyclohexylphosphine adducts using ortho-metallated N-donor ligands (Figure 1.1 a and b) which displayed high activity in Suzuki couplings using electron deficient and rich aryl chlorides.[43] In the following publication, mixed tricyclohexylphosphine-triarylphosphite complexes of palladium also showed a very high activity using aryl chlorides as substrate (Figure 1.1 a and c).[44]

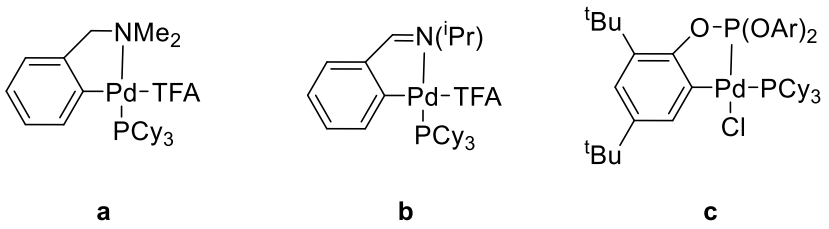

a **b** **c**

Figure 1.1 Bedford catalysts active for aryl chlorides cross-coupling.

The cross-coupling of alkyl halides has also been reported using boron complexes as nucleophiles. Fu and co-workers reported the sp^3-sp^3 Suzuki coupling of primary alkyl bromides with alkyl 9-Borabicyclo[3.3.1]nonane (9-BBN) derivatives using a mixture of $Pd(OAc)_2$ and PCy_3, using K_3PO_4 H_2O as the base. 9-BBN was shown to react with the base forming the hydroxyl complex K[(OH)(R)-9-BBN] (Scheme 1.23). This result is known as the

first catalysis using a β-hydrogen containing alkyl halide with palladium.[45]. This system was later extended to the coupling of secondary alkyl halides using a nickel salt with a diamine ligand.[46] Fu also managed to use alkyl chlorides possessing β-hydrides as substrates with a system that tolerates functional groups on the electrophile such as amines, esters and olefins.[39]

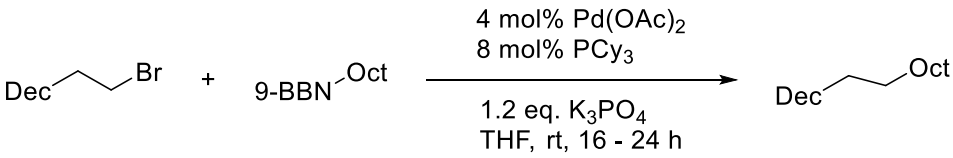

Scheme 1. 23 Suzuki coupling of alkyl bromides with β-hydrogens

A drawback to the use of alkyl-9-BBN derivatives is that they are air sensitive and are not commercially available. Fu developed a cross-coupling method using aryl, vinyl and alkyl boronic acids with a range of alkyl bromides (Scheme 1.24).[47]

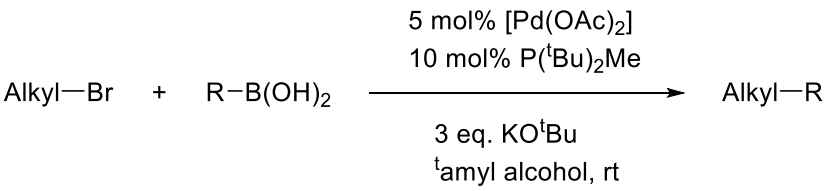

Scheme 1. 24 Cross-coupling of primary alkyl bromides with aryl, vinyl and alkyl boronic acids.

The Suzuki-Miyaura coupling reaction is applied in the synthesis of natural products and other biologically relevant molecules, for instance, biphenomycine A[48] (Figure 1.2). Also, this reaction has found extensive use in the synthesis of a polymeric rigid rod used in high-performance engineering materials.[49]

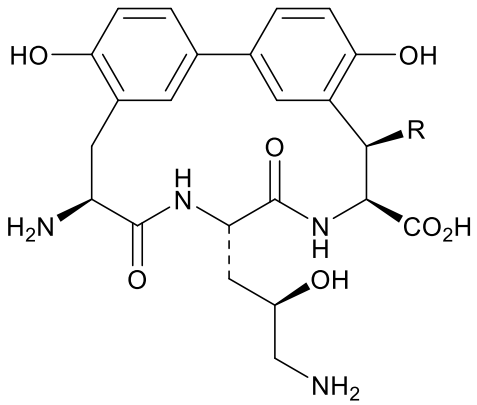

Figure 1. 2 Biphenomycine A

1.5 Iron as a catalyst

Despite its significant catalytic activity, selectivity and compatibility with a range of functional groups, the use of palladium in the industry have some disadvantages because of its toxicity, cost and scarcity. Regulatory agencies such as the European Medicines Agency, require palladium to be removed from final products to a concentration limit of 10 ppm in oral pharmaceutics.[50] Removing metals from products means an additional process which results in a higher cost of production. The cost of palladium has fluctuated between 600 USD to over 1000 USD per ounce troy in the past five years,[51] this is owing in part to Palladium existing in the crust of the earth only in parts per trillion. This scarcity and the continuous need for palladium in other industries such as the automotive and electronics add up to the fluctuation in the price of the metal. Other alternatives such as nickel come with other drawbacks like toxicity.

In contrast, iron is the fourth most abundant element in the Earth's crust which translates into a lower cost (the price of iron ore is 73.03 USD per tonne).[52] Likewise iron has a significant role in the human body, playing a vital role as part of haemoglobin which is essential for oxygen transport. This metal role in life extends to an essential role in glucose metabolism, scavenging free radicals and the synthesis of DNA.[53]

Iron reserves are estimated to be over 100 billion tonnes, and due to its availability, there are many salts and complexes commercially available. It is present in the Earth's crust as some different ores; the most abundant is haematite (Fe_2O_3), then it can be found in magnetite (Fe_3O_4), goethite (FeO(OH), lepidocrocite (FeO(OH)) and siderite ($FeCO_3$).[54]

Iron possesses many accessible oxidation states. It is most commonly found as iron(II), and iron(III). However, oxidation states ranging from (-II) to (IV) have all been reported. Iron in low oxidation states is especially interesting for organometallic chemistry as they confer a nucleophilic nature to the metal.[55]

Iron has been used for many years as a heterogeneous catalyst, most importantly in the Haber-Bosch process, Which produces ammonia from nitrogen and hydrogen.[56]

1.5.1 Iron catalysed cross-coupling using Grignard reagents

Iron catalysts for cross-coupling reactions often show high activities and short reaction times, outperforming those of the group 10 transition metals. In early experiments, the formation of the desired products came with the formation of β-hydride elimination side products as well as homo-coupling products due to the high activity of the catalytic systems. A successful coupling of alkenyl halides requires the deployment of large amounts of an alkenyl reagent with moderate yields based on the Grignard reagents. The start of cross-coupling reactions using iron as catalyst began in 1941 when Kharash and co-workers reported that $FeCl_3$ could catalyse the cross-coupling of bromobenzene with phenyl magnesium bromide, but this work did not attract much attention as this line of research was not pursue any further (Scheme 1.25).[5]

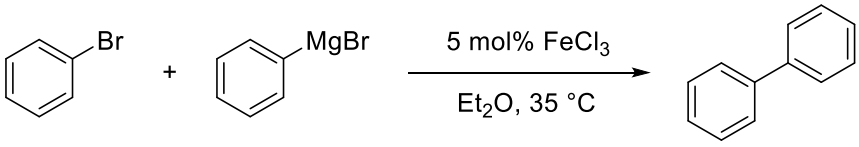

Scheme 1. 25 Iron-catalysed biaryl coupling by Kharasch

1.5.1.1 Alkenyl Electrophiles

Much later in 1971, Kochi and Tamura attempted the coupling of alkenyl halides with alkyl Grignard reagents catalysed by $FeCl_3$.[6,57] In their research, they found that a mixture of alkanes and alkenes was formed, nevertheless under the same conditions, vinyl bromides could be cross-coupled with alkyl Grignard reagents in high yields, retaining the *cis/trans* configuration (Scheme 1.26), a large excess of vinyl halide was required. This work was extended for the use of secondary and tertiary alkyl Grignard reagents.

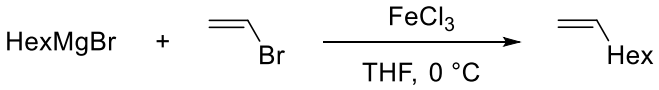

Scheme 1. 26 First example of iron-catalysed cross-coupling, by Kochi and co-workers.

Work by Molander,[58] Marchese[59] and Naso[60] in the 80s showed that iron could catalyse the reaction between alkyl and aryl Grignards. In the study by Molander the reaction between alkenyl halides and aryl Grignards demonstrated that using the solvent dimethylether (DME) and a low temperature reaction, the reaction does not need an excess of electrophile in order to get high yields of cross-coupling product (Scheme 1.27, a).[58] Interestingly, if the reaction was performed in the presence of bromobenzene, the reaction was entirely selective for the coupling with the vinyl derivative, recovering the unreacted aryl halide. Naso reported the use of a range of iron reagents such as $[Fe(dbm)_3]$, $[Fe(acac)_3]$ and $FeCl_3$ in the catalysis of both cis or trans isomers of 1-bromo-2-phenylthioethenes with alkyl Grignard reagents, obtaining high chemo- and stereo-selectively, whereas mixtures of isomers are obtained using palladium or nickel catalysts (Scheme 1.27, b).[60]

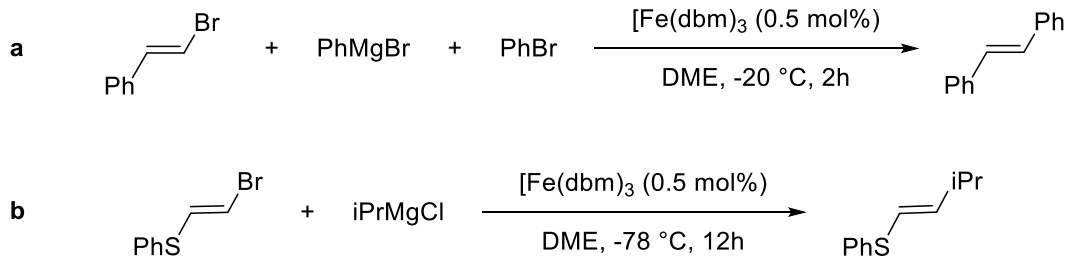

Scheme 1. 27 Molander and Naso examples of iron-catalysed cross-coupling

In 1996 Cahiez and co-workers reported a procedure for the alkenylation of organomanganese nucleophiles using $FeCl_3$ or $Fe(acac)_3$, effectively cross-coupling alkenyl halides with alkylmanganese chlorides under very mild conditions to afford the substituted olefin in excellent yield (Scheme 1.28). This system required a solvent system of THF and NMP.[61]

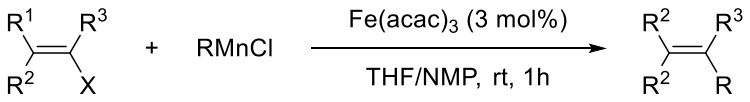

Scheme 1. 28 Fe-Catalysed Alkenylation of RMnCl

In 1998, Cahiez reported again the use of NMP (N-methylpyrrolidone) as co-solvent with $Fe(acac)_3$ as catalyst for the coupling of alkenyl halides and alkyl Grignard reagents (Scheme 1.29).[62] This work demonstrated the importance of selecting the correct solvent system when carrying out catalysis, as the use of only THF yielded low conversion to products. The research showed an impressive stereoselectivity, functional group tolerance (alkyl and aryl bromides, amides, esters and ketones) and high yields. NMP was assumed to stabilise an intermediate of reaction and lower the activity of this iron species, avoiding decomposition of the active species.

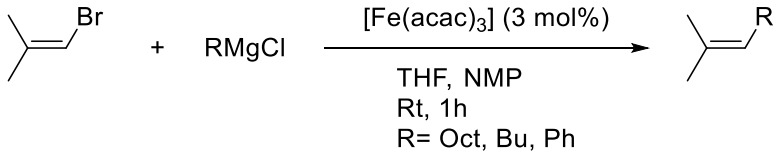

Scheme 1. 29 Cahiez's iron catalysed cross-coupling with organomagnesium nucleophiles and NMP as an additive.

Knochel and Cahiez collaborated and worked on the cross-coupling of functionalised arylmagnesium reagents with ester, cyano, nonaflate, or trialkylsilyloxy substituents generated by halogen-metal exchange with iPrMgBr. The reaction was rapid using alkenyl iodides or bromides in the presence of $Fe(acac)_3$ at -20 °C, and resulted in the production of exclusively E isomers with good yields (Scheme 1.30).[63]

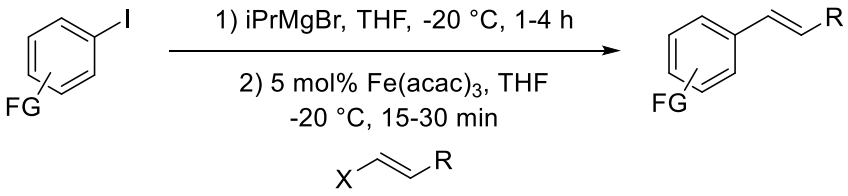

Scheme 1. 30 $Fe(acac)_3$ catalysed cross-coupling of aryl Grignard reagents with alkenyl halides.

Cassar and co-workers recently reported the coupling of allylic and vinylic bromides with aryl Grignard reagents using D-glucosamine HCl as a biocompatible, sustainable and cheap ligand.[64]

Hoffmann used a chiral Grignard reagent which had the magnesium in the stereogenic centre, testing the reactivity with vinyl bromide using a different catalyst. Pd or Ni catalyst gave a product with full retention of the stereo-configuration, whereas the use of [$Fe(acac)_3$] and [$Co(acac)_2$] resulted in racemisation (Scheme 1.31). The conclusion was that the Pd and Ni catalysis occurred as a concerted S_E2-ret process, while the use of iron and cobalt involved a single electron transfer (SET) operating.[65]

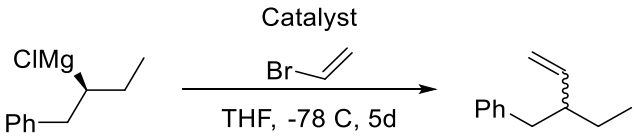

Scheme 1. 31 Cross-coupling of chiral Grignard with vinyl bromide

Fe-catalysed Kumada coupling has found applications in the synthesis of natural products, like the synthesis of Latrunculin B which is a known toxin which binds to actin monomers preventing them from polymerising (Scheme 1.32). [66]

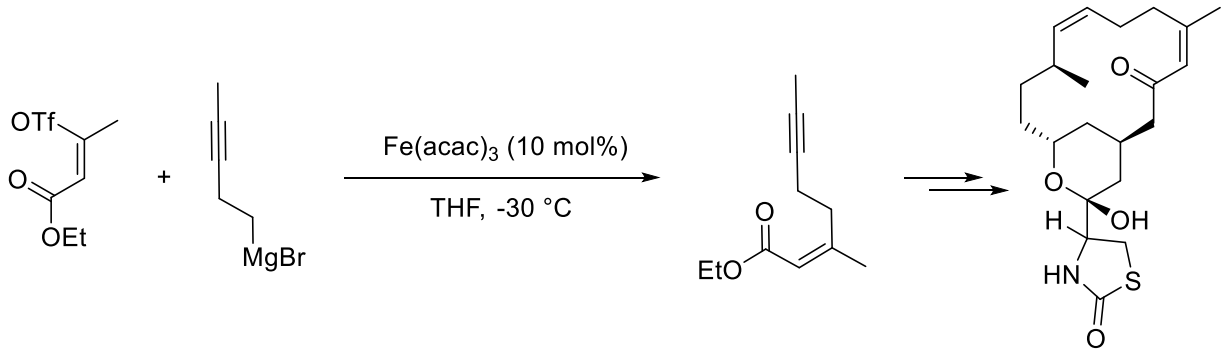

Scheme 1. 32 Synthesis of Latrunculin B and the Fe-catalysed cross-coupling step involved.

Hayashi used [Fe(acac)$_3$] as the catalyst for the coupling of enol triflates with Grignard reagents in the synthesis of C2-symmetric bicyclo[2,2,1]hepta-2,5-dienes (Scheme 1.33). This work compared the performance of the iron catalyst with palladium and nickel, resulting in a 98% yield using Fe and 45% using Ni or Pd.[67]

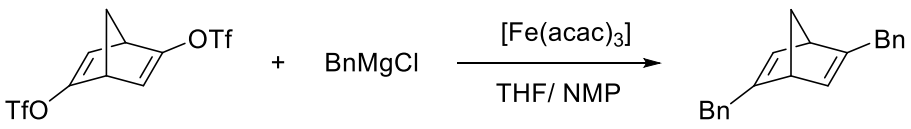

Scheme 1. 33 Cross-coupling of enol triflates

1.5.1.2 Aryl Electrophiles

Fürstner and co-workers reported the iron catalysed cross-coupling between aryl halides, triflates and tosylates with alkyl Grignard reagents, substrates that were inactive in previous investigations (Scheme 1.34).[68,69] This work used initially [Fe(acac)$_3$] as a pre-catalyst, but iron chlorides (II or III) and [FeCl(salen)] salts were shown to have the same efficiency. The chemistry was tolerant of functional groups. Straight-chain and secondary alkyl Grignards gave great conversions, as well as trialkylzincates ([R_3Zn]$^-$) and organomanganese reagents (RMnX, R_2Mn, $R_3MnMgCl$). Further tests with other nucleophiles showed that no cross-coupling was obtained with triethylaluminium or n-butyllithium.[68]

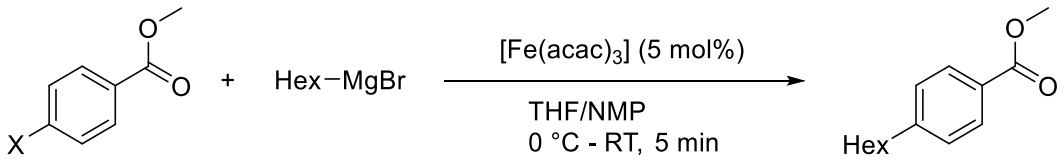

Scheme 1. 34 Cross-coupling of aryl halides, triflates or tosylates and alkyl Grignard reagents reported by Furstner.

This work has the advantage of using aryl chlorides which were found to give a higher yield than the corresponding bromides and iodides.[69]

Fürstner later reported the cross-coupling of heteroaromatic chlorides with aryl Grignard reagents, obtaining high yields by using Fe(acac)$_3$ in a mixture of THF and NMP.[70] It is important to note that electron-rich aryl halides failed as cross-coupling partners and the only product obtained was the homo-coupling of the arylmagnesium reagent. Fe(salen)Cl was tested as the catalyst for this reaction, but it did not show activity for heteroaromatic chlorides.[68]

Aryl Grignard reagents are difficult to work with due to their propensity to undergo homocoupling reaction caused by oxidation with organic halides or iron-catalysed halogen-metal exchange.[71] Nakamura published a report using a catalyst system of iron(III) fluoride and N-heterocyclic (NHC) ligands (Scheme 1.35). This system suppresses homocoupling, and

it was hypothesised that this is due to the presence of fluoride anions. This assumption was tested using iron(III) chloride and adding potassium fluoride as an additive, obtaining a good selectivity although reduced compared to that of the FeF_3. It was suggested that the formation of ferrate complexes ([ArAr'$_3$Fe] or [Ar$_2$Ar'$_2$Fe] would be prevented by coordination of the fluoride ion to the iron centre, avoiding the non-selective reductive elimination that yields the homocoupling product.

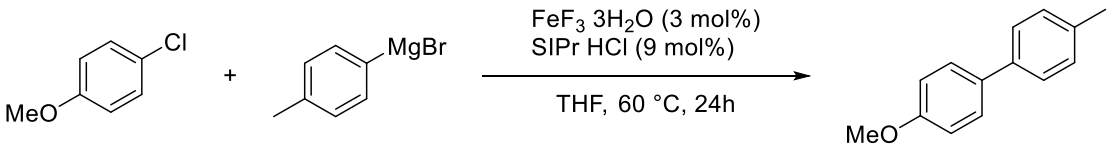

Scheme 1. 35 Fe-catalysed aryl-aryl cross coupling

Duong and co-workers, inspired by the work of Nakamura, used alkoxide ligands to enhance selectivity and inhibit the formation of ferrate complexes that produce the homo-coupled product (Scheme 1.36),[72] different sources of iron show good activity, with iron(III) triflate showing the best performance.[73] Compared to fluoride ligands, alkoxide ligands are stronger π-donors, and its donor nature is tuneable by changing the alkyl substituent.[74] It was shown that both electron rich and deficient substrates were compatible with this system as well as sterically bulky aryl chlorides. A recent paper by the same authors tested a range of NHC ligands and it was found that bulky substituents on the carbene and the degree of unsaturation of the NHC backbone influence the reaction outcome, with sterically demanding ligands giving the highest yields of the desired biaryl.[75]

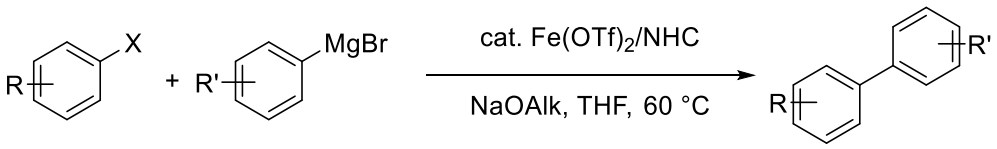

Scheme 1. 36 Use of alkoxides as homo-coupling inhibiting ligands

Knochel and co-workers reported that an isoquinoline additive accelerates the coupling of N-heteroaromatic halides with aryl Grignard.[76] This work was expanded to the use of

heteroaromatic electrophiles with heteroaromatic nucleophiles.[77] Without the additive, the yield was lowered drastically. It was concluded that the isoquinoline additive would coordinate to the iron tribromide salt, stabilising the reaction.

1.5.1.3 Alkyl electrophiles

Alkyl halides are challenging cross-coupling partners in Pd- and Ni- catalysed system, because the alkyl-metal complex formed in situ are prone to β-hydride elimination to form alkene by-products.[78]

Reports of cross-coupling reactions with vinyl Grignard reagents and alkyl halides are rare. In 1983, Konig used $FeCl_3$ for the synthesis of cyclobutylidene derivatives, vinylmagnesium bromide proved to be an excellent coupling partner with cyclobutyl bromide (Scheme 1.37).[79]

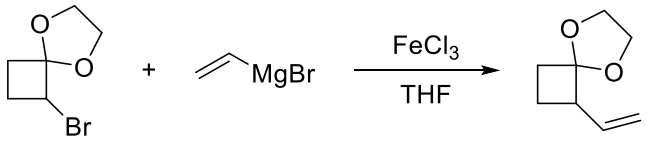

Scheme 1.37 Vinylation of cyclobutyl bromide

Cossy and co-workers studied the conditions for the cross-coupling of vinyl Grignard reagents with primary and secondary alkyl iodides and bromides. The first attempt on this reaction was using the already well-known $Fe(acac)_3$/THF/NMP, but this protocol did not work with these substrates. A new system using $FeCl_3$/TMEDA afforded the desired products in high yields (Scheme 1.38).[80] These conditions did not give positive results using aromatic halides and using secondary halides led to the formation of β-elimination products.

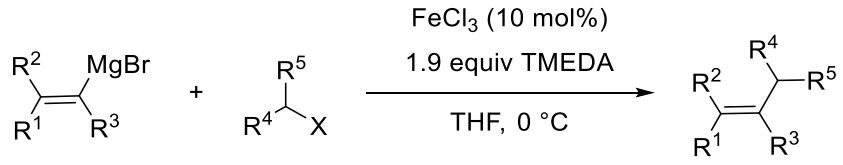

Scheme 1.38 Alkenylation of alkyl halides

In 2004, Nakamura reported the cross-coupling of inactivated secondary alkyl halides and aryl Grignard reagents. It was shown that if tetramethylethylenediamine (TMEDA) is used as an additive with iron(III) chloride as the catalyst, the cross-coupling product would be formed in high yields (Scheme 1.39). If no additives were added or monoamines, phosphine ligands or DABCO (1,4-diazabicyclo[2.2.2]octane) were added, very little selectivity for the cross-coupling reaction was obtained.[81]

Denmark presented a similar method using the Fe TMEDA system for cross-coupling aryl Grignards and alkyl sulfones or alkyl thioethers. The Bedford group have suggested that the role of TMEDA in these reactions is to remove available iron, reducing its overall reactivity in order to avoid side reactions (Scheme 1.40).[82]

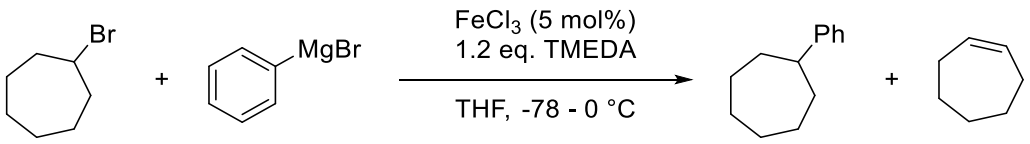

Scheme 1. 39 Nakamura's Fe-catalysed cross-coupling Kumada reaction with secondary alkyl halides.

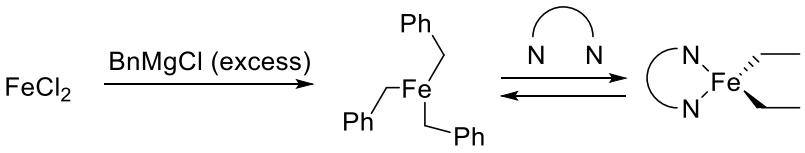

Scheme 1. 40 Role of TMEDA in cross-coupling reactions

Hayashi and co-workers showed that by switching the catalyst from $FeCl_3$ to $Fe(acac)_3$ and using Et_2O as the solvent instead of THF, high yields of the cross-coupled product could be obtained without the need to add slowly any reagent (Scheme 1.41). $Fe(acac)_3$ could be used for subsequent cross-coupling of vinyl and aryl halides in THF/NMP mixtures and changing the solvent to a THF/NMP mixture, which cross-couples allyl halides or aryl triflates.[83]

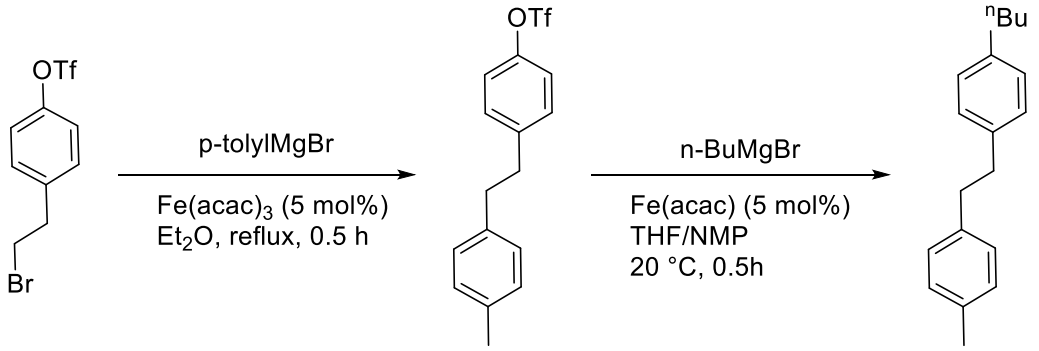

Scheme 1. 41 Subsequent cross-coupling using Hayashi and Furstner system.

Fürstner used iron salen complexes for the catalysis between secondary alkyl Grignards and aryl halides.[84] Bedford and co-workers expanded this work with the coupling of alkyl halides featuring β–hydrogen atoms with aryl Grignard reagents under NMP additive free conditions using the same iron(III)-salen complexes (Scheme 1.42).[85] As mentioned before, the coupling of alkyl halides has proven to be problematic due to the propensity of metal-alkyl complexes to undergo β-hydride elimination. [1]

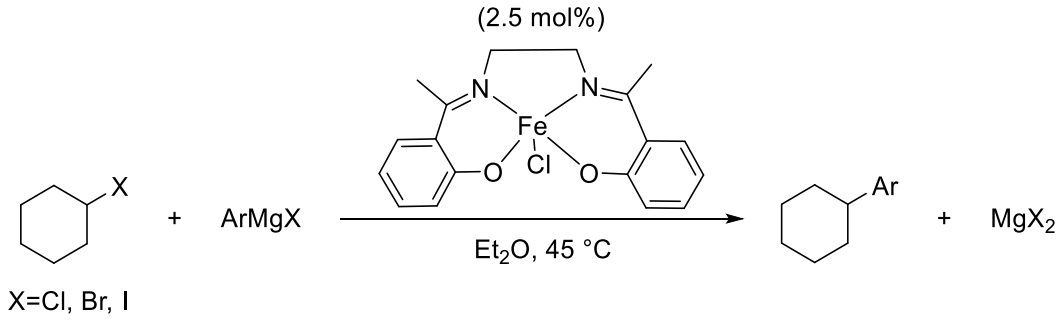

Scheme 1. 42 Cross-coupling of alkyl halides with tolylmagnesium bromide utilising an iron-salen complex as reported by Bedford and co-workers.

Bedford expanded these findings by using a more convenient procedure using catalytic amounts of simple amine ligands (TMEDA, DABCO) and $FeCl_3$ catalyst in one pot for the coupling of secondary alkyls bearing a β-hydrogen with aryl Grignards (Scheme 1.43). [86] This reaction did not need a slow addition of the Grignard Reagent.

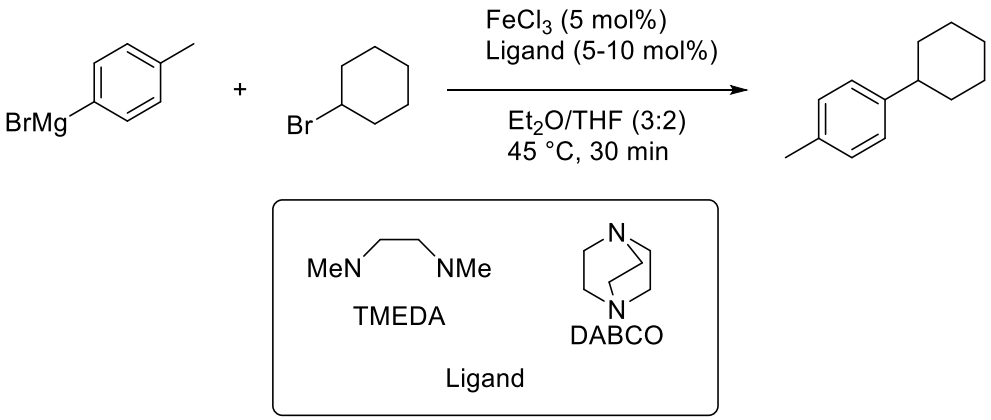

Scheme 1. 43 Fe-catalysed Kumada coupling using simple amine ligands.

Later the same group published iron phosphine, phosphite, arsine, and carbene based catalyst systems.[87] The best results were obtained using alkyl bromides, with a general trend of reactivity found to be Br > I > Cl. Nakamura reported that phosphine ligands did not work well under their condition,[81] while Bedford introduced a new system for which both mono- and di-phosphines where effective. N-heterocyclic carbene ligands were used for the first time in iron cross-coupling within the same studies. In the reactions reported by Bedford, the reaction mixtures were observed to turn black. Transition Electron Microscopy analysis demonstrated that nanoparticles of iron were formed.[88] Polyethylene glycol (PEG) was added in an attempt to stabilise the in situ formed nanoparticles with excellent results, improving the yield of the reaction without the need for amine additives (Scheme 1.44).

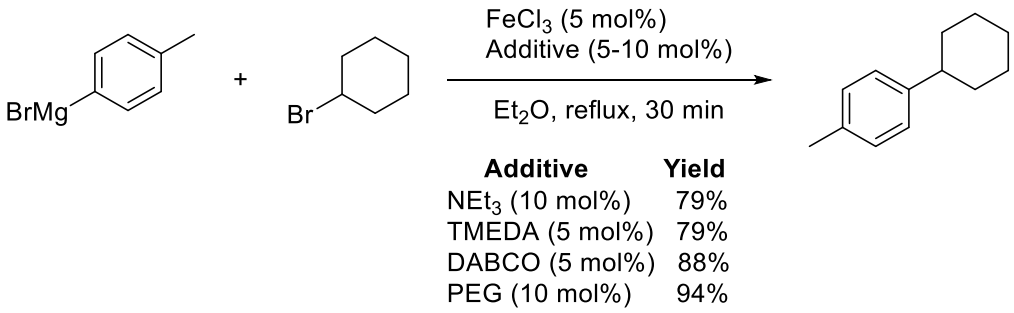

Scheme 1. 44 Cross-coupling using nanoparticles in the presence of catalytic additives.

Nakamura and co-workers presented a system capable of producing cross-coupling of primary and secondary alkyl chlorides with aryl Grignards as the coupling partner. SciOPP ligand showed better results than the similar dpbz ligand (Scheme 1.45). This system was compatible with electron withdrawing and electron donating substituents on the aryl group but was not successful with tertiary alkyl chlorides.[89]

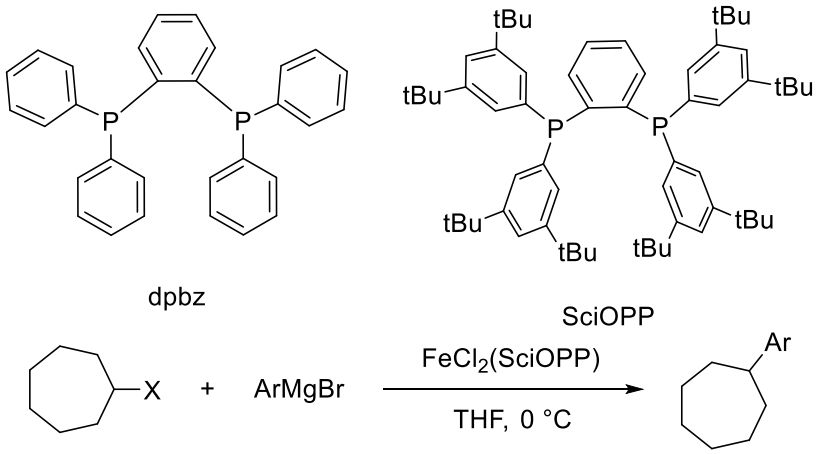

Scheme 1. 45 Use of Phosphine SciOPP ligand for cross-coupling of alkyl halides with aryl Grignard reagents.

Fürstner studied sterically encumbered aryl Grignard reagents and iron dichloride complex $FeCl_2(depe)_2$ (Scheme 1.46, a),[90] discovering the formation of a bisarylated bisphosphine complex without the production of the homoleptic $[Mes_3Fe]$-, which Neidig has attributed to the homo-coupling product formation of Grignard reagent.[91] The group used this knowledge to couple sterically hindered aryl Grignard reagents with primary alkyl bromides and iodides. The use of secondary alkyl halides resulted in the elimination product (Scheme 1.46, b)

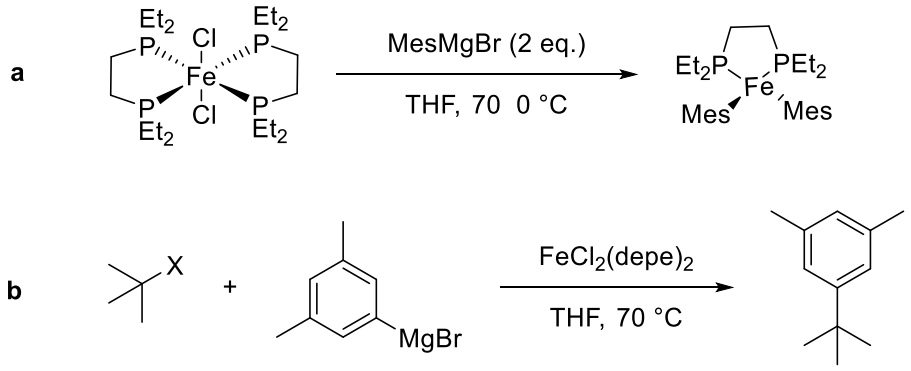

Scheme 1. 46 (a) Formation of phosphine adduct with bulky Grignard reagents. (b) cross-coupling of alkyl halides with aryl Grignard in presence of phosphine complex.

Früstner and co-workers reported the use of $[Fe(C_2H_4)_4][Li(tmeda)]_2$ for the arylation of alkyl, allyl and propargyl halides containing reactive functional groups (Scheme 1.47).[92]

This pre-catalyst with a formal oxidation state of Fe(-II) has four kinetically-labile ligands, wich offers a highly nucleophilic active site. However, this pre-catalyst is not simple to prepare as it requires ferrocene treated with lithium under an ethene atmosphere and the pre-catalyst is highly reactive, making its handling difficult.

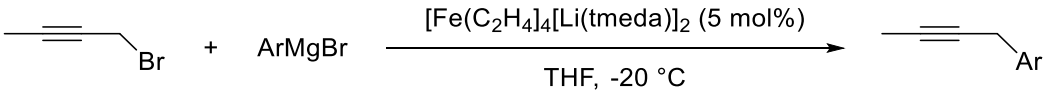

Scheme 1. 47 Iron-catalysed arylation with a Fe(-II) complexes pre-catalyst

The more challenging iron-catalysed sp^3-sp^3 couplings have been studied recently. Chai and co-workers used a primary alkyl bromide and primary alkyl Grignard reagents with $[Fe(OAc)_2]$ and Xantphos to form the pre-catalyst.[88] This reaction is promising, but it does not provide high yields. Cárdenas and co-workers expanded this work using *N*-heterocyclic carbene precursor IMes.HCl (Scheme 1.48).[93] Nitrogen- and oxygen-containing heterocycles, as well as esters were compatible with this system.

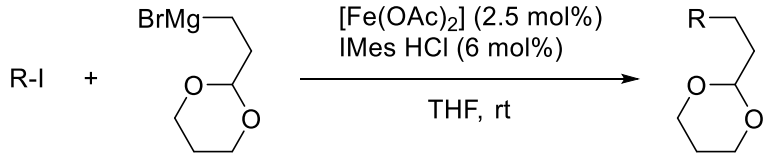

Scheme 1. 48 sp3-sp3 cross-coupling reaction

Hu and co-workers used alkynyl Grignard reagents as coupling partner with alkyl halides (Scheme 1. 49).[94] This reaction used a mixture of $FeBr_2$ and NMP without the use of any ligand or slow addition of the reagents.

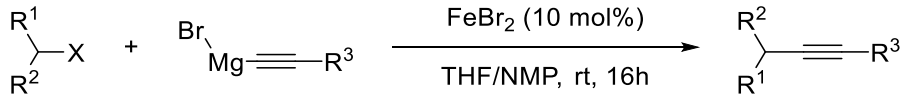

Scheme 1. 49 Alkynyl Grignard reagents and alkyl halides cross coupling

1.5.2. Zinc-based nucleophiles

Experiments using 'soft' nucleophiles in iron cross-coupling with a better functional group tolerance has also been reported actively. Zinc organometallic compounds had been shown to work efficiently with palladium catalysts, and in the early 2000s, Fürstner demonstrated that alkyl zincates could undergo cross-coupling selectively if used in conjunction with $[Fe(acac)_3]$ and ethyl 4-chlorobenzoate. [68,69]

Nakamura reported the use of zinc salts in 2005 using the already known system $FeCl_3$/TMEDA system [81] which permitted a better temperature tolerance (Scheme 1.50).[95] This improvement allowed to carry out the reaction at 50 °C and for the diaryl zinc reagent to be added in a single portion giving high yields without over-reducing the iron centre in the reaction. Curiously, this reaction needed the use of magnesium salts as an additive. Diphenylzinc prepared from $ZnCl_2$ and two equivalents of phenyl lithium was not active for the reaction. Also, it was shown that diorganozinc reagents were necessary: monoorganozinc regents were not nucleophilic enough. This disadvantage reduces the atom economy of the

reaction making it a disadvantage of the method. A more recent paper by the same author describes the use of alkyl sulfonates as substrates using arylzinc reagents.[96]

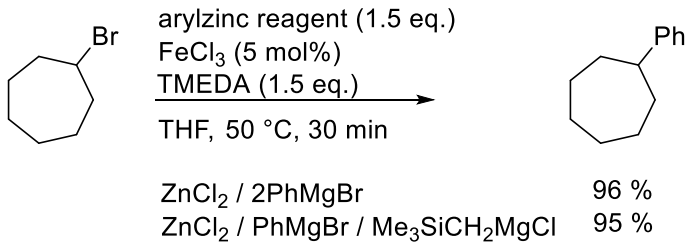

Scheme 1. 50 Arylzinc cross-coupling to an alkyl bromide in the presence of an excess of TMEDA, and a catalytic amount of $FeCl_3$

In 2009, Bedford reported Negishi coupling using $[FeCl_2(dpbz)_2]$ (**1a**) or similar to couple benzyl halide with diaryl zinc reagents (Scheme 1.51).[97] The formation of the pre-catalyst $[FeCl_2(dpbz)_2]$ increased the activity in the reaction affording the best yields of the desired product and suppressing the formation of homo-coupled products.

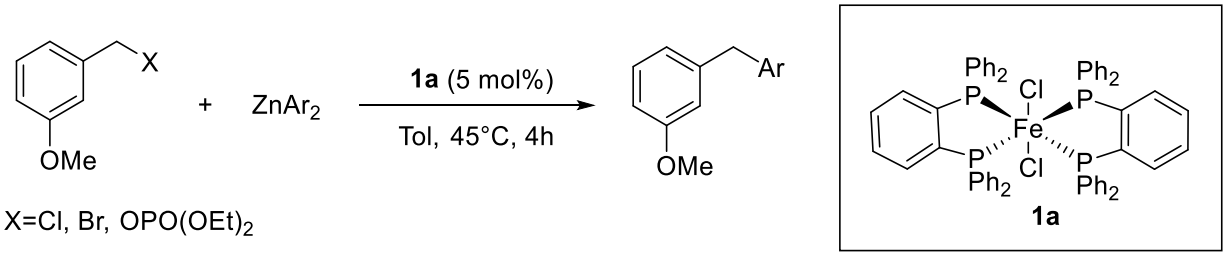

Scheme 1. 51 Iron-catalysed Negishi reaction for the arylation of benzyl halides

The diarylmethane moiety is of particular interest because it is a common structural unit in biologically active compounds such as avrainvilleol and trimethoprim. Having discovered an easy method for the synthesis of this diarylmethane motifs, Bedford reported a broad range of substrates for the Negishi reaction, reporting a good yield of cross-coupled product in the reaction of di-p-tolyl zinc and 2-halopyridines and pyrimidines.[98] The use of sub-stoichiometric amounts of the arylating agent or the use of aryl zinc halides was detrimental in the reaction, indicating the need for two aryl rings on the nucleophilic zinc centre, similar

to the system previously reported by Nakamura.[95] The use of a non-transferable "dummy" ligand in place of one of the aryl rings improved in the atom efficiency of the reaction (Scheme 1.52).[97]

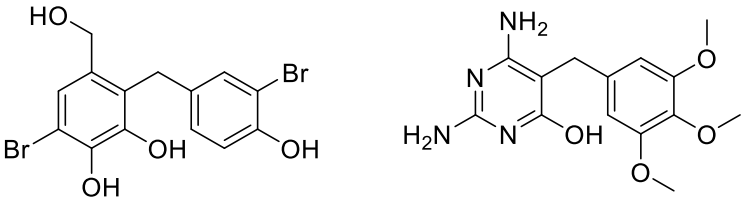

Avrainvilleol Trimethoprim

Figure 1. 3 Biphenomycine A

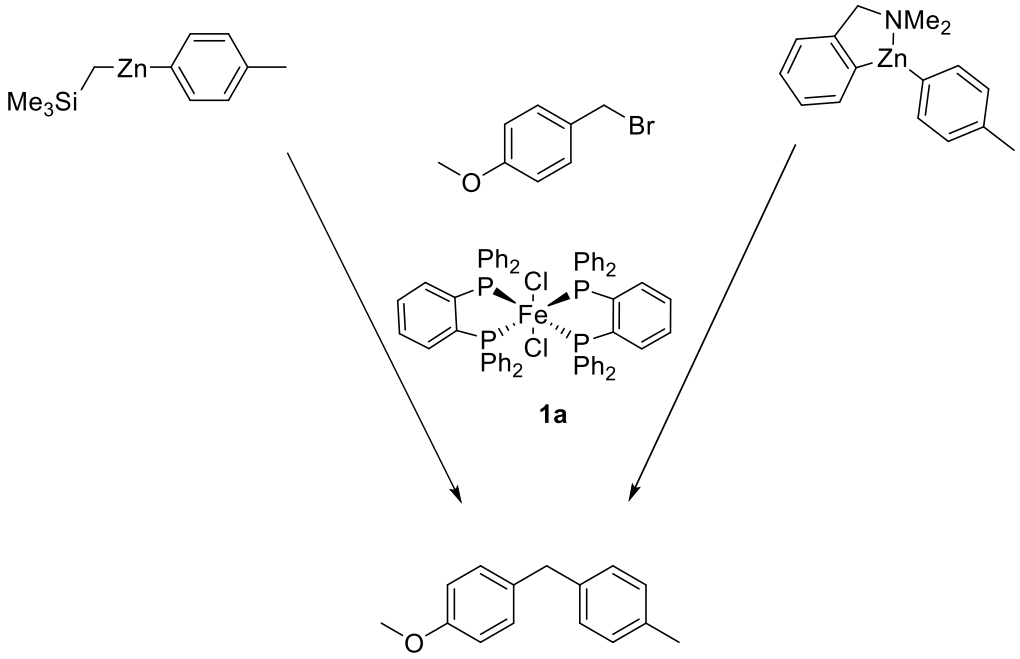

Scheme 1. 52 Fe-catalysed Negishi reaction using a non-transferable 'dummy' ligand

Further studies by Bedford showed the formation of Fe(I) complexes from the reaction of $[FeCl_2(dpbz)_2]$ with arylzinc reagents. These complexes showed catalytic competence. A comparison between these complexes suggested that the complex $[FeBr(dpbz)_2]$ was consistent with an on-cycle intermediate, whereas $[Fe(4\text{-tolyl})(dpbz)_2]$ seems to be an off-cycle species.[99] Previous screening using the ligand dppe did not show significant yields, but

the complex [FeBr(dppe)$_2$] proved competent for cross-coupling, suggesting that the dppe used in optimal conditions is as active as the ligand dpbz. These findings show the importance of being cautious when testing a new catalytic system.[100]

Similarly, Nakamura reported the cross-coupling of alkyl halides with polyfluorinated diaryl zinc reagents using iron halides and the same dpbz bis-phosphine ligand (Scheme 1.53).[101] This reaction was unachievable with TMEDA. This system suppresses sp^2 C-F bond cleavage and E_2-elimination reactions.

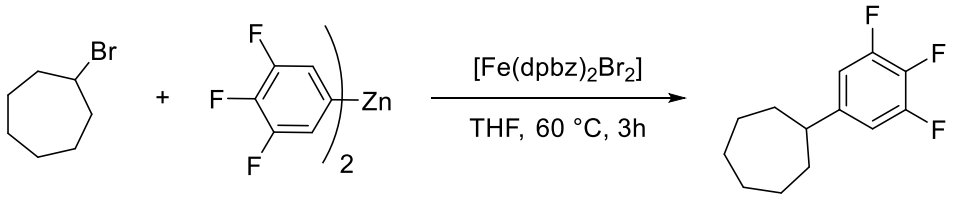

Scheme 1. 53 Fe-catalysed coupling reaction of fluoroaromatic zinc reagents.

Quing *et al.* reported the first example of iron catalysed cross-coupling of α-halo-β,β–difluoroethylene containing compounds with aryl Grignard reagents. For this system, $ZnCl_2$ TMEDA was necessary as an additive, pointing to the formation of the arylzinc reagent. This reaction needed TMEDA and dppp as ligands.[102]

1.4.3 Boron based nucleophiles

To date, efficient protocols for iron cross-coupling reactions using organoboron transmetallating reagents are rare. All the known reports involve the activation of the boron compound and the presence of Zn or Mg additives. In 2009, Bedford reported the iron-catalysed cross-coupling of boron nucleophiles with benzyl and heteroaryl halides (Scheme 1.54).[98] This reaction required the presence of a zinc halide or diarylzinc co-catalyst; it is also of note that there is no transfer of the aryl groups from the diarylzinc. It was suggested that zinc additive role is the stabilisation of active iron species to prevent its decomposition.

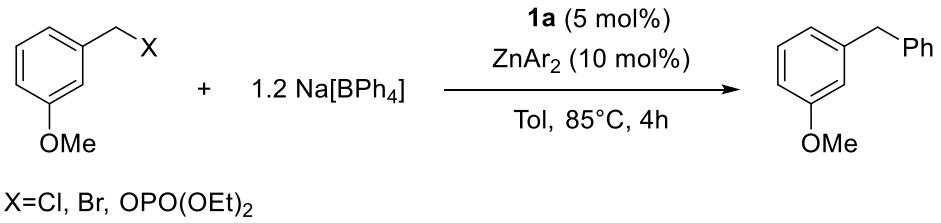

Scheme 1. 54 Iron-catalysed cross-coupling of sodium tetraphenylborate and benzyl bromide with co-catalytic ditolyl zinc as reported by Bedford

Later, Nakamura reported the cross-coupling of alkyl halides with lithium arylborates in the presence of catalytic amounts of magnesium salts (Scheme 1.55).[103] The coupling improved when an iron(II) chloride pre-catalyst, incorporating a bulky dpbz based ligand (SciOPP), was used. The bulk of the ligand prevents a second chelating ligand from coordinating to the iron centre, forcing the complex into a tetrahedral environment. The role of the magnesium dibromide was unknown, but it was hypothesised that it accelerated the slow transmetallation step.

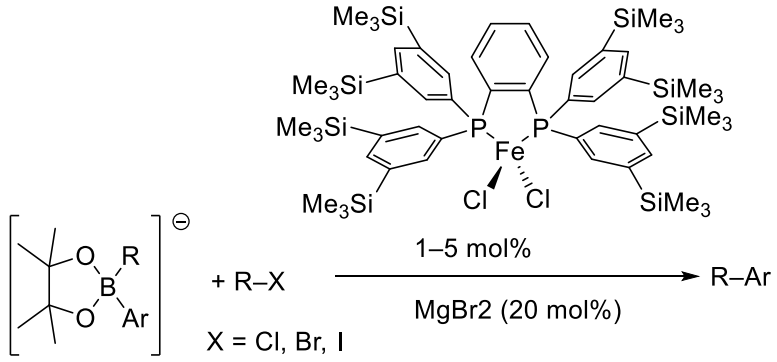

Scheme 1. 55 Cross-coupling of alkyl halides with lithium arylborates using co-catalytic magnesium salts and a [$FeCl_2$(SciOPP)] pre-catalyst, as reported by Nakamura and co-workers.

Further studies by Nakamura showed that lithium vinylborates could be coupled with alkyl halides under similar conditions as those reported previously (Scheme 1.56 a).[104] In a recent report, Nakamura and co-workers made a significant advance in developing an iron-catalysed sp^3-sp^3 coupling, demonstrating the cross-coupling of primary and secondary alkyl halides with magnesium arylborates. This reaction was catalysed by $Fe(acac)_3$ pre-catalyst with added

Xantphos ligand (Scheme 1.56 b).[105] This reaction showed excellent functional group compatibility.

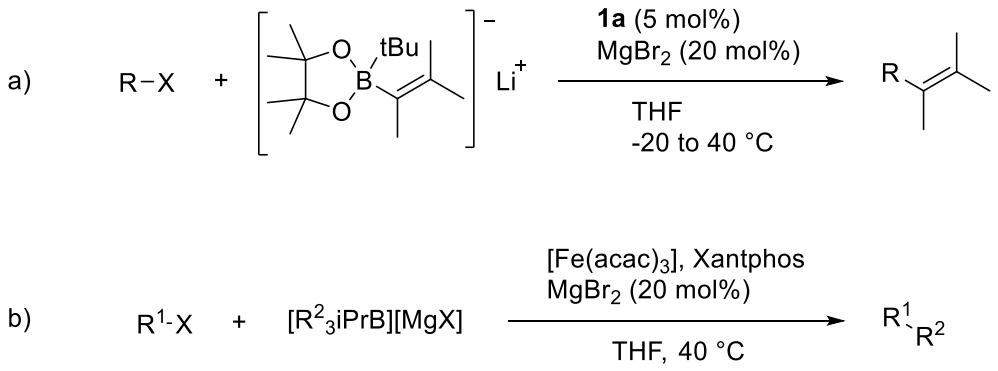

Scheme 1. 56 Nakamura's cross-coupling using a) vinyl borate complexes and b) alkyl borate complexes

Further work by Bedford and co-workers described the cross-coupling of alkyl halides with aryl pinacol boronic esters in the presence of ^{t}BuLi and co-catalytic amounts of magnesium salts (Scheme 1.57).[106] It is worth noting that these couplings happened with $Fe(acac)_3$ and bisphosphine ligands and, in some cases, just $Fe(acac)_3$ in the absence of any additional ligand. Ligands dppe and dppp show good performances, surpassing that of the SciOPP ligands. This system worked for the cross-coupling of alkyl, benzyl and allyl halides.

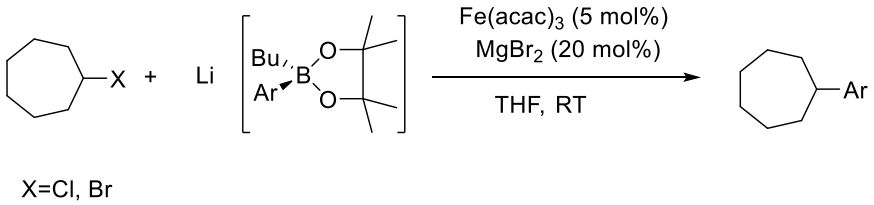

Scheme 1. 57 Cross-coupling of alkyl halides with lithium arylborates utilising co-catalytic magnesium dibromide and bench stable $Fe(acac)_3$ pre-catalysts

Additional work by Bedford and co-workers showed that 2-halobenzylhalides could couple at both benzylic and aromatic positions. To date, this is the only example of an iron-catalysed

biaryl coupling. It was suggested that the initial coupling of the benzyl halide allows the iron catalyst to coordinate, effectively activating the aryl halide. (Scheme 1.58).

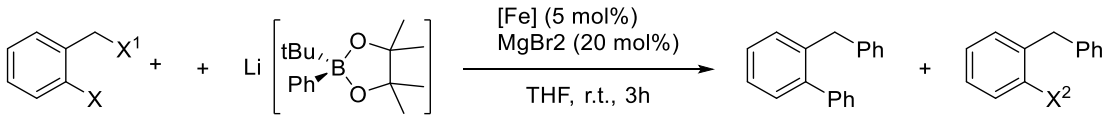

Scheme 1. 58 cross-coupling of halobenzylhalides using arylborates.

The investigation into iron-catalysed cross-coupling reactions has provided a range of procedures for the formation of C-C bonds. Iron has the potential to replace palladium and nickel. In this thesis, the mechanistic aspects of the existing coupling reaction are explored. Also, a new procedure for the cross-coupling of benzyl bromides with zinc reagents was attempted using manganese as the catalyst.

Chapter 2. Exploring Fe(I) reactivity in Negishi Cross-Coupling

2.1 Introduction

2.1.1 Mechanism of iron catalysed cross-coupling reactions

Fe-catalysed reactions are challenging to study due to the redox chemistry of iron which provides a source of complexity in the study of mechanisms of reaction. Due to its electronic characteristics, Fe forms paramagnetic species which introduces difficulties in NMR spectroscopy studies.

Since Kochi reported his seminal work in cross-coupling,[6] the mechanism of iron-catalysed cross-coupling reactions has been studied. There are many aspects to consider for elucidating the mechanism of these reactions, such as the formation of radical intermediates, the oxidation state of the catalyst, and the chemistry of the ligand. Also, there is evidence suggesting that different cross-coupling systems have different mechanisms due to the diverse pathways operative and interactions between the electrophile, nucleophile and pre-catalyst in the reaction.[107] Moreover, active catalysts are very difficult to study and characterise due to their limiting activities and lifetimes, inherent to the nature of the metal and the reaction, added to the paramagnetic nature of many intermediates.

2.1.1.1 Oxidation State of the Active Catalyst

Characterisation of the active catalyst is one of the most critical aspects to resolve in order to understand a catalytic reaction. Fe(II-III) salts are the sources of stable pre-catalysts due to commercial availability and ease of handling. There is a universal agreement in that before catalysis initiates, a preliminary reduction of the iron is made by the nucleophilic. The nature of these low-valent iron complexes has been the subject of debate in the reported mechanistic studies summarised in this section.

Kochi and co-workers examined for the first time the mechanism of iron catalysed cross-coupling between alkenyl halides and alkyl Grignard reagents.[108] They determined the oxidation state of the active catalyst by reacting Fe(III) salts and methylmagnesium bromide, forming methane and ethane (Scheme 2.1); quantifying the amount of product they deduced

the number of times the iron centre was reduced, concluding that a Fe(I) species was formed. However, they could not exclude a Fe(0) species as an active form. It was suggested, using the palladium-catalysed Kumada cross-coupling mechanism as a template,[3] that the mechanism involved the oxidative addition of the alkenyl halide to an activated iron centre, followed by transmetallation with the nucleophile and a reductive elimination, reforming the putative active Fe(I) species (Scheme 2.2).

Scheme 2. 1 Reduction of Fe(III) by CH_3MgBr

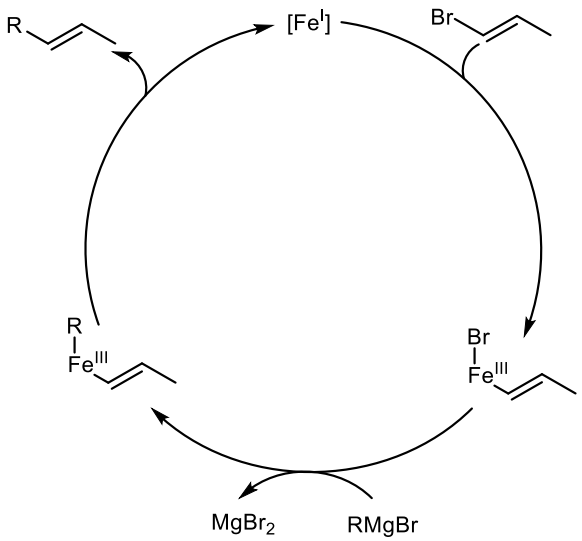

Scheme 2. 2 Mechanism proposed by Kochi

Fürstner and co-workers studied the cross-coupling of aryl chlorides and Grignard reagents, observing a different behaviour when methylmagnesium bromide or ethyl magnesium bromide was used.[92] Methylmagnesium bromide was not active in the reaction whereas ethyl magnesium bromide forms the expected cross-coupling product in good yields. The group credited the different results to the lack of β-hydrogens in the methyl Grignard, which favour the formation of a homoleptic organoferrate. Previous work by Bogdanovic[109] found the

formation of the iron species [Fe(MgX)$_2$] when four equivalents of ethyl magnesium bromide are mixed with a Fe(II) (Scheme 2.3). This compound forms small clusters, and the iron centre is in a formal oxidation state of (-II). A highly nucleophilic character was found for these reagents, and they are the subject of oxidative addition of aryl halides, so the authors concluded that Fe(-II) was the active species. This conclusion was supported by mixing aryl chloride and Fe(0) powder in the presence of an alkyl Grignard. Insertion of the aryl chloride into the Fe(0) was observed, forming the coupling product, whereas without the Grignard reagent the reaction would not proceed, indicating the role of the Grignard as reducing agent for the Fe centre.

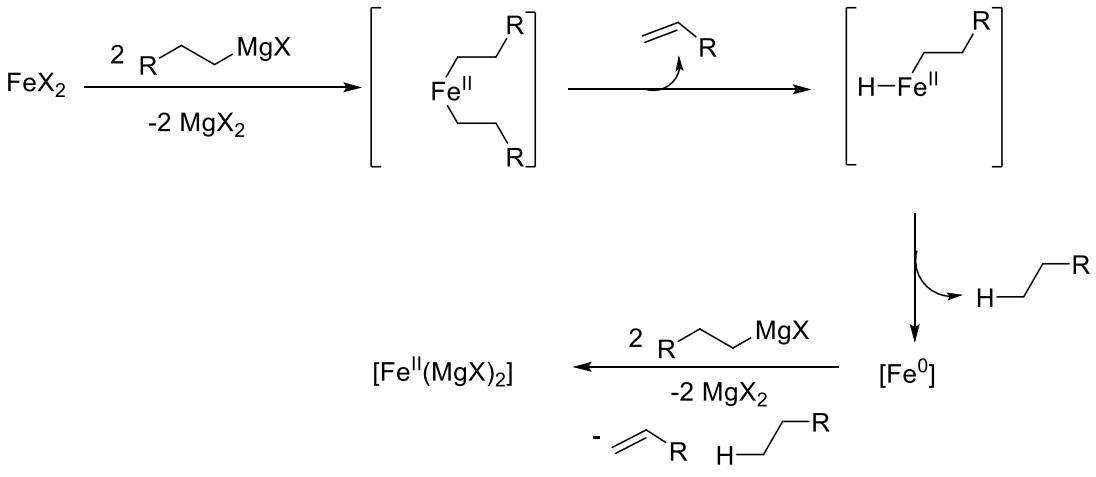

Scheme 2. 3 Formation of Fe(-II) species

More evidence of the relevance of the Fe(-II) ferrate complex was provided when Fürstner reported the isolation of a [Li(TMEDA)]$_2$[Fe(C$_2$H$_4$)$_4$] as an analogue to the [Fe(MgX)$_2$] complex. This ferrate was used successfully in the coupling between aryl halides and alkyl Grignard reagents and alkyl halides with aryl Grignards, supporting the possibility of Fe(-II) having a relevant role in the catalytic cycle (Scheme 2.4).

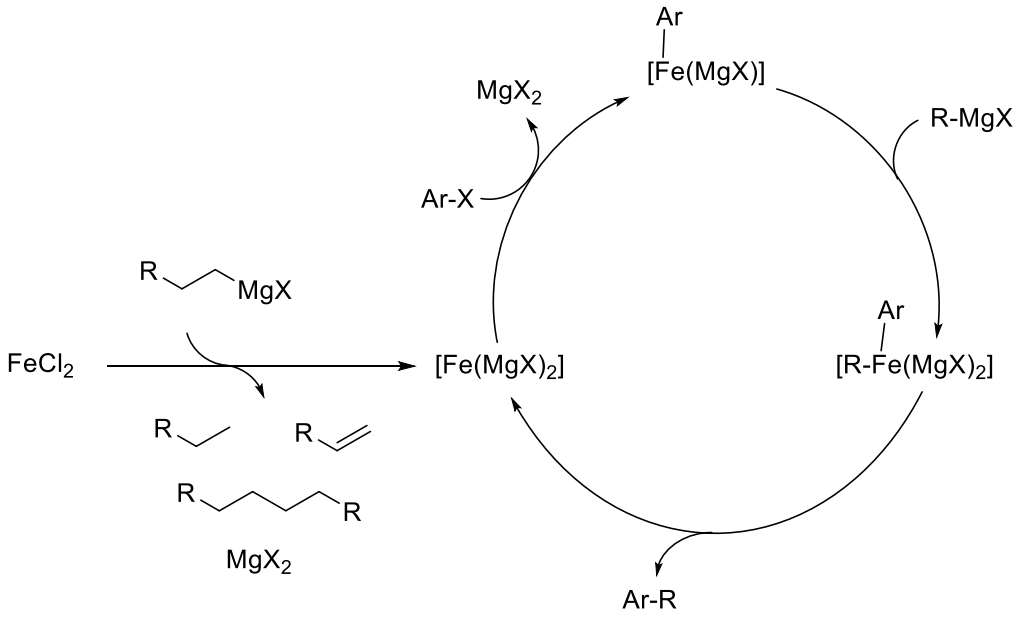

Scheme 2. 4 Fe(-II/0) Mechanism proposed by Fürstner

Norrby and co-workers reported studies of the iron-catalysed cross-coupling between aryl chlorides and alkyl Grignard reagents.[110] They monitored the effect of incremental amounts of octylMgBr with a fixed amount of aryl chloride, quantifying the starting material, coupling product and the side product octane at the end of the reaction. They found three phases in the reaction: an initiation phase where the iron salt is reduced, a second phase in which the cross-coupling takes place, and a deactivating phase. A Hammett study was performed using different substituted electrophilic partners. This study displayed that the reaction is accelerated with electron-withdrawing groups in the electrophile, obtaining an ρ= +3.8, which indicates that a negative charge is built upon the aromatic ring during the transition state of the oxidative addition. Two possibilities were suggested, one where the catalytic cycle proposed by Kochi is operative, and another where the transmetallation occurs prior to the oxidative addition followed by the reductive elimination of the product (Scheme 2.5).

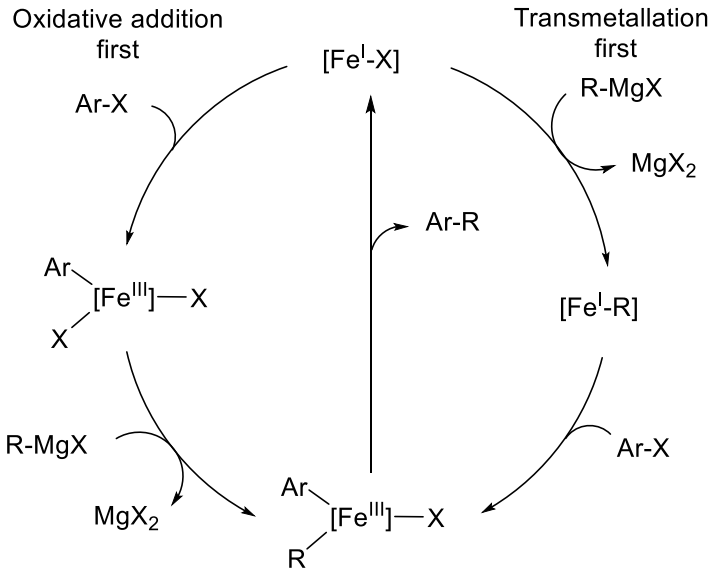

Scheme 2. 5 Pathways proposed by Norrby

Computational studies by Norrby were conducted where four active catalysts were studied, with each of these species having an oxidation state of Fe(-II) through Fe(I). The study was focused on the reductive elimination reaction's free energies, which is a shared step in both pathways. In the presence of Fe(-II) and Fe(-I), high endergonic energies where calculated, meaning that the oxidation states are thermodynamically unfavourable. Studying the Fe(-II)/Fe(0) and Fe(III)/Fe(I) routes, the activation barrier for the reductive elimination (ΔG) showed a low value for the Fe(III)/Fe(I) couple, which supports the mechanism proposed in Kochi's report.[111] The role of Fe(-II) species in cross-coupling reactions reported by Fürstner was explained by Norrby as the result of a double oxidative addition between the aryl bromide and the Fe(-II), forming a $R_2Fe(II)$ species that undergoes a binuclear reductive elimination with another Fe(II) salt, releasing a Fe(I) species (Scheme 2.6). The computational study could not discriminate between the oxidative addition and the transmetallation pathways because the DFT calculations showed the two routes were very close in energies. It was suggested that an excess of one of the substrates favours one pathway over the other, with the oxidative addition being the rate-limiting step in both cases.

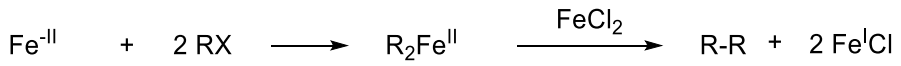

Scheme 2. 6 Fe(-II) reactivity with aryl halides proposed by Norrby.

Norrby and co-workers reported a Hammett study for the cross-coupling of *p*-substituted aryl Grignard reagents and cyclohexyl bromide.[112] A small correlation between the relative rates and the σ values of ρ=-0.5 was calculated. This value suggests that Grignard reagents that possess an electron-withdrawing substituent are less active in cross-coupling due to the increase of positive character in the transition state. The small correlation was explained proposing that two different mechanisms could be operating depending on the nucleophilicity of the Grignard reagents. A computational study suggested that instead of a standard oxidative addition, an atom transfer process could be operating.[113]

Bauer and co-workers used X-ray absorption spectroscopy to elucidate the nature of the active catalyst. Mixtures of $Fe(acac)_3$ with increasing amounts of PhMgCl showed that 3 equivalents of the Grignard reagent were necessary to produce Fe(I) species. Analysis of the biphenyl product also confirmed this. [114] Extended X-ray absorption fine structure (EXAFS) showed that the structure of the Fe species were clusters of Fe(I). $[Fe(I)\text{-}Ph]_n$ species were proposed as active species instead of the [Fe(I)-X] complex suggested by Norrby. A mechanism was proposed considering these discoveries with a Fe(I)/Fe(III) system similar to the one proposed by Kochi.[6]

Jutand and co-workers investigated the mechanism of iron-catalysed aryl-aryl cross-coupling using NMR and EPR spectroscopy alongside cyclic voltammetry.[115] They obtained results pointing to a reduction of $Fe(acac)_3$ to the Fe(I) complex $[MgBr]^+[PhFe(I)(acac)]^-$ in the presence of phenylmagnesium bromide. This Fe(I) disproportionates to a Fe(II) and a Fe(0) species as a black precipitate. Reaction of $[PhFe(I)(acac)]^-$ with phenyl iodide and 2-chloropyridine showed different reactivity. PhI is reduced to give a phenyl radical that reacts with the solvent forming benzene and the complex [PhFe(II)(acac)]. This Fe(II) species does not react any further with PhI and addition of excess Grignard regenerates the Fe(I) complex. No cross-coupling product is formed under these conditions. On the other hand, using 2-

chloropyridine, the coupling product and Fe(I) complex are isolated. DFT calculation suggested an S_NAr-type oxidative addition forming a 2-Py-Fe(III) complex which reductively eliminates (Scheme 2.7).

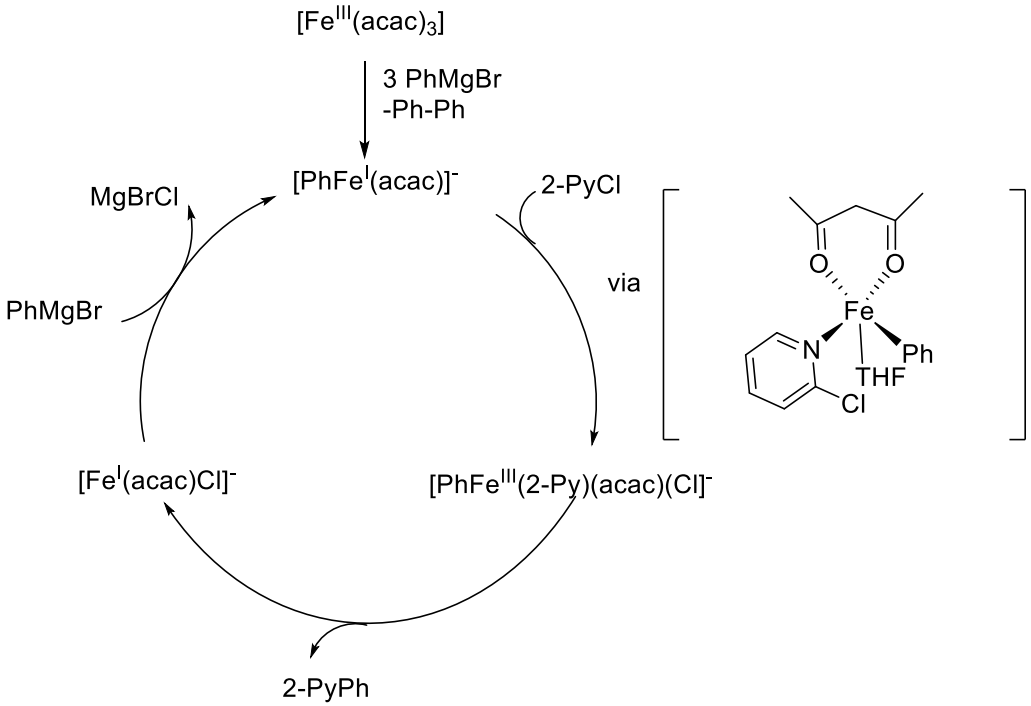

Scheme 2. 7 Reaction of Fe(I) complex with 2-chloropyridine

Nakamura used iron fluoride for the cross-coupling of aryl halides and aryl Grignard reagents in combination with an NHC ligand, obtaining good selectivity for the cross-coupling product, whereas the use of iron chloride favoured the homocoupling reaction.[71] The authors suggested that a ferrate complex $[Ph_4Fe]^-[MgX]_2^+$ is formed with iron chloride and then subsequent reductive elimination bore the homocoupling product. The fluorides on the iron centre avert the formation of the ferrate complexes, inhibiting the homocoupling reaction. A mechanism in concordance with these suggestions was proposed, a rapid reductive elimination was expected to outperform the homocoupling reaction (Scheme 2.8).

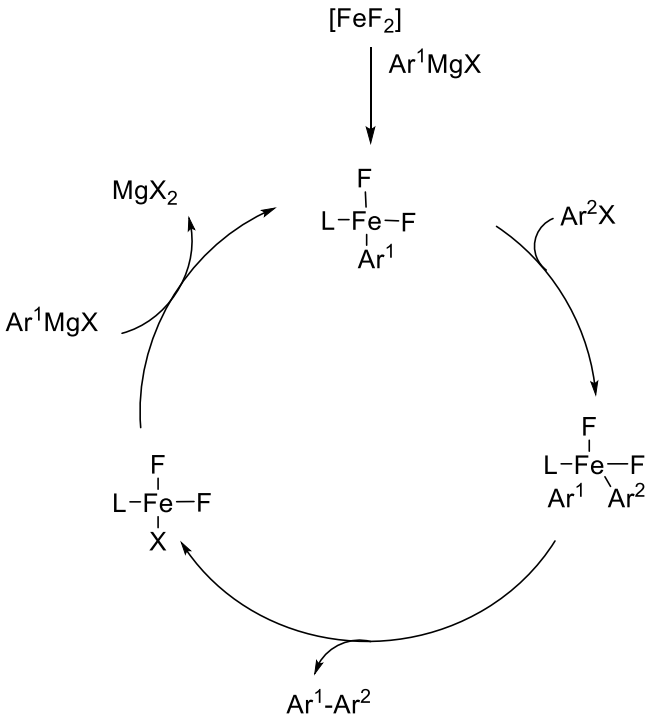

Scheme 2. 8 Aryl-aryl cross-coupling cycle suggested by Nakamura

Cárdenas studied the system $Fe(OAc)_2$/IMes HCl, in alkyl-alkyl cross-coupling. Increasing amounts of alkyl Grignard reagent were added to a solution of the catalyst, quantifying the homocoupling product. The quantity of homocoupling product stays at 0.5 mmol per 1 mmol of Fe which is in agreement with a reduction to Fe(I) (Scheme 2.9).[93]

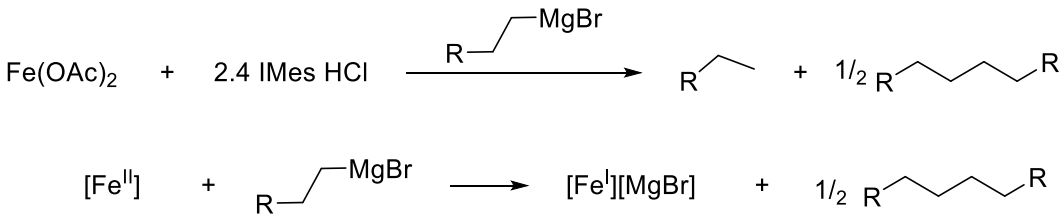

Scheme 2. 9 Formation of Fe(I) with alkyl Grignards.

2.1.1 2 Free radical mechanism of reaction.

In opposition to the different proposals of two-electron systems, there are reports with evidence for the formation of radical intermediates during iron-catalysed cross-coupling. Nakamura demonstrated that in the cross-coupling of 1-Br-4-*t*-butylcyclohexane and an aryl Grignard reagent, the same diastereomer would be produced independently of the starting configuration of the substrate, suggesting the presence of a radical intermediate.[116] In Fürstner´s work, when an optically active bromo-alkane is used as a coupling partner, complete loss of the stereo centre happens which also indicates the formation of a radical. Reactions using radical-clocks have been performed to confirm the formation of radical intermediates. In most cases, a cyclization/ring-opening takes place (Scheme 2.10).[80,89,117]

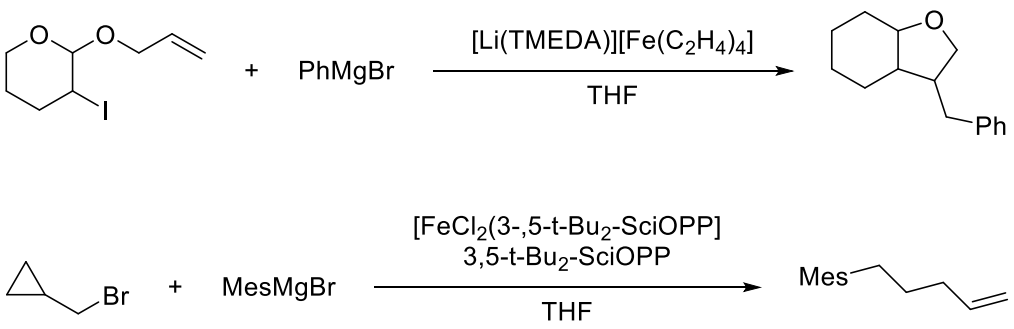

Scheme 2. 10 Radical clocks in iron-catalysed cross-coupling

The formation of radicals has been explained as the oxidative addition step being substituted by a single electron transfer. There is uncertainty over whether SET or transmetallation happens first (Scheme 2.11). Norrby proposed another explanation for the formation of radicals; who suggested an atom transfer where the halide is coordinated to the iron centre, thus releasing a radical that could recombine with the Fe(II) species to give rise to an Fe(III) species (Scheme 2.12).[118]I

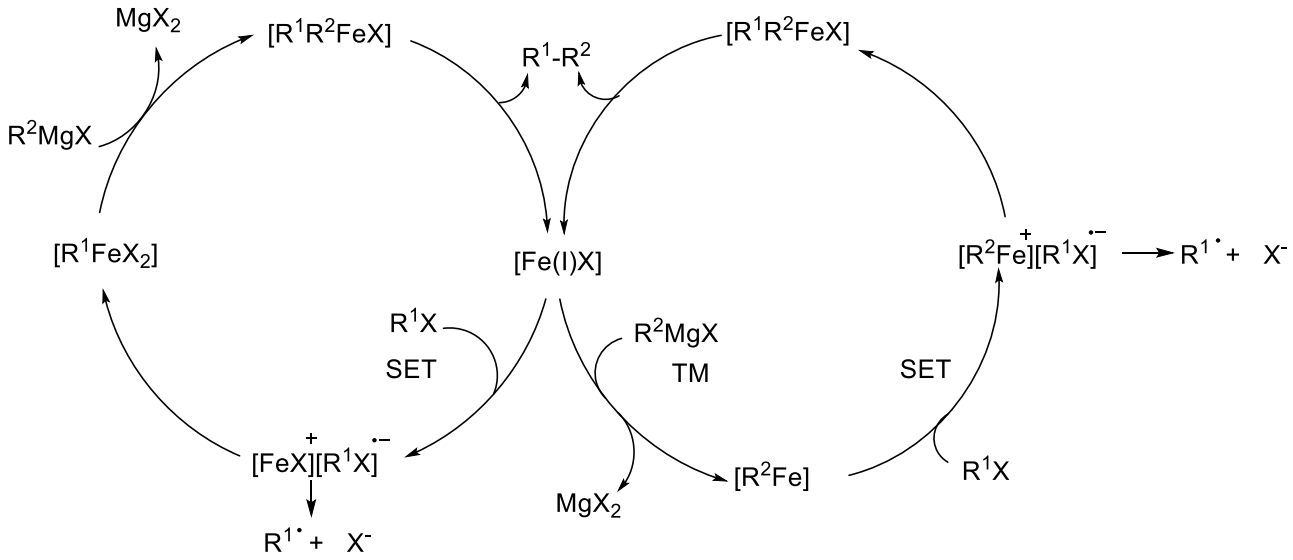

Scheme 2. 11Mechanism with radical intermediates.

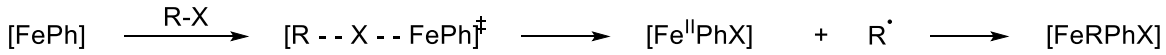

Scheme 2. 12 Atom transfer reaction

2.1.1.3 Effect of ligand in the cross-coupling reactions

One of the more critical aspects of mechanistic studies is to understand the role of the ligand in the reaction. In the case of iron-catalysed cross-coupling reactions, the precise effect of the ligand has not been clarified due to the different ligands that are used depending on the chemical nature of the substrates. A significant obstacle in this area is the fact that the nature of the ligand changes with the type of cross-coupling (Csp^3-Csp^2, Csp^2-Csp^2, Csp^3-Csp^3).

Nakamura studied the role of TMEDA in the cross-coupling of alkyl halides and aryl Grignard reagents. [(TMEDA)Fe$(Mes)_2$] was isolated in the absence of alkyl halide.[119] Addition of 1-bromooctane formed the complex (TMEDA)Fe(Mes)Br and the cross-coupling product. Radical clock experiments showed the formation of radicals and a mechanism was proposed accordingly (Scheme 2.13). This cycle proposes the formation of an alkyl radical which upon reaction with the arylated iron centre forms the cross-coupling product.

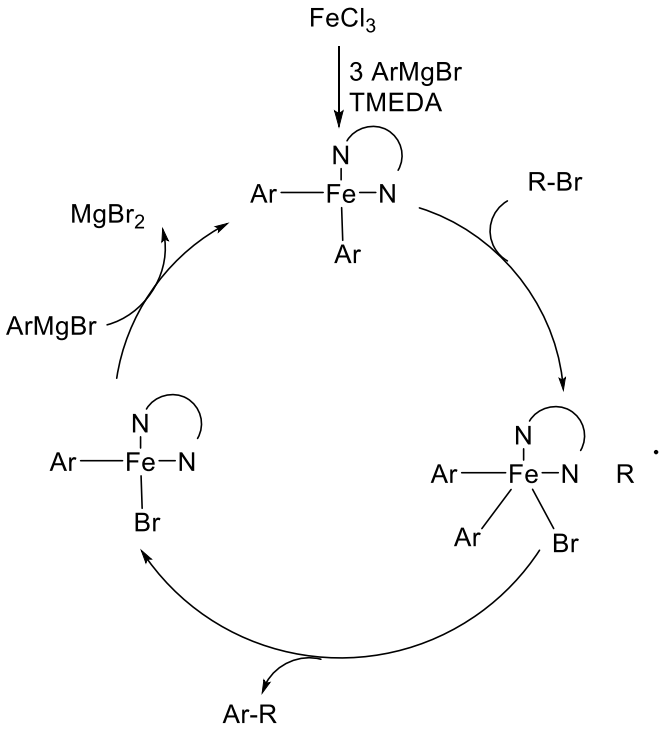

Scheme 2. 13 Mechanism proposed for the role of TMEDA

Bedford and co-workers expanded the study on TMEDA. An excess of TMEDA was employed in the presence of mesitylmagnesium bromide, emulating catalytic conditions.[82] Surprisingly the complex (TMEDA)Fe(Mes)$_2$ was not detected, and the complex [Fe(Mes)$_3$]$^-$ was identified (Scheme 2.14). Upon reaction with 1-bromooctane, the homoleptic mesityl complex produces the cross-coupling product faster than the complex studied by Nakamura. It was suggested that TMEDA is necessary as an off-cycle stabiliser, trapping iron intermediates that promote the formation of by-products.

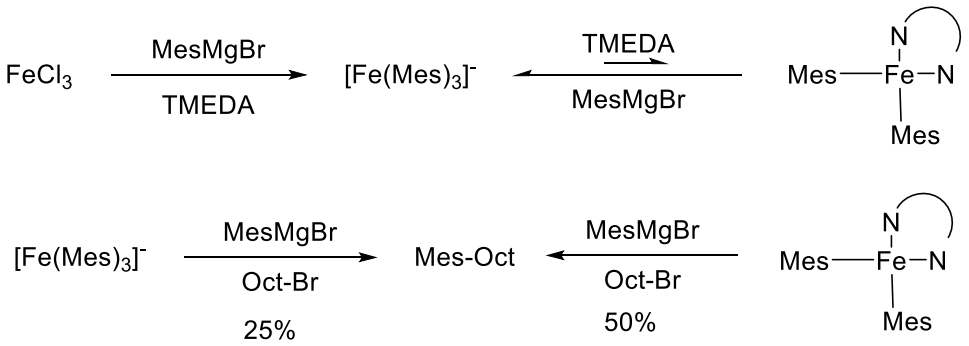

Scheme 2. 14 Reactions of MesMgBr with iron TMEDA complexes

Phosphine ligands have demonstrated great versatility as they have been used in Kumada, Negishi and Suzuki cross-coupling reactions.[120] Neidig group used both spectroscopic techniques and DFT calculations to study the complexes Fe(Mes)Br(ScioPP) and ($Fe(Mes)_2$(SciOPP).[91] Reaction between $FeCl_2$(SciOPP) and increasing amounts of mesitylmagnesium bromide where done. When 1 equiv of MesMgBr is used, Fe(Mes)Br(SciOPP) is detected but upon the addition of 2 equivalents, a mixture of $Fe(Mes)_2$(SciOPP), $[Fe(mes)_3]^-$ and Fe(Mes)Br(SciOPP) forms. If a large excess of Grignard reagent is added (20 equiv), the ate complex is detected alongside $Fe(Mes)_2$(SciOPP). These two complexes showed very different reactivity. Addition of 1-iododecane to the SciOPP complex produces mesityldecane, whereas the homoleptic complex yields a mixture of mesityldecane and decene. The differences between the chemistry of mesityl homoleptic complexes and the TMEDA system reported by Bedford can be associated with a better ability of the TMEDA to coordinate to Fe than that of the phosphine ligand. No iron Fe(I) was formed in this reaction according to EPR spectroscopy, so an Fe(II)/Fe(III) couple mechanism was hypothesised (Scheme 2.15). Nakamura and co-workers studied a Suzuki type cross-coupling using the same ligand and proposed a similar mechanism for the reaction.[103]

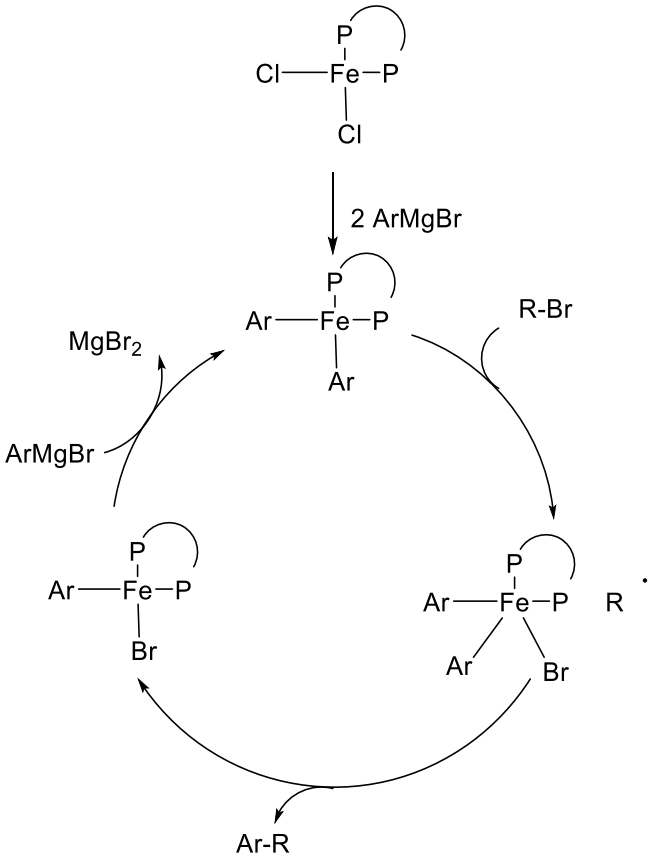

Scheme 2. 15 Mechanism for the coupling of alkyl halides with MesMgBr

Further studies by Neidig used less bulky aryl nucleophile phenylmagnesium bromide. Addition of 2 equivalents of the Grignard on a $FeCl_2$(SciOPP) complex formed the Fe(0) complex [Fe(η^6-biphenyl)SciOPP]].[121] This complex reacted very slowly with chloro-cycloheptane, thus not being kinetically relevant. Complexes [Fe(Ph)X(SciOPP)] and [$Fe(Ph)_2$(SciOPP)] were isolated; the former showed good activity with alkyl halides, resulting in cross-coupling product with low concentrations of the β–elimination product, and the latter gave an equimolar mixture of these products. The complex [Fe(Ph)X(SciOPP)] was proposed as the active catalytic species in the reaction between aryl Grignard reagents and alkyl halides.

N-heterocyclic carbene ligands have also been subject to mechanistic studies. Deng and co-workers studied IMes complexes $(IMes)_2FePh_2$ prepared from $FeCl_2$, phenylmagnesium bromide and IMes.[122] Stoichiometric amounts of alkyl halide added to a solution of this

complex resulted in excellent yields of the cross-coupling product. Radical clock experiments with cyclopropylmethyl bromide showed the opening of the ring, interpreted as a possible radical mechanism. It was found that the main iron complex in solution was $(IMes)_2FePhX$. It was hypothesised that after a single-electron transfer from the Fe(II) complex to the alkyl halide, the formed radical interacts with a Fe centre. Under catalytic conditions, the reaction produced alkanes and alkenes, which could be due to the formation of $[IMes]_2FeAr_3]^-$ or $[FeAr_4]^-$ attributed to the excess of Grignard reagent in the reaction mixture. Studies by Tonzetich showed the radical trap BHT completely inhibited the coupling between cyclohexyl bromide and the Grignard reagent,[2] increasing the evidence for a free radical mechanism.

2.1.2 Previous developments of iron catalysed Negishi cross-coupling reactions

Most of the mechanistic studies on iron catalysed cross-coupling are from Kumada type reactions. There are not many studies related to the use of zinc reagents or boron compounds, but the studies done with Grignard reagents serve as a good foundation for understanding the reactions using nucleophilic partners of different nature.

Early studies by Bedford and co-workers on the Negishi cross-coupling reaction examined a range of amines and phosphine ligands. It was found that the best results were obtained using diphosphine ligands. From the range of phosphines studied, 1,2-bis(diphenylphosphino)Benzene (dpbz) showed the best performance. (Table 2. 1 Ligand screen for the cross-coupling of a benzyl halide and a preformed diarylzinc).[97]

Table 2. 1 Ligand screen for the cross-coupling of a benzyl halide and a preformed diarylzinc

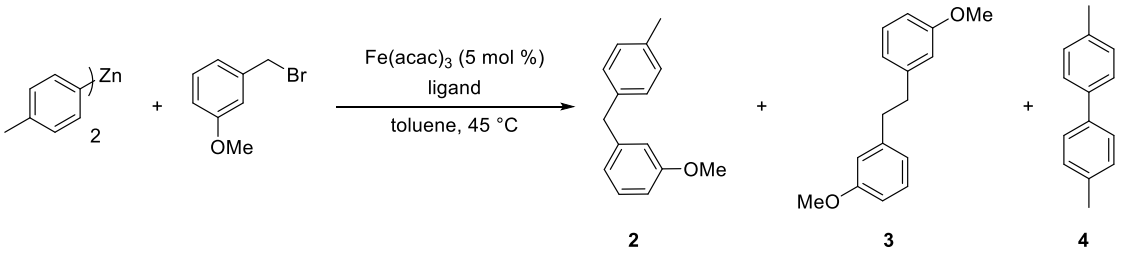

2 3 4

Entry	Ligand (equivalents)	Yield of **5** (%)	Yield of **6** (%)	Yield of **7** (%)
1	-	0	0	0
2	-	43	7	21
3	TMEDA (1)	28	6	12
4	PCy_3 (2)	26	8	16
5	PPh_3 (2)	28	4	16
6	dppm (1)	50	5	10
7	dppe (1)	48	3	10
8	dppp (1)	69	2	6
9	dpbz (1)	79	0	12
10	dpbz (2)	80	0	10
11	dpbz (3)	91	0	10

Conditions: 3-methoxybenzylbromide (1.0 mmol), di(4-tolyl)zinc (1.0 mmol), $Fe(acac)_3$ (0.05 mmol), ligand (1-2 eq), toluene, 45 °C, 4h; [b] no $Fe(acac)_3$ added.

Preformed complexes $FeCl_2(dpbz)_2$ **(1a)**, $FeCl_2$(deppe) and $FeCl_2$(dppp), performed better than the mixture of $FeCl_2$ and the corresponding ligand. $FeCl_2(dpbz)_2$ was easy to handle and synthesise making it a good candidate for kinetic studies (Table 2.2). It was noted that the use of an extra equivalent of the ligand was necessary for the complexes $FeCl_2$(dppe) and $FeCl_2$(dppp) to achieve a performance comparable to the complex $FeCl_2(dpbz)_2$.[124]

Table 2. 2 Pre-catalyst screen in the iron-catalysed Negishi cross-coupling using different Fe complexes

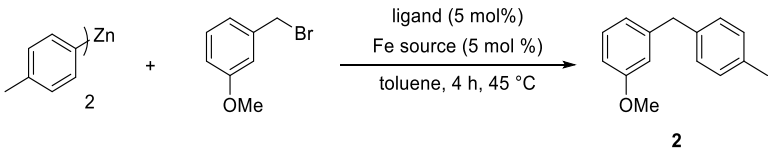

Entry	Iron source	Ligand	Yield %
1	$FeCl_2$	-	36
2	$[FeCl_2(dpbz)_2]$ (**1a**)	-	94
3	$[FeCl_2(dppe)]$	-	31
4	$[FeCl_2(dppe)]$	dppe	91
5	$[FeCl_2(dppp)]$	-	70
6	$[FeCl_2(dppp)]$	dppp	92

Conditions: 3-methoxybenzylbromide (1.0 mmol), di(4-tolyl)zinc (1.0 mmol), $Fe(acac)_3$ (0.05 mmol), ligand (0.05 mmol, if appropriate), toluene, 45 °C, 4h.

Neeve undertook a kinetic study of the iron-catalysed Negishi cross-coupling using **1a** as the pre-catalyst. The reaction was performed at 45 °C and -10 °C. The yield of both reactions was the same, but at -10 °C the reaction was slow enough to allow a study in greater detail (Figure 2.1). 4,4'- bitolyl was always formed in the reaction due to the reduction of the iron pre-catalyst to iron(I) complex. [124]

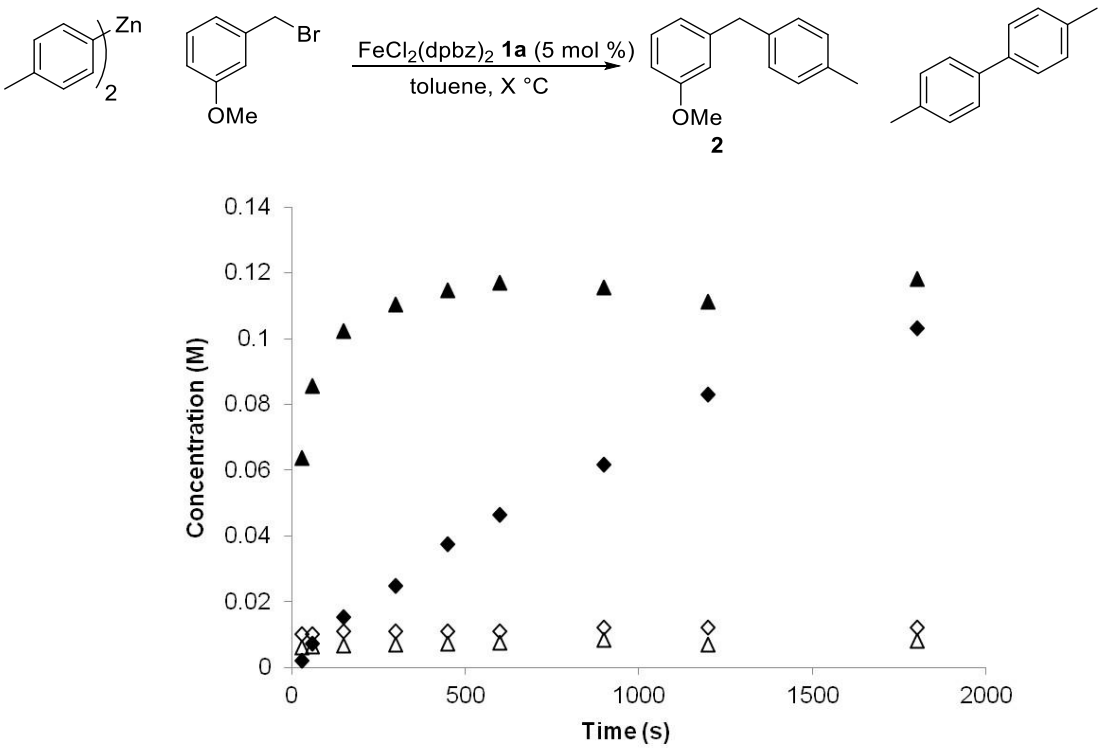

Figure 2. 1 Concentration-time profiles for the cross-coupling of 3-methoxybenzyl bromide and di(4-tolyl)zinc catalysed by $FeCl_2(dpbz)_2$ at the specified temperature; Cross-coupled product at 45 °C (▲), Cross-coupled product at –10 °C (♦), 4,4'-bitolyl at 45 °C (Δ), 4,4'-bitolyl at –10 °C.

A kinetic analysis at -10 °C was performed to get the order of reaction of the different compounds involved in the reaction. The empirical rate law for the standard iron-catalysed Negishi reaction established by Neeve is shown in Figure 2. 2 The empirical rate law for the standard iron-catalysed Negishi reaction as established by Neeve. It is shown a second order dependence on the concentration of precatalyst, first order in benzyl bromide and ditolyl zinc and zero order dependence on the ligand. [124]

$$r = -\frac{d[prod]}{dt} = k[\mathrm{FeCl_2(dpbz)_2}]^{1.9(\pm 0.3)}[\mathrm{ditolylzinc}]^{1.3(\pm 0.1)}[\mathrm{BnBr}]^{1.15(\pm 0.1)}[\mathrm{dpbz}]^{0.1(\pm 0.1)}$$

Figure 2. 2 The empirical rate law for the standard iron-catalysed Negishi reaction as established by Neeve.

It was suggested that the second order dependence in the pre-catalyst was due to a bimolecular process where two Fe species react with each other. Due to the characteristics of products and previous studies on the mechanism of the reaction, a feasible option is the bimolecular reductive elimination of two different iron species (Scheme 2.16).

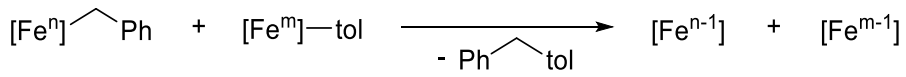

Scheme 2. 16 Second order dependence on the iron pre-catalyst

2.1.3 Oxidation states of iron catalyst in cross-coupling

Studies on the Negishi cross-coupling have shown the transformation of iron(II) or iron(III) pre-catalyst into new species under the conditions of reaction. A preliminary qualitative sign of chemical change is the change in colour observed from yellow to red when an iron salt (irrespective of its oxidation state) is mixed with the appropriate ligand and a nucleophile reagent like a Grignard reagent or arylzinc reagent, the reaction mixtures consistently became deep red (Figure 2.3). Fe(II) solutions have a light-yellow colour, and in the absence of ligand, the addition of reducing agents results in the formation of black suspensions of iron (0).

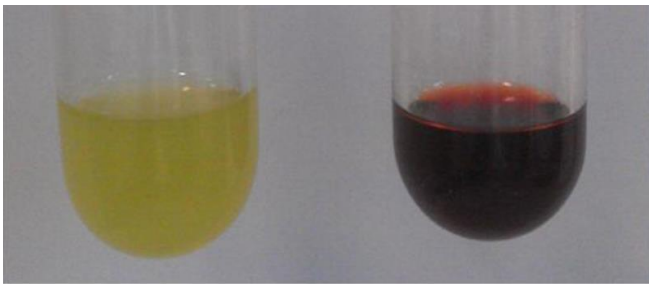

Figure 2. 3 $FeCl_2(dpbz)_2$ pre-catalyst suspension in toluene (left); solution of pre-catalyst after addition of di-p-tolyl zinc (right)

Neeve quantified the formation of 4,4'-bitolyl at a range of temperatures in the reaction of **1a** and di(4-tolyl)zinc. It was concluded that a reduction to Fe(I) happened very fast, and it was hypothesised that reduction to lower oxidation states could happen but at slower rates.

After 20 minutes of reaction, reactions run at 45 °C had produced enough bitolyl to correlate an average oxidation state of (-II) on the Fe centre. Cross-coupling reactions at this temperature are complete within 90 seconds, discarding lower oxidation states as the active catalysts. Comparing the time it takes to produce these low valent complexes with the time it takes the cross-coupling reaction to reach completion, it was found that the speed of formation of cross-coupling product matched the reduction to Fe(I). These results are strong evidence to suggest the hypothesis that Fe(I) is the lowest relevant oxidation state in the reaction.

Bedford and Huwe previously found that the species $[Fe(dpbz)_2]^+$ and $[Fe(4\text{-tolyl})(dpbz)_2]$ were present in the reaction mixtures of this reaction using ESI mass spectrometry (Figure 2.4). Later Cartes isolated the sensitive iron(I) complex with a tolyl moiety. The trigonal bipyramidal complex $Fe(4\text{-tolyl})(dpbz)_2$ (**5**) was found to be a low-spin d^7 iron(I) complex due to its 1.8 μ_B magnetic moment (Scheme 2.17).

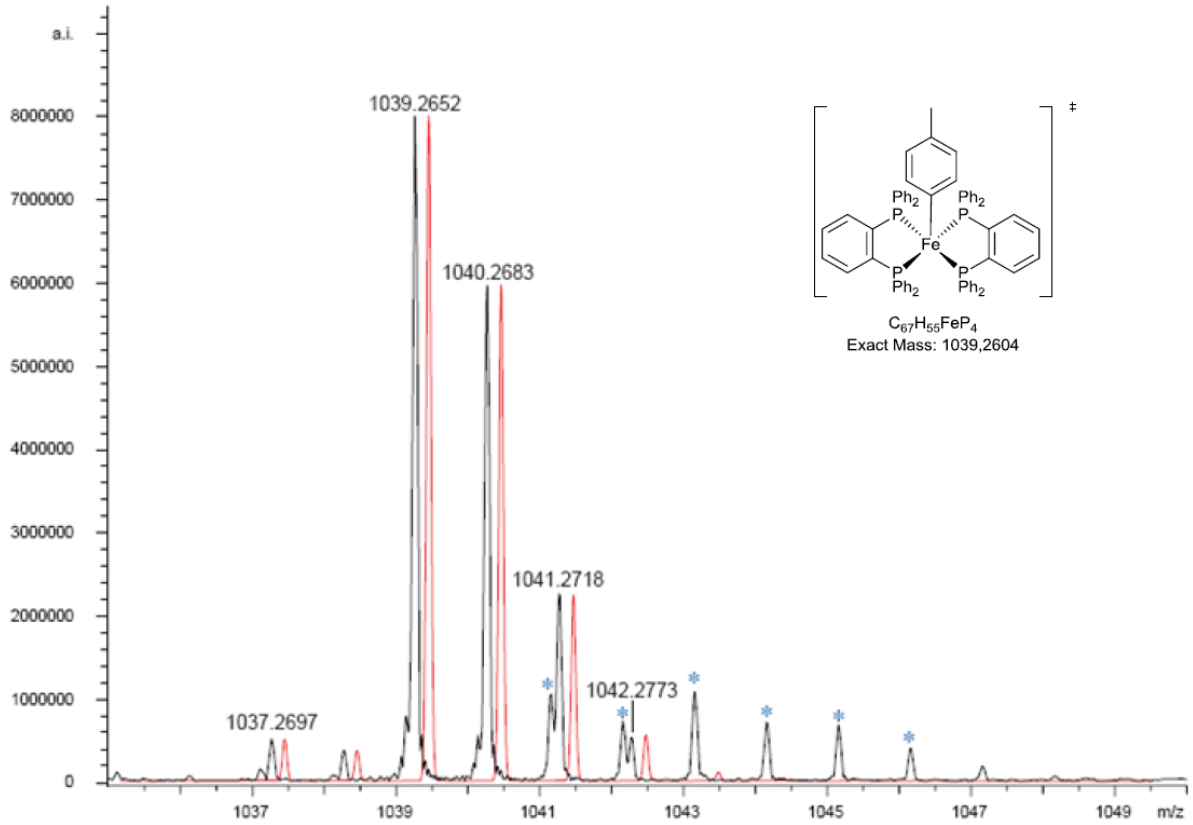

Figure 2. 4 ESI-MS obtained by Michael Huwe from a mixture of $FeCl_2(dpbz)_2$ and 2 equivalents of ditolylzinc. Red trace marks the calculated isotope distribution for $[Fe(tol)(dpbz)^{2+}$

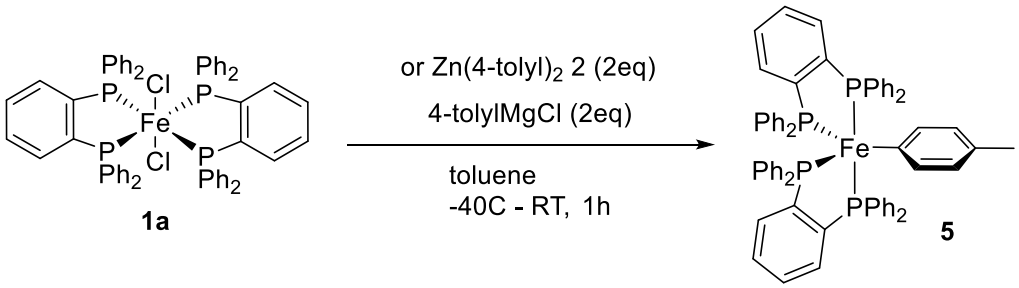

Scheme 2. 17 Synthesis of the complex $Fe(4\text{-tolyl})(dpbz)_2$ by Cartes

The electron paramagnetic resonance (EPR) spectrum of **5** was recorded by Gower (Figure 2.5). The spectrum of this compound at room temperature showed that a single electron was coupling with two different pairs of phosphorus atoms of which two are identified as equatorial and two axial. As a result of this, it is rationalised that at this temperature the trigonal bipyramidal structure was maintained.[125]

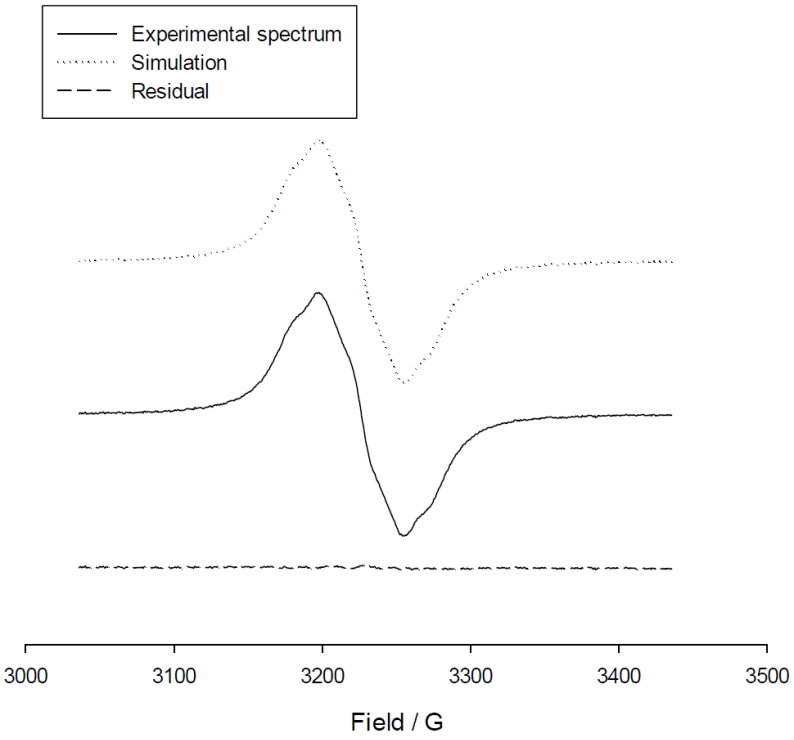

Figure 2. 5 EPR spectra of **9** measured by Nick Gower.

Nick Gower tested the activity in catalysis of this new complex in the Negishi cross-coupling, obtaining a 97% conversion, which was a slight improvement from the 94% obtained using the complex **1a**. If this Fe(I) complex is mixed with 3-methoxybenzyl bromide in the absence of Zn(4-tolyl), the cross-coupling product is obtained in low yield (12%) and the tolyl is recovered in the homo-coupled product 4,4'-bitolyl. In the presence of $Zn(4\text{-tolyl})_2$, cross-coupling product is obtained quantitatively with a little yield of homo-coupling products (Table 2.3). Interestingly, if the nucleophile used in the reaction was diethyl zinc, no formation of cross-coupling between the tolyl moiety of the iron complex and any of the cross-coupling partners product was found, suggesting that the complex **5** is not an on-cycle compound (Scheme 2.18).

Table 2. 3 Negishi cross-coupling using 3-methoxybenzyl bromide

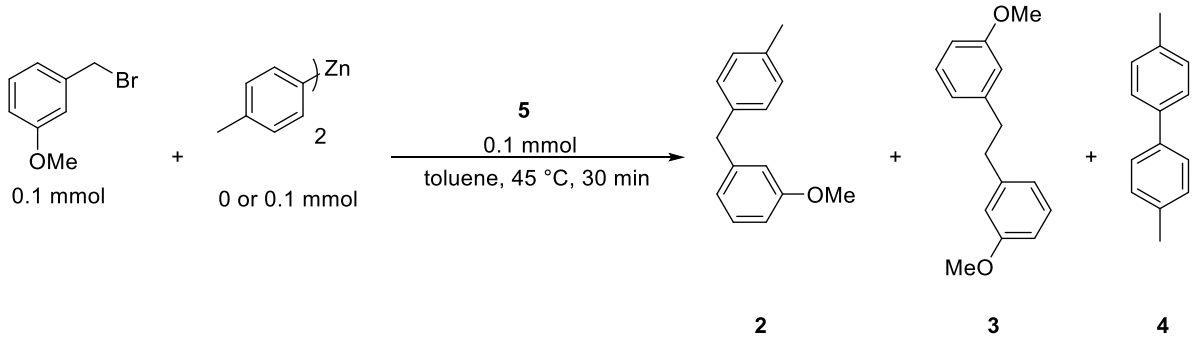

			Conversion (mmol)		
Entry	**Zn(4-tolyl)**	**5**	**2**	**3**	**4**
1	*none*	1 equiv	0.012	0.020	0.003
2	1 equiv	1 equiv	0.097	0.002	0.002

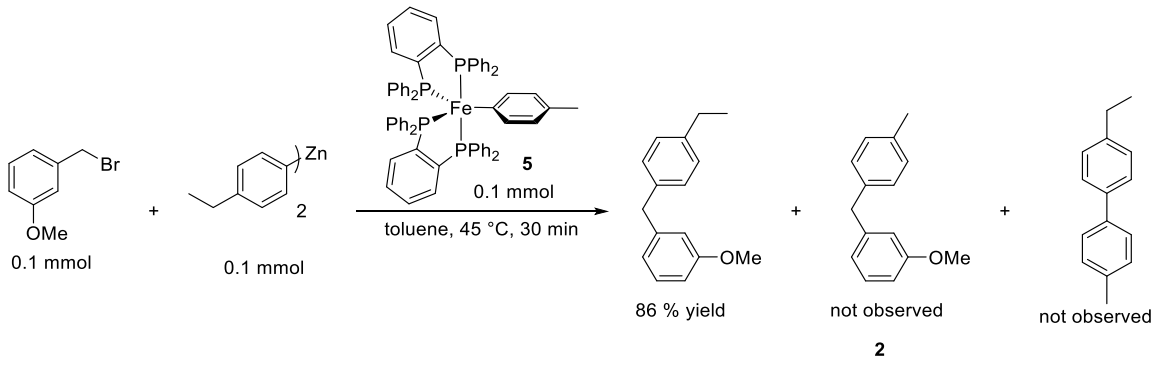

Scheme 2. 18 Reaction of **2** with MeOBnBr in the presence of di(4-ethylphenyl)zinc.

Further experiments isolated iron complexes formed from the reaction of $FeBr_2(dpbz)_2$ (**1b)** with BnMgBr. The Bedford group isolated the complex $FeBr(dpbz)_2$ (**6b**) shown to be trigonal bipyramidal by X-ray crystallography (Scheme 2.19). The analogous $FeCl(dpbz)_2$ (**6a**) was also isolated exhibiting similar characteristics to **6b**. Characterisation of **6b** was done and the magnetic susceptibility obtained with the Evans method gave a magnetic moment of 2.0 μ_B, indicating a single unpaired electron on the iron centre. The solid state magnetic moment obtained was 1.9 μ_B.

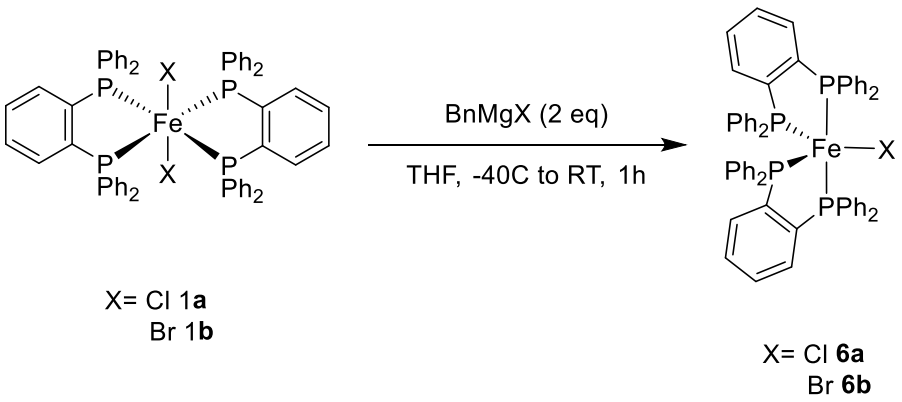

Scheme 2. 19 Synthesis of iron(I) halide complexes

Gower investigated the catalytic activity of complex **6b** in the standard Negishi reaction, having similar performance to pre-catalyst **1a.**[125] If the complexes **1a** and **6b** are mixed with stoichiometric amounts of 4-methoxybenzyl bromide, bibenzyl is formed in both cases. One possible explanation for this is the abstraction of the halide from the benzyl halide, forming

the Fe(II) dihalide and a benzyl radical which collapse with another benzyl radical (Scheme 2.20). In these studies, it was observed that the chloride has a strong halide effect, making the reaction of benzyl chloride slower and active in comparison with benzyl bromides. A similar comparison using the tolyl complex **5** showed that when using benzyl bromide, the reaction was faster than using benzyl chloride. The strength of the Fe-X bonds in **6a** and **6b**, as well as the carbon-halide bond account for this observation.[125]

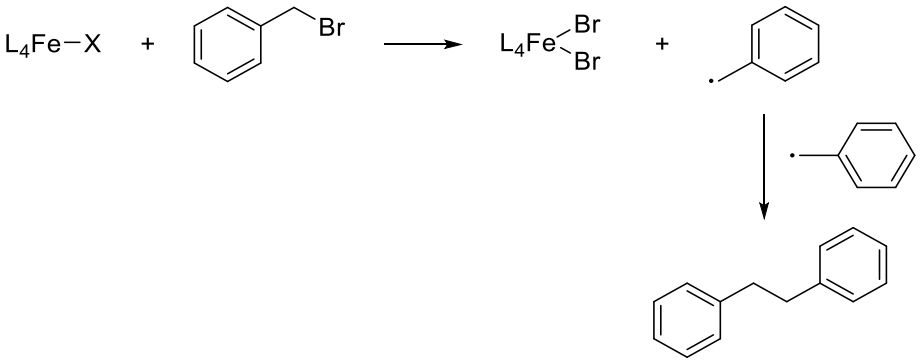

Scheme 2. 20 Formation of Bibenzyl with complex **6b**

Complexes **6a** and **6b** were tested in the cross-coupling reaction as pre-catalysts in the iron-catalysed Negishi reaction by Neeve (Figure 2.6). It was found that complex **6b** gave a reaction profile for the formation of the cross-coupled product which was identical to the standard iron(II) pre-catalyst **1a**. Complexes **5** and **6a** resulted in slower reactions. **6b** is a relevant complex in the catalytic cycle according to these results, whereas **5** and **6a** must be off-cycle intermediates due to the slow rate of reaction observed. **6a** was expected to have a better performance considering the excellent performance compared to that of the chloride containing **1a**, showed in previous experiments. The similar rates obtained using the complex **1a and 6b** is suggested to be due to a halide abstraction of benzyl bromide in the iron centre forming in situ the complex **6b**.

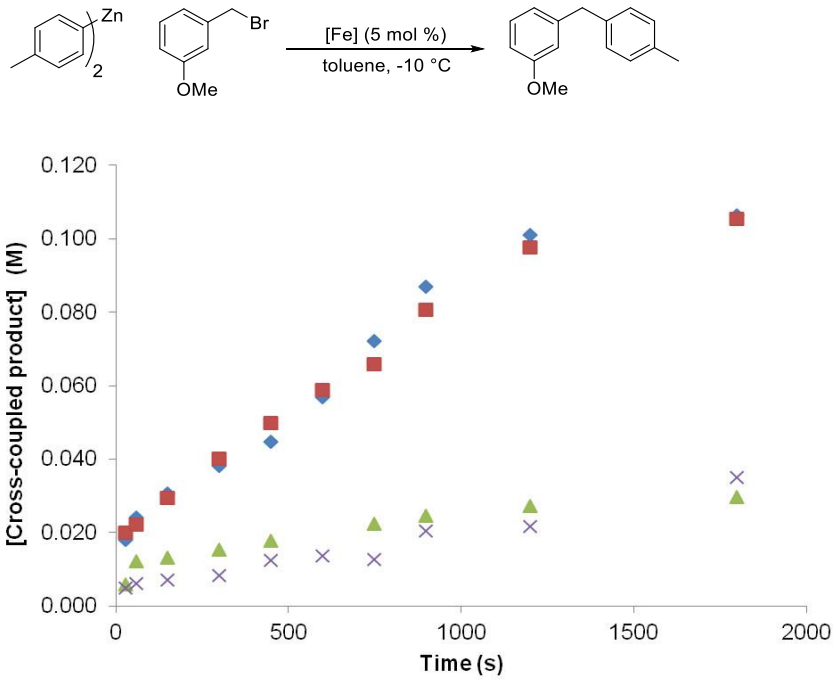

Figure 2. 6 Concentration-time profiles for cross-coupled product formation in the Negishi reaction catalysed by the specified pre-catalyst; $FeCl_2(dpbz)_2$ **1a** (♦), $FeCl(dpbz)_2$ **6a** (X), $FeBr(dpbz)_2$ **6b** (■), Fe(4-tolyl)$(dpbz)_2$ **5** (▲).

2.1.4 EPR analysis

EPR studies were performed by Coswell in collaboration with Murphy and Richards at Cardiff University. The tolyl complex was tested at different temperatures, and no change was observed, therefore, all further experiments were conducted at 140 K. The EPR spectra of complexes **6b** and **6a** were measured, and it was observed that the EPR spectra compared well with DFT calculated spectra using the B3LYP functional, showing rhombic g-tensors which are consistent with low-spin iron(I) centres (Figure 2.7).

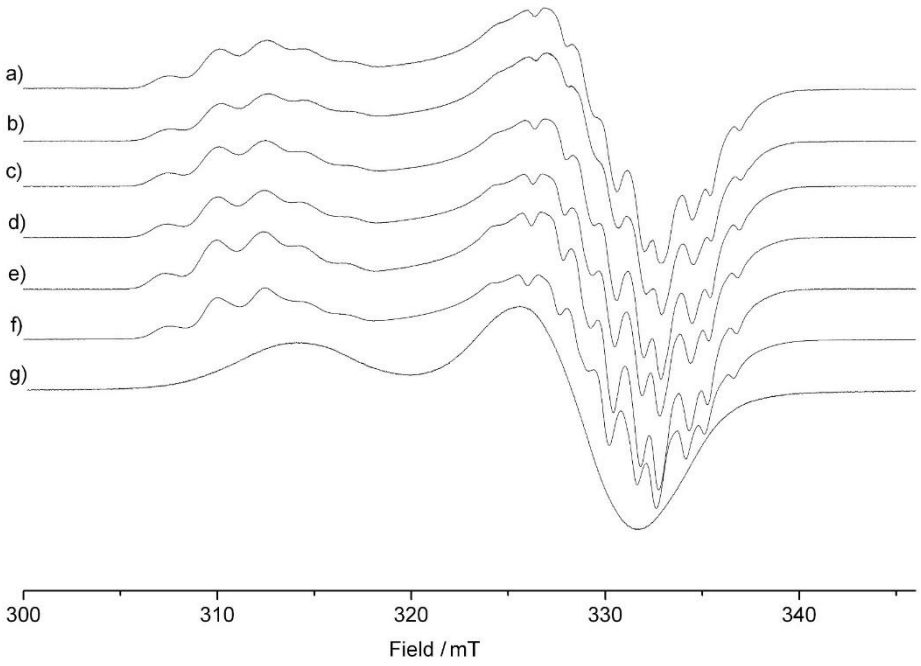

Figure 2. 7 X-band CW-EPR spectra of **5** in a THF/toluene (15 : 1) solution at the specified temperature; a) 5 K, b) 10 K, c) 20 K, d) 30 K, e) 50 K, f) 140 K, g) 220 K

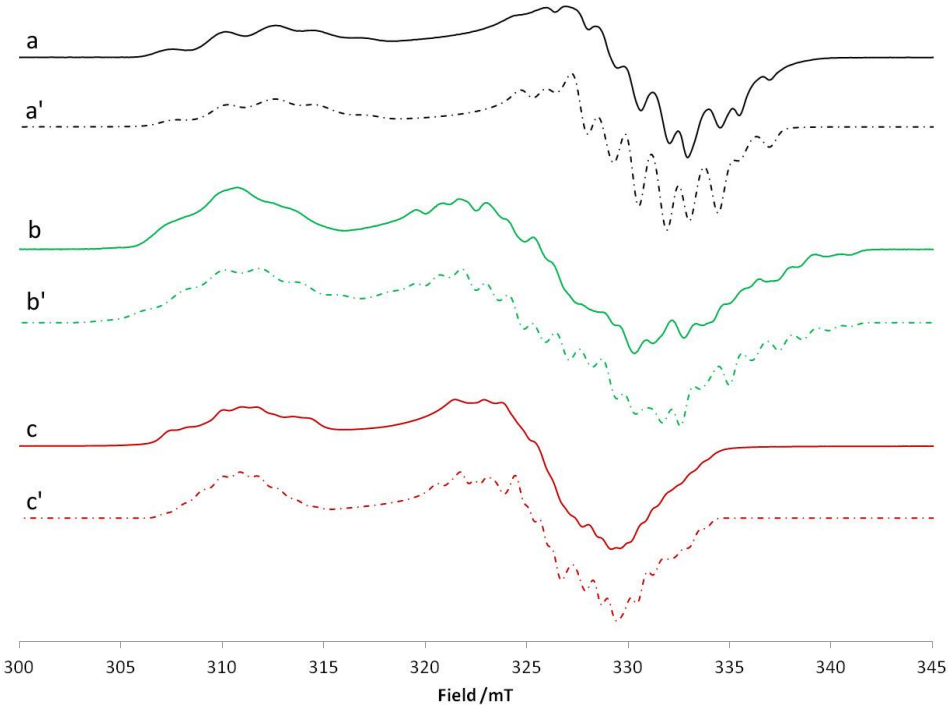

Figure 2. 8 Continuous wave X-band EPR spectra (140 K) of **5** (a), **6a** (b), and **6b** (c) recorded in a THF/toluene (15: 1) solution; corresponding simulations shown as dashed lines in a', b' and c'.

Isotropic EPR at room temperature for **6b** showed that at this temperature the complex still has a low-spin character in concordance with the magnetic moments obtained at room temperature (Figure 2.9).

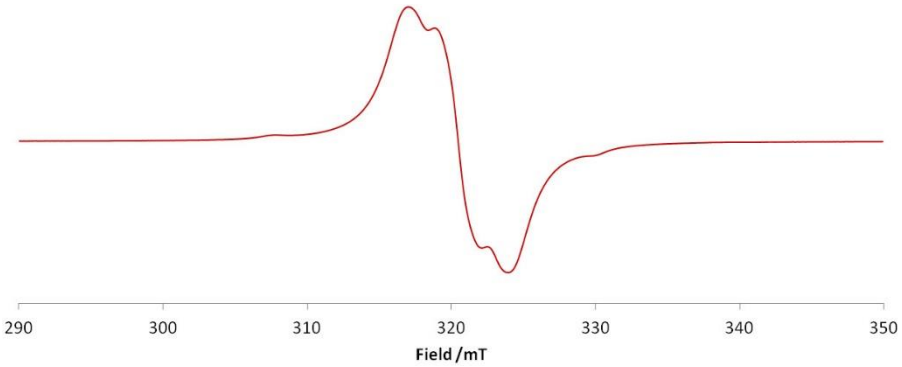

Figure 2. 9 Continuous wave X-band EPR spectrum (298 K) of 6**b.**

Further EPR experiments tested the presence of the iron(I) intermediates in the reaction mixture. Cogswell examined the distribution of iron(I) complexes formed in situ by monitoring mixtures of arylating reagents and the iron(II) complexes. Stoichiometric addition of di(4-tolyl)zinc to a solution of **1a**, produced an EPR spectrum that fitted the data recorded from the isolated complexes **6a** and **6b** (Figure 2.10). An excess of Zn(4-tolyl)$_2$ would also result in an EPR reminiscent of the one obtained from the isolated compound as well. If an excess of 4-tolylMgCl was used as arylating reagent, the resulting EPR showed that all the iron was converted to the complex **6b**. It is implied that Zn(4-tolyl)$_2$ is not nucleophilic enough to produce the iron(I) tolyl complex **5**, eliminating this complex as an off-cycle or on-cycle species candidate for the iron-catalysed Negishi cross-coupling.

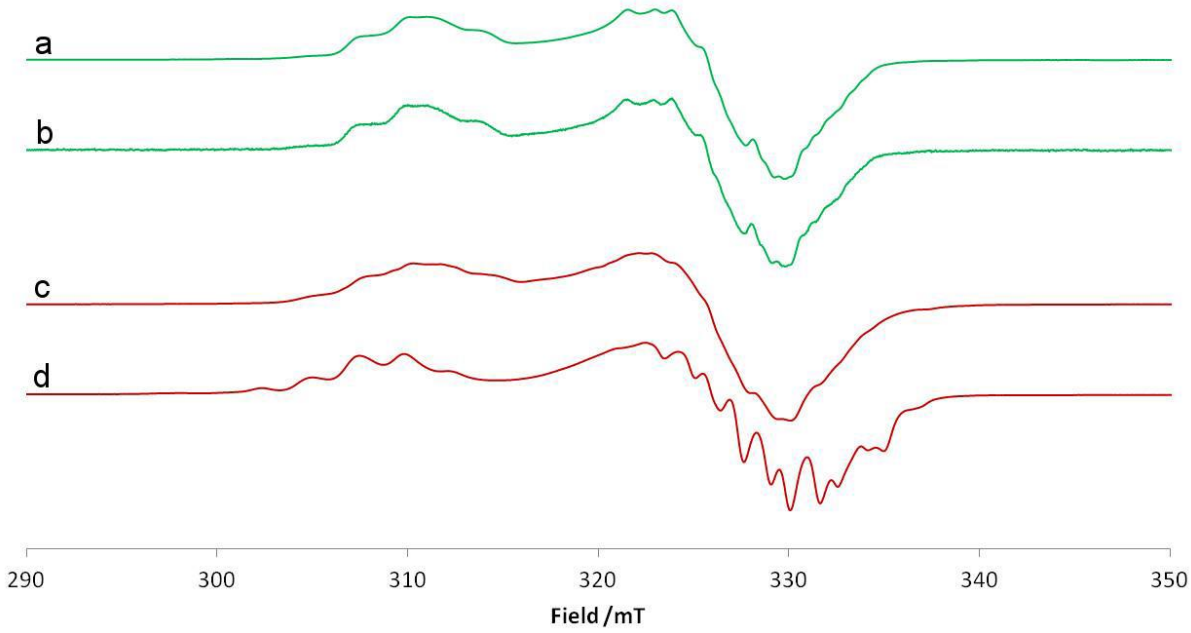

Figure 2. 10 Continuous wave X-band EPR spectra (140 K) of the reaction mixtures of **6a** with 1eq of Zinc(4-tolyl)$_2$ (a), **6a** with 20 eq of Zinc(4-tolyl)$_2$, (b), **6a** with 4-tolylMgCl (20 eq) (d).

2.2 General Considerations

The following work is a study exploring the reactivity of the iron(I) complex FeBr(dpbz)$_2$ focusing on the reaction kinetics.

In Section 2.3, UV-Vis spectroscopy is used to determine the formation of iron(I) complexes and the effect on the formation of iron(I) using different reducing mixtures. Section 2.4 covers the effects of various additives on the reaction speed, and a kinetic study of the oxidation of the iron(I) complex is conducted to get insight on the elemental steps that involve the reaction. In Section 2.5, a linear free energy relationship is undertaken with a range of substituted benzyl bromides in the oxidation of iron(I). An Eyring analysis to estimate the reaction activation parameters is presented in Section 2.6. Finally, Section 2.7 considers all the results in this chapter to propose a plausible mechanism of reaction in the Negishi cross-coupling.

2.3 Preliminary UV-Vis studies in Fe catalysed cross-coupling.

Complex **6b** was the focus of the preliminary UV-Vis studies as it was found to be present in the catalysis and shown to be catalytically competent in cross-coupling reactions, therefore, likely to be the active catalyst. To simplify the analysis, the compounds chosen were bromides, meaning that the starting materials for the Negishi coupling would consist of [FeBr(dpbz)$_2$] **6b**, 4-tolylMgBr, ZnBr$_2$ and 3-methoxybenzyl bromide or benzyl bromide.

In collaboration with Messinis, a UV-Vis spectroscopic study was conducted to examine the inorganic components in the reaction mixture of the iron-catalysed Negishi cross-coupling. The reaction was monitored using a dip-probe performing the reaction in standard conditions in a Schlenk tube. An excess of the zinc reagent was added to a solution of **1b**, and after the concentration of Fe(I) plateaus, an excess of BnBr was added (Scheme 2.21). Addition of an excess of the electrophile (180 equiv) depletes the concentration of **6b** to zero (Figure 2.11), and the formation of more Iron(I) complex is no longer detected. It is assumed that an iron(II) complex is formed upon addition of BnBr. It was suggested that the excess of electrophile consumes the complex **6b** faster than it can be generated by the action of the nucleophile, leading to the fast disappearance and absence of Fe(I) thereafter.

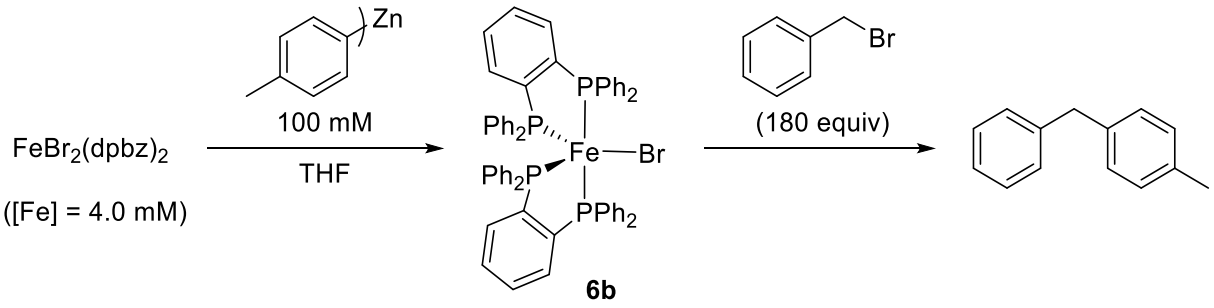

Scheme 2. 21 Monitoring of the formation of Fe(I) with an excess of Zn(4-tolyl)$_4$ and subsequent addition in excess of BnBr

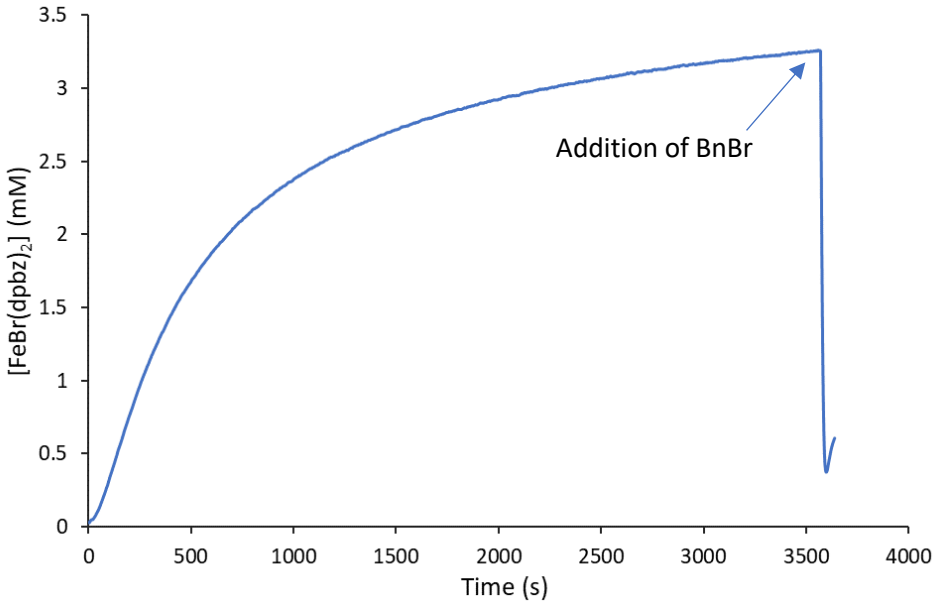

Figure 2. 11 Reaction profile for the formation of **6b** with posterior addition of BnBr

The reaction was repeated with half an equivalent of electrophile (Scheme 2.22) respect to $Zn(tolyl)_2$. It was observed that upon addition of the benzyl bromide, the concentration of **6b** lowered drastically. Once the electrophile was consumed, the concentration of Fe(I) increased again. It is important to note that this time the formation of Fe(I) was faster than the initial reduction (Figure 2.12).

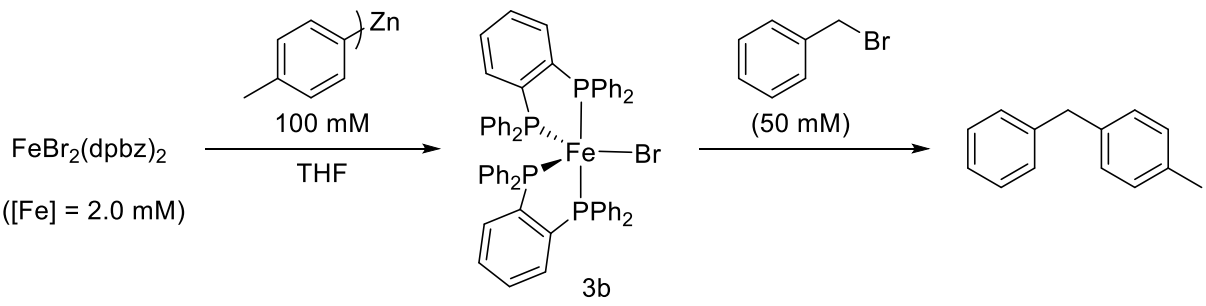

Scheme 2. 22 Formation of Fe(I) and subsequent effect of benzyl bromide (0.5 equiv).

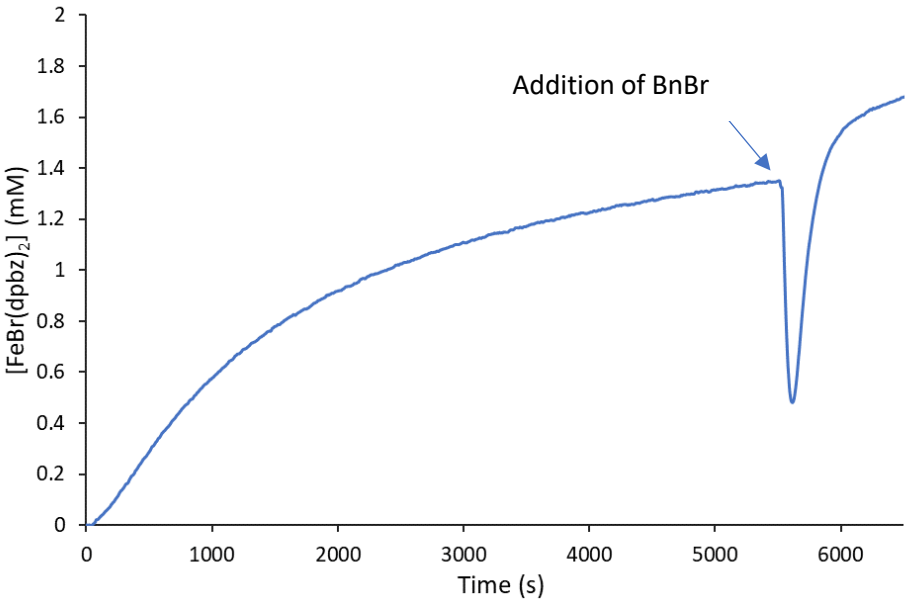

Figure 2. 12 Concentration profile of the formation of **6b** in the absence of electrophile and following addition of BnBr.

These results indicate that **6b** immediately reacts with the benzyl bromide, making the cross-coupled product, and while the reaction is happening, very little Fe(I) complex is present in the reaction mixture. Once the cross-coupling finishes the excess of arylating reagent can reduce the iron back to **6b**, suggesting that the Fe(I) complex can enter the catalytic cycle, participate, reform and enter again, the fast reaction with benzyl bromide shows that the rate of this reaction is more rapid than the production of Fe(I).

Previous work by Nunn explored the in situ formation of the complex **6b** with different reductants.[126] Grignard reagents are subject to the Schlenk equilibrium in solution; it is well known that the presence of additive or solvents can modify the equilibrium of the different species. Thus, the influence of different reducing agents towards the production of Fe(I) species **6b** from Fe(II) was tested (Figure 2.13). Diphenyl zinc mixtures were prepared via different routes, Ph_2Zn was prepared with PhLi and $ZnBr_2$; a mixture of pure Ph_2Zn and $MgBr_2$, which would provide similar concentrations of atoms to those in the reaction produced by the mix of PhMgBr and $ZnBr_2$; and finally, a mixture of pure Ph_2Zn and $ZnBr_2$ was tested. When the mixture of Ph_2Zn and $MgBr_2$ was used, a profile similar to the one obtained in the formation of 6**b** using $ZnBr_2$ and PhMgBr was obtained. On the other hand, Ph_2Zn on its own resulted in a fast formation of **6b**, but less of it was formed compared to the experiment using

$MgBr_2$ and showed a fast decomposition rate. The absence of $MgBr_2$ seems to be detrimental to the stability of the Fe(I) complex leading to the suggestion that an adduct between the Fe(I) complex and the $MgBr_2$ in solution can be formed which improves the stability of the complex (Scheme 2.23). When the mixture of Ph_2Zn and ZnBr was used, no formation of Fe(I) could be detected. A possible explanation for this behaviour is that the zinc reagent could be involved in a similar Schlenk equilibrium as the Grignard reagents leading to the lack of formation of **6b,** this equilibrium would make the zinc compound less nucleophilic, hindering the reducing power of the mixture. It has been reported that ArZnBr reagents have a poor performance in cross-coupling reaction, which is in agreement with the low reducing power shown with iron.[124]

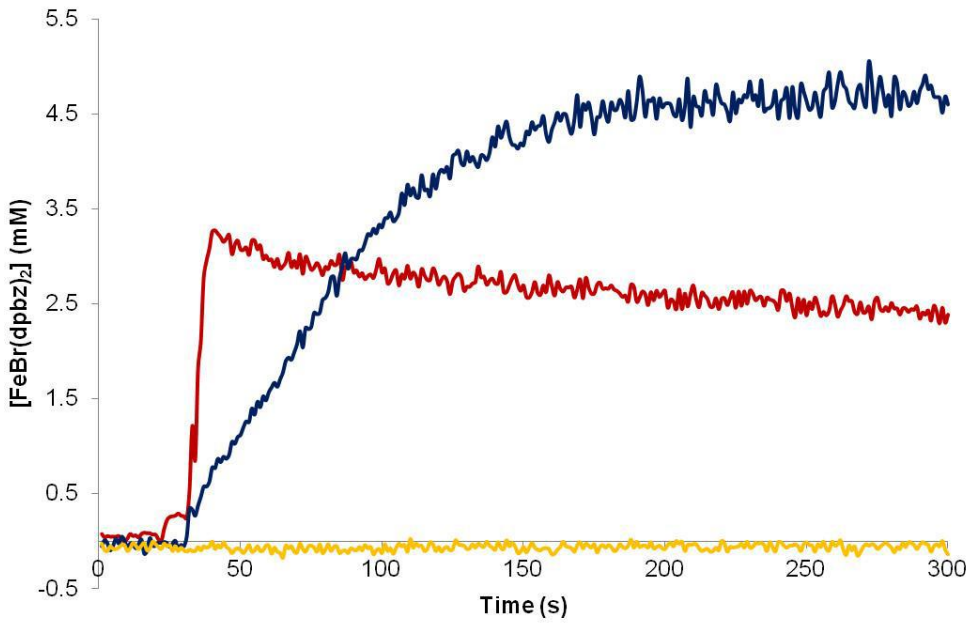

Figure 2. 13 In-situ formation of **6b** at 45 °C from **1b** (5.0 mM) with Ph_2Zn (20 eq) (–), Ph_2Zn (20 eq) + $MgBr_2$ (20 eq) (–), Ph_2Zn (20 eq) + $ZnBr_2$ (20 eq) (–). Reagents added at 25 s.

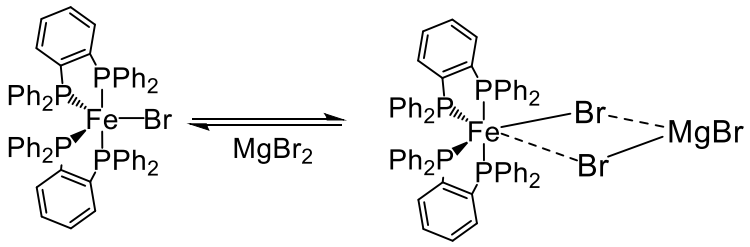

Scheme 2. 23 Putative stabilisation of **6b** with $MgBr_2$

2.4 Kinetic studies on the oxidation of Fe(I)

After the initial experiments using complex **6b**, there is enough evidence that Fe(I) species **6b** has a vital role in the cross-coupling reaction. Some of the evidence that supported this is that a mixture of Fe(II) pre-catalyst with diarylzinc reagent produces Fe(I). Tests using the Fe(I) aryl **5** suggest that it is an off-cycle intermediate due to the reaction was 5 times slower than using a Fe(II) pre-catalyst. Both Fe(I) halides showed activity in the cross-coupling, but the bromide complex performed better than the chloride, and the bromide showed an identical profile to that of the pre-catalyst **1a**. It is hypothesised that the complex **6b** is an on-cycle intermediate in iron catalysed Negishi type reactions. The first step taken for understanding the mechanism of reaction with this complex was to observe the interaction of the Fe(I) species with the electrophile, studying the oxidative addition step of benzyl bromide.

2.4.1 Preliminary UV-vis experiments of $FeBr(dpbz)_2$

The complex **6b** was examined using a stopped-flow UV-Vis spectrometer located in a glove box to observe any characteristic peak in order to have a reference in the changes in concentration throughout the catalysis and use it in kinetic experiments. The complex exhibited some transitions and an isolated peak at 742nm (Figure 2.14). This peak is strong and remote enough, making it ideal for the subsequent kinetic studies, and it is assigned to a metal-ligand transition from d_{yz} -- π^*_{dpbz}.[127]

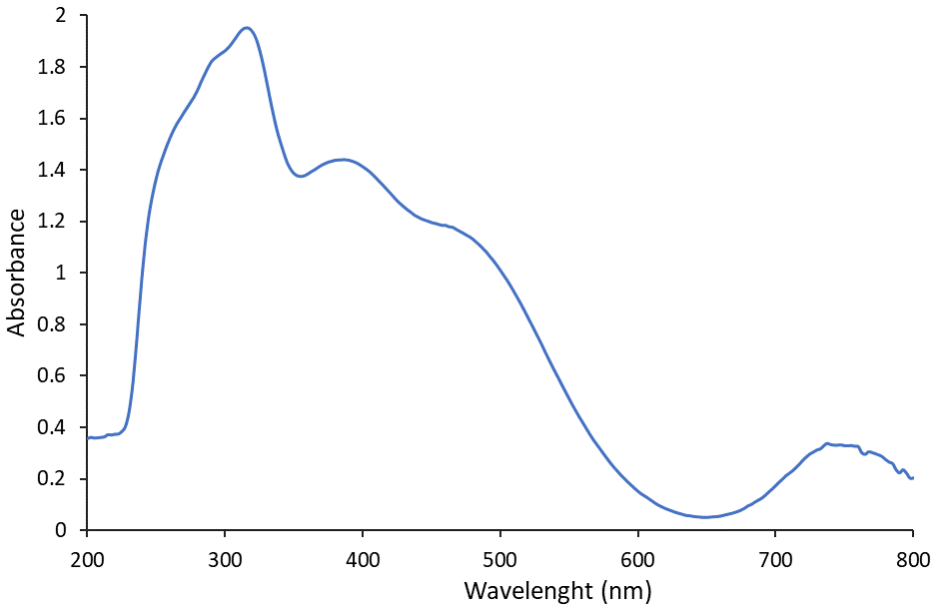

Figure 2. 14 Recorded UV-Vis spectra of [FeBr(dpbz)$_2$]

Using the peak at 742 nm, single wavelength kinetic experiments were conducted following the concentration of **6b** as indicative of the reaction progression.

The stability of complex **6b** in THF was determined in a range of concentrations at 40 °C. It was observed that the solutions were stable, not observing any variation in absorbance at the time of the observation (Figure 2.15).

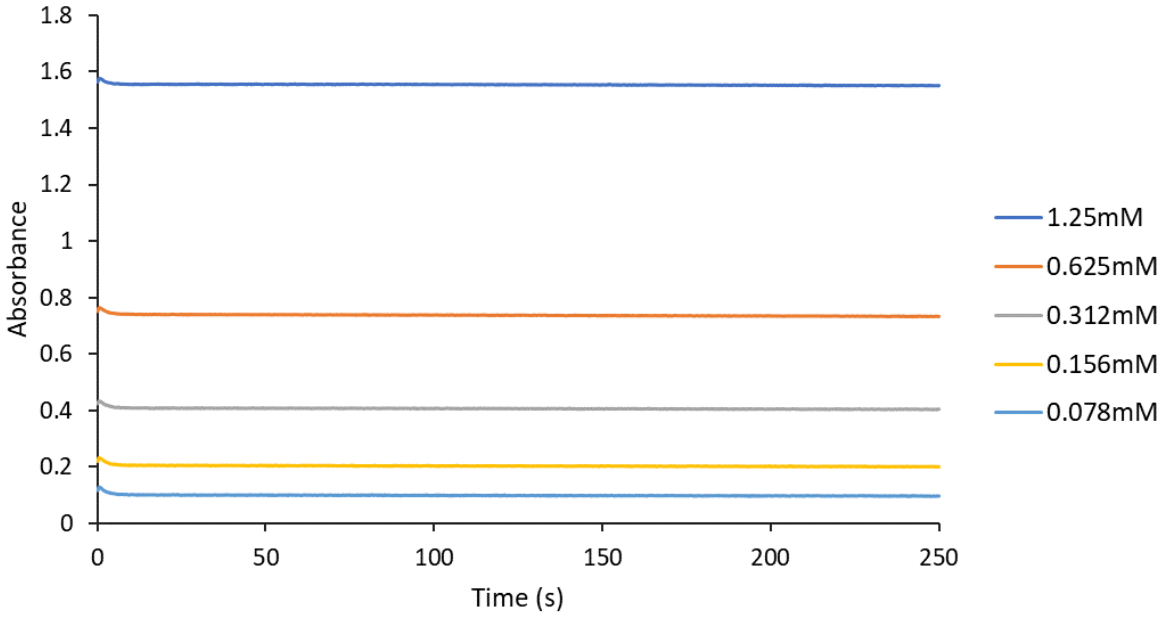

Figure 2. 15 Stability test of a range of **6b** concentrations in THF.

These data allow us to get the extinction coefficient value of 1.217 $L \cdot mol^{-1} \cdot cm^{-1}$ using the Beer-Lambert law (equation 1), where A is the absorbance, ε is the extinction coefficient, d the longitude of the cell and C the concentration of the solution.

$$A = \varepsilon dC \quad (1)$$

2.4.2 Effect of additives

It is hypothesised that complex **6b** could be the active species in the iron-catalysed cross-coupling. The effect of the different substrates was analysed to observe their effect on the complex using a set concentration of **6b** (0.625 mM) and. The reaction profiles are shown in Figure 2.16. It was observed that BnBr (10 mM) in absence of $Zn(4\text{-tolyl})_2$ produced a decrease in concentration of **6b**, this reaction finished in around 200 seconds. The addition of $Zn(4\text{-tolyl})_2$ (10 mM) did not affect the concentration of **6b**. Upon addition of a mixture of $Zn(4\text{-tolyl})_2$ (10 mM) and BnBr (10 mM), Fe(I) is consumed immediately, then a small amount of Fe(I) is formed to then gradually decays to 0. The presence of $Zn(4\text{-tolyl})_2$ must have an accelerating effect, but it was suggested that Zn^{+2} was responsible for this effect, with the nucleophilic $(4\text{-tolyl})^-$ responsible for the slight recovery of **6b.**

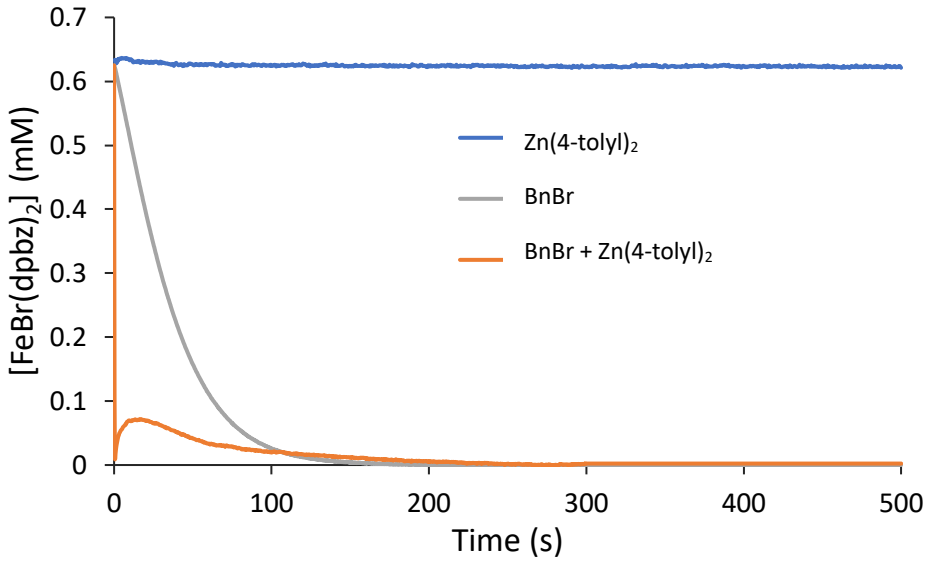

Figure 2. 16 Reaction profiles of the interaction of **6b** (0.625) with different substrates.

In order to test the influence of Zn^{+2}, some experiments were conducted. Neeve reported that cross-coupling reaction of BnBr with Zn(4-tolyl)$_2$ catalysed by [FeCl(dpbz)$_2$], after approximately 20 seconds, was 50% complete which corresponds to 12 turnovers.[124] If **6b** is an active catalyst, it is expected to react at rates similar to those of the catalysis. The reactions between **6b** and solutions of $ZnBr_2$ and BnBr were monitored. In Figure 2.17, the reaction between BnBr and **6b** seems to be too slow compared with the catalytic reaction to be relevant in catalysis, suggesting that the presence of zinc is necessary for reaching the timescales observed in the catalysis. This is supported by the reaction of BnBr in the presence of Zn(4-tolyl)$_2$ shown in Figure 2.16. In order to test this hypothesis, the effect of $ZnBr_2$ was observed in **6b** in the presence and absence of BnBr (Figure 2.17).

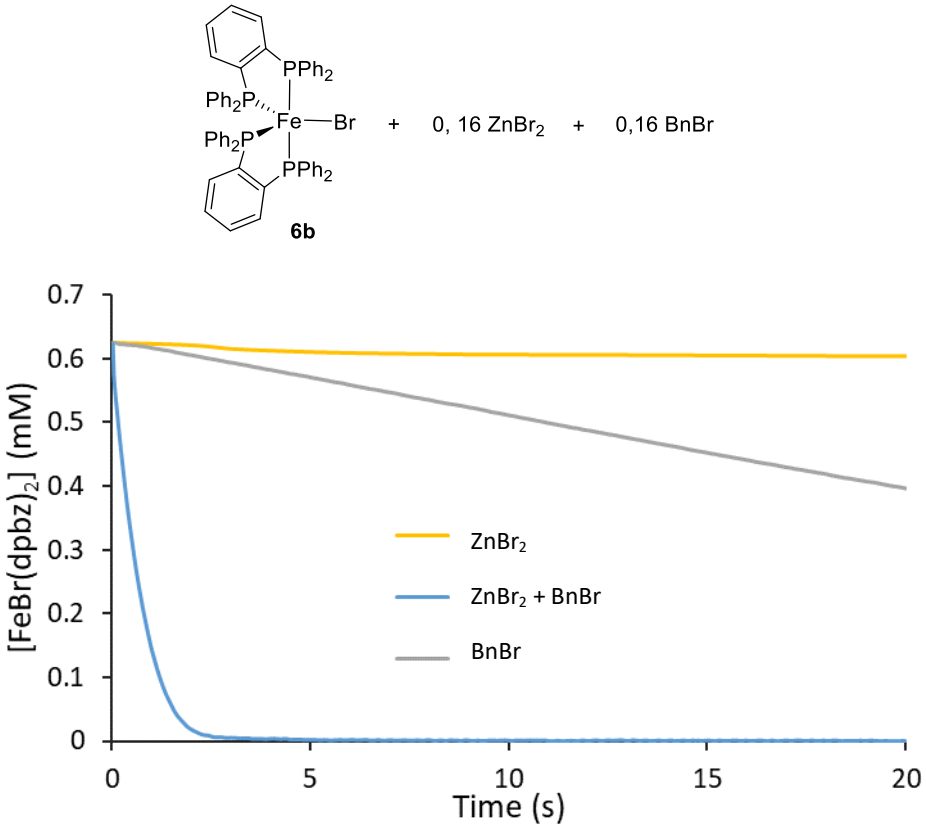

Figure 2. 17 Influence of $ZnBr_2$ (20 mM), a mixture of $ZnBr_2$ (20 mM) with BnBr (20 mM) and BnBr in the reaction between **6b** (0.625 mM)

It is evident that the presence of $ZnBr_2$ hugely accelerates the reaction. Two pathways are suggested for the accelerating effect of $ZnBr_2$ (Scheme 2.24). The first pathway involves the abstraction of a single phosphine ligand to form the monophosphine complex **7** which oxidises in the presence of benzyl bromide. The second pathway involves the abstraction of the bromide from **8** and subsequent oxidation with the benzyl bromide. The absence of a zinc species would involve kinetically unfavoured oxidation with benzyl bromide as shown in a third pathway.

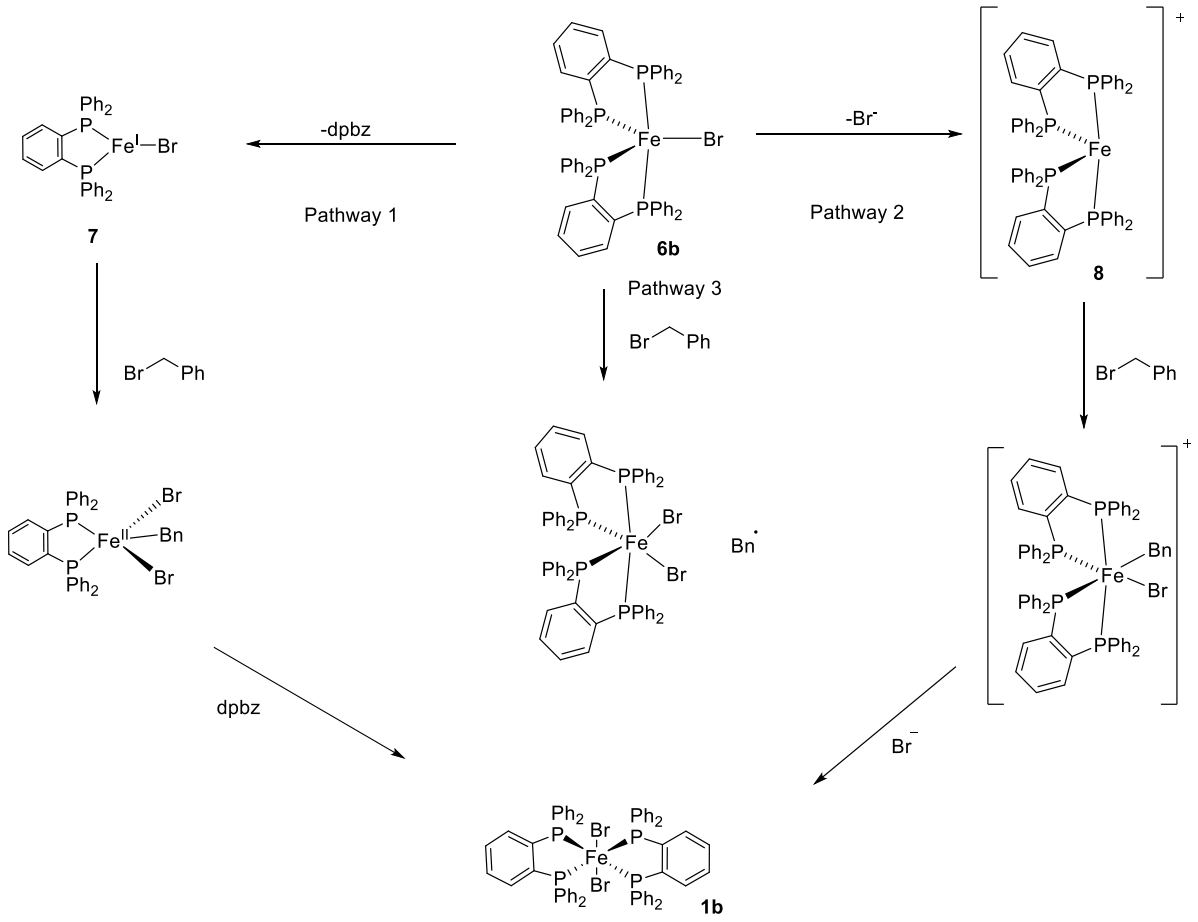

Scheme 2. 24 Suggested mechanism for the acceleration of reaction in the presence of $ZnBr_2$

In order to test the plausibility of the halide abstraction from Fe(I) as shown in pathway 2, a range of bromide salts was tested as bromide donors, expecting them to reduce the rate of reaction and inhibit oxidation. Also, $Li[B(Ar_f)_4]$ ($Ar_f = C_6H_3$-3,5-$(CF_3)_2$) was tested as a bromide abstractor.

The effect of different concentrations of zinc bromide in the absence of BnBr was tested. It was expected that, as the concentration of $ZnBr_2$ increases, the decay of **6b** would be accelerated due to Zinc´s Lewis acid character, abstracting a bromide from the metal complex, and thus accelerating the decomposition of **6b**. Surprisingly, as the concentration of zinc salt increased, the rate of decay was reduced, although the concentration of Fe(I) still fell at a faster rate than in the complete absence of $ZnBr_2$ (Figure 2.18). It is suggested that in the absence of BnBr, the $ZnBr_2$ acts as a Lewis base, forming the adduct **9** which slows the decay of Fe(I) (Scheme 2.25).

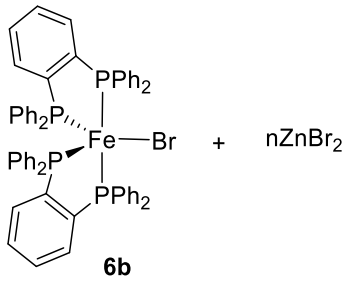

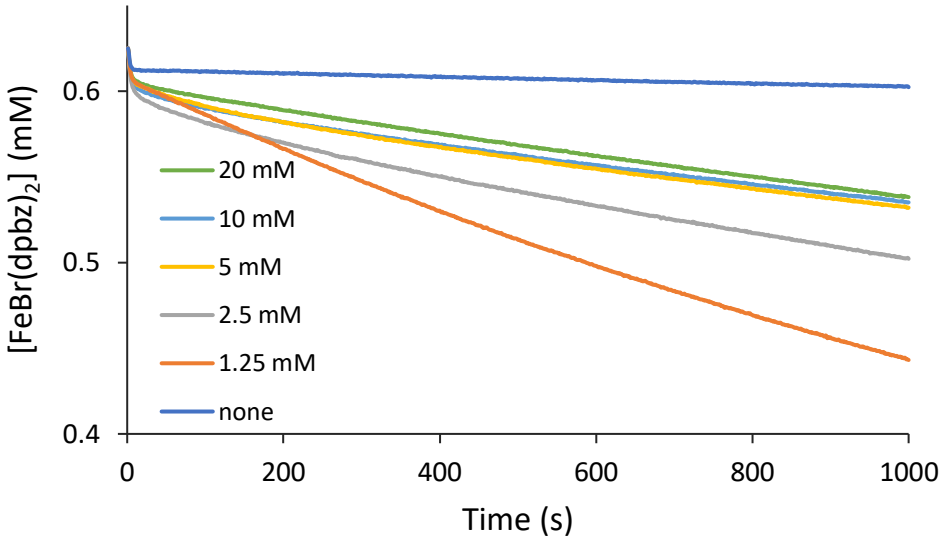

Figure 2. 18 Reaction of $[FeBr(dpbz)_2]$ (0.625 mM) with a range of $ZnBr_2$ concentrations

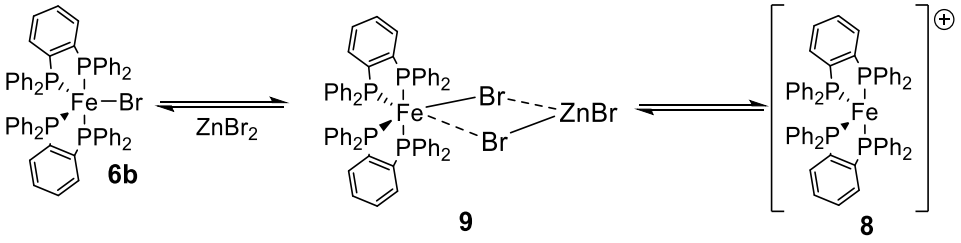

Scheme 2. 25 Proposed equilibrium between **6b** and $ZnBr_2$ in the absence of BnBr.

A range of $ZnBr_2$ concentrations was tested in the presence of BnBr to observe if the rate of reaction with Fe(I) was different from the results shown in absence of the electrophile. Contrasting with the previous result, as the concentration of $ZnBr_2$ increases the rate of reaction is accelerated (Figure 2.19). An explanation for this could be that the reaction of BnBr with the dehalogenated Fe(I) species **8** which has donated its bromide ion to the zinc is faster than the equilibria between **6b, 9** and **8** (Scheme 2.26). Also, zinc could have an accelerating effect in the oxidative addition of BnBr to **6b.**

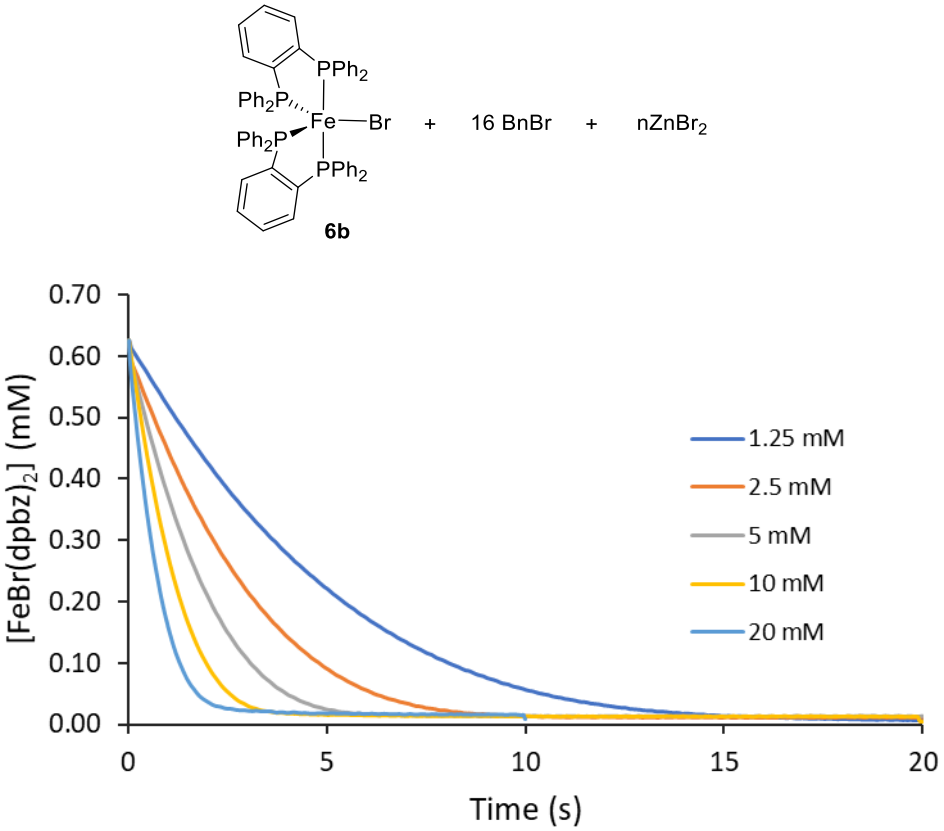

Figure 2. 19 Reaction of $FeBr(dpbz)_2$ (0.625 mM) with BnBr (10mM) with a range of concentrations of $ZnBr_2$

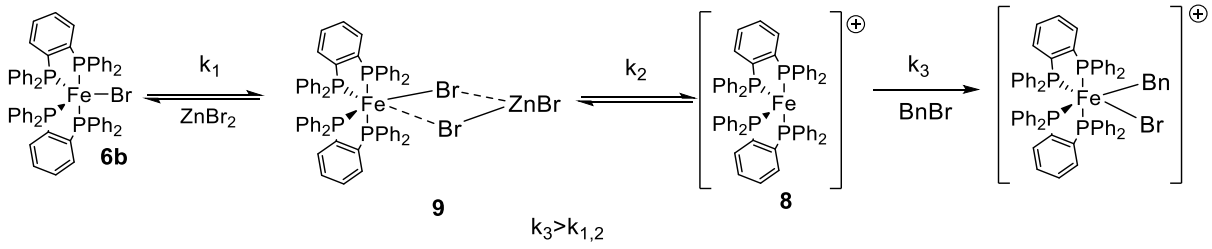

Scheme 2. 26 Proposed interaction between **6b** and $ZnBr_2$ in the presence of BnBr

The next salts to be tested were magnesium bromide, lithium bromide and aluminium bromide in the presence of BnBr. As shown in figure 2.20, increasing the amount of magnesium bromide and lithium bromide decreased the rate of reaction, whereas aluminium bromide accelerates the oxidation. This result shows that $AlBr_3$ and $ZnBr_2$ are more likely to behave as Lewis acids in the presence of BnBr, whereas LiBr and $MgBr_2$ act as a bromide donor, suggesting the formation of an adduct similar to **9**.

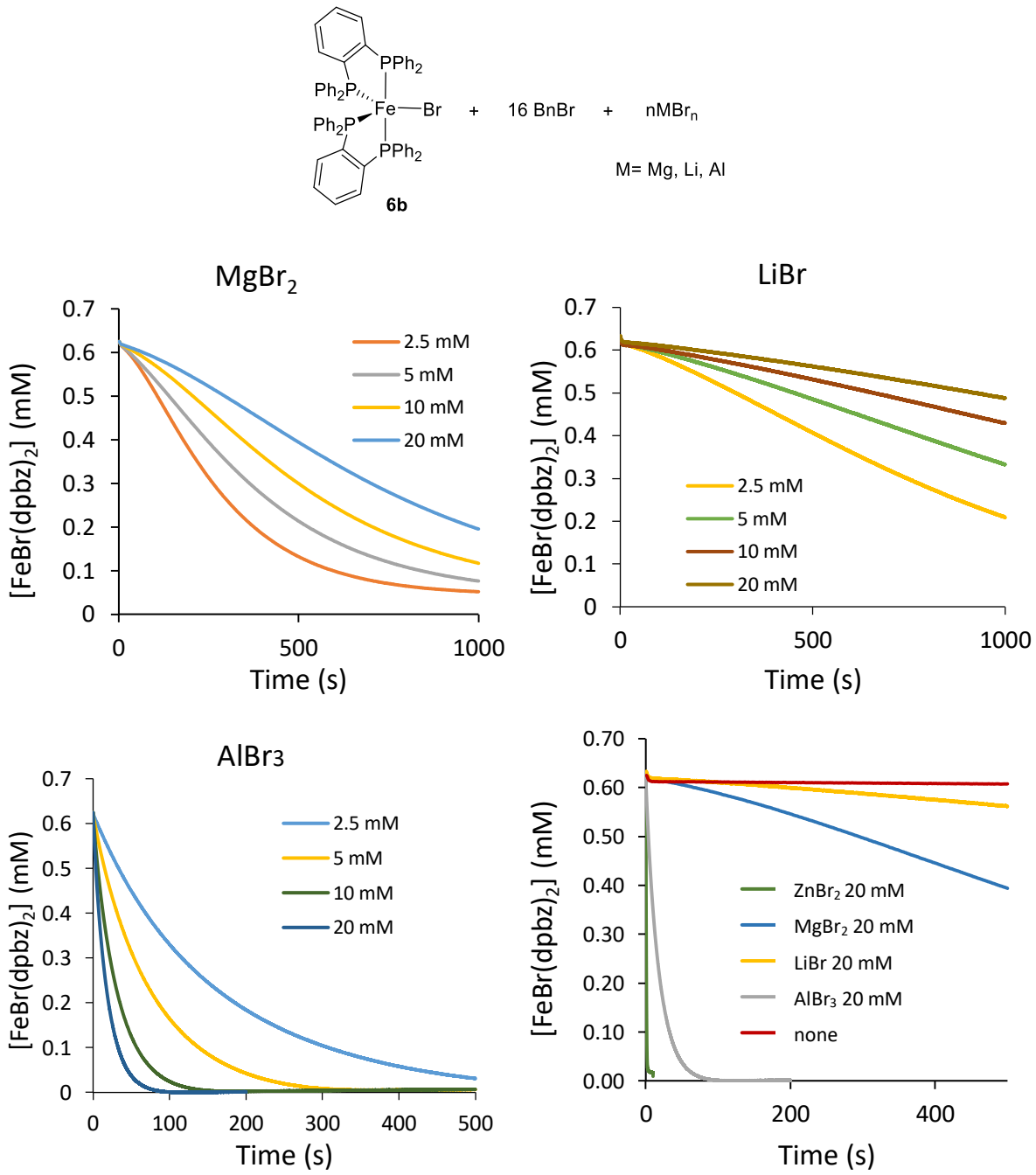

Figure 2. 20 Effect of Bromide salts in the reaction with **6b** (0.625 mM) and BnBr (20 mM) and a range of concentrations of $MgBr_2$, LiBr, $AlBr_3$.

The next step was testing $Li[B(Ar_f)_4]$ as a bromide abstractor. This salt showed that the lithium ions could compete with the Fe(I) for the bromide ion, increasing the rate of decay of **6b** as the concentration of the salt rises (Figure 2.21). The reaction was faster than the reaction using $ZnBr_2$, demonstrating the impressive effect that the lithium cation can have in accelerating the oxidation by abstracting a bromide from **6b**. It can be observed that the

concentration of **6b** at the beginning of the reaction is lower than the original concentration of the solution. This outcome may be because the reaction with $Li[B(Ar_f)_4]$ is instant, decreasing the apparent initial concentration of the iron complex.

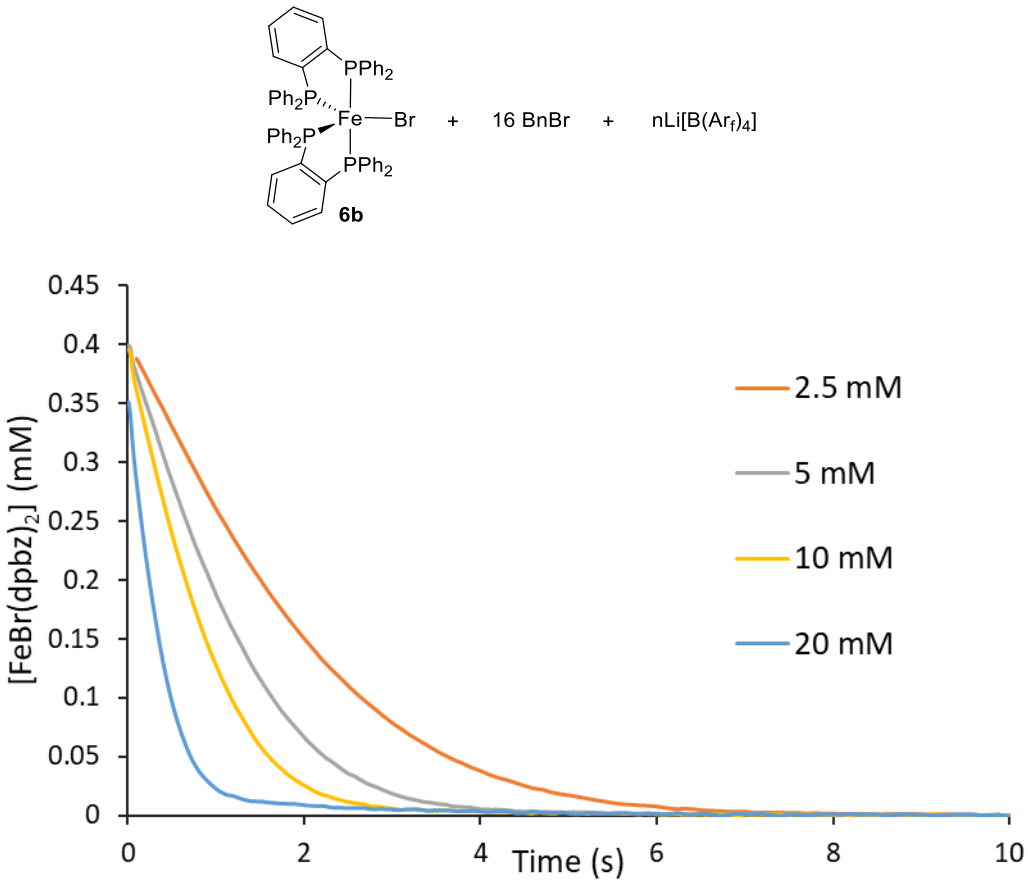

Figure 2. 21 Effect of $Li[B(Arf)_4]$ in the reaction between **6b** (0.625 mM) and BnBr (20mM)

As a final experiment to understand the effect of the investigated salts, they were tested in the reaction of **6b** with BnBr and $ZnBr_2$ in order to see if its effect kept constant on the rate of the oxidation reaction (Figure 2.23) in the presence of the zinc salt. As with the previous reactions, the presence of $Li[B(Arf)_4]$ and $AlBr_3$ accelerated the reaction, whereas the addition of LiBr reduced the rate of the oxidation. It is important to note that again, on the use of $Li[B(Ar_f)_4]$ an $AlBr_3$, the concentration of **6b** was reduced drastically before the measurement started, confirming the fast rate of reaction between the salts and the Fe(I) species.

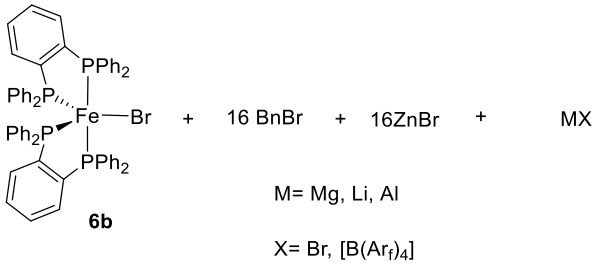

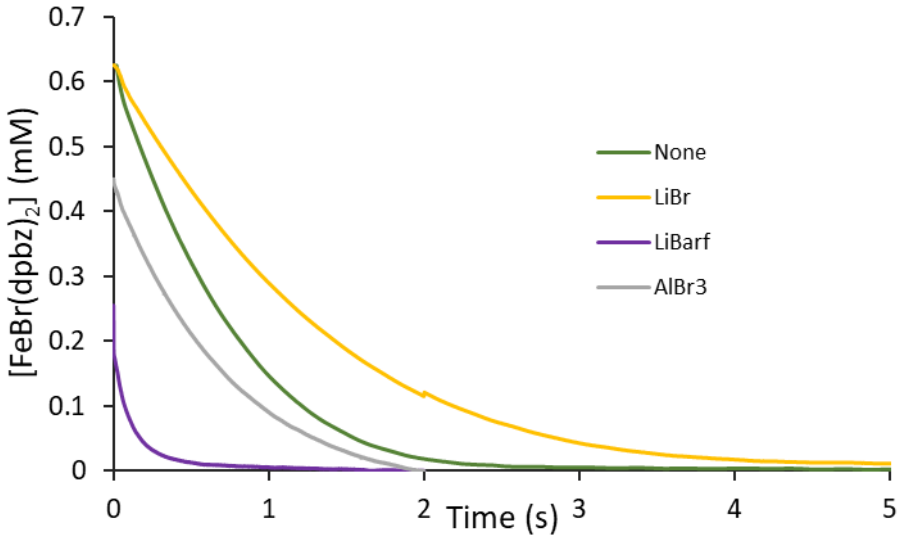

Figure 2. 22 Effect of salts in the rate of reaction between 6**b** (0.625), BnBr (10 mM) and ZnBr (10 mM)

In order to investigate the pathway 2, shown in Scheme 2.24, the influence of dpbz was tested in the oxidation of **6b** in the absence of $ZnBr_2$ (Figure 2.23). It is observed that as the concentration of dpbz ligand increases, the rate of consumption is decreased. This result could be explained by the fact that dpbz could shift the equilibrium to the formation of **6b**, effectively reducing the amount of monocoordinated complex (Scheme 2.27).

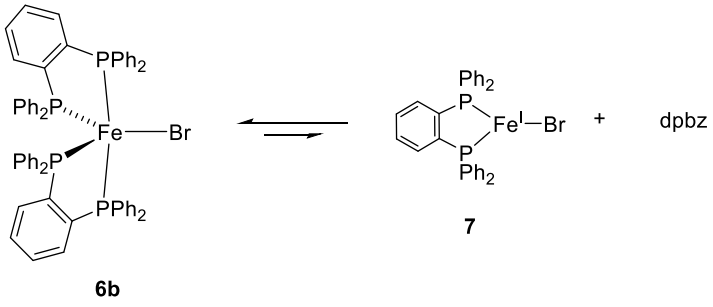

Scheme 2. 27 Effect of dpbz in the oxidation of Fe(I)

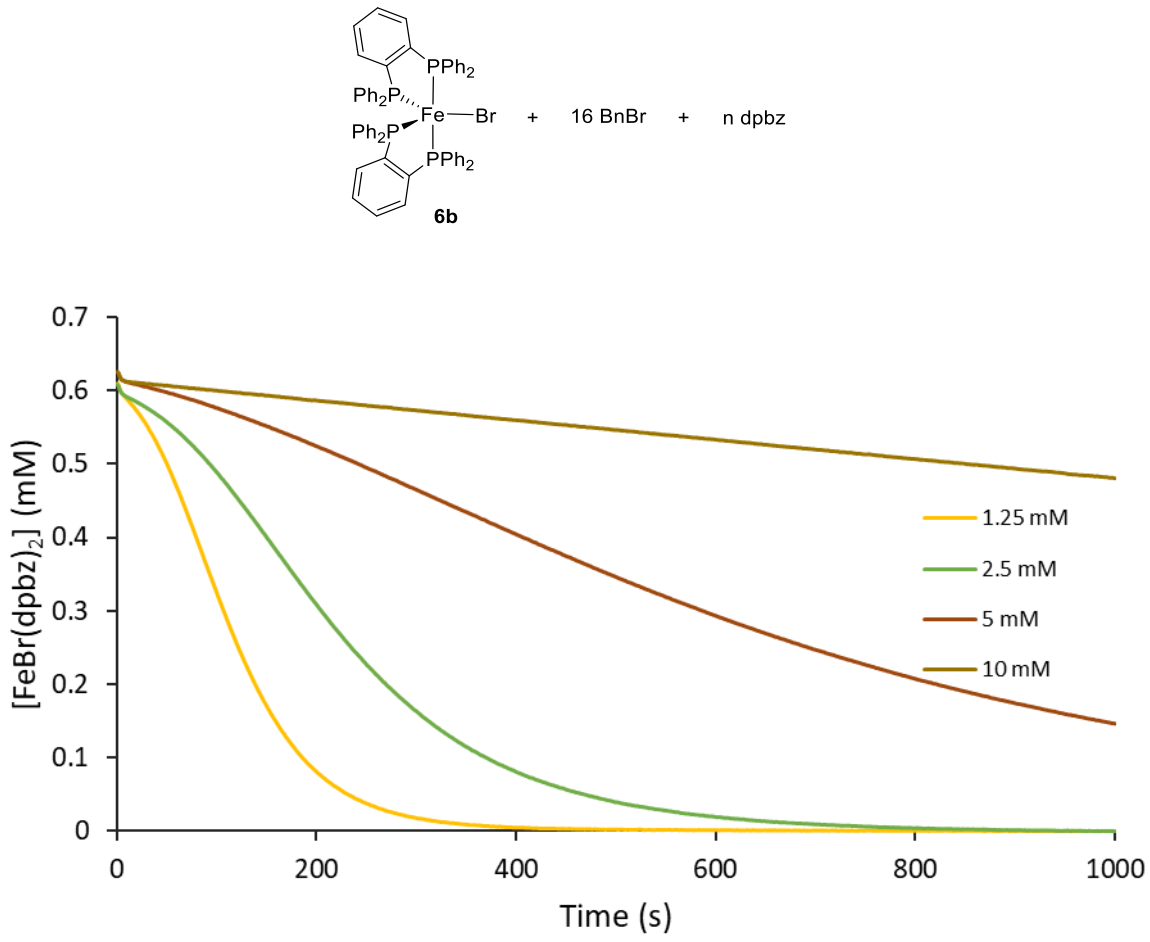

Figure 2. 23 Effect of a range of concentrations of dpbz in the rate of reaction between **6b** (0.625 mM), BnBr (10 mM)

Figure 2.24 shows the effect of dpbz in the presence of $ZnBr_2$ (20 mM). At low concentrations of ligand (2-8 eq), the reaction was not affected by the increasing amounts of ligand. When an excess of dpbz with respect to Zn is used (16-64 eq), the ligand decreases the rate of oxidation of Fe(I). This observation suggests that if the pathway 2 is operative, an excess of dpbz removes free $ZnBr_2$ from the solution slowing down the abstraction of bromide, thus hindering the formation of **8.**

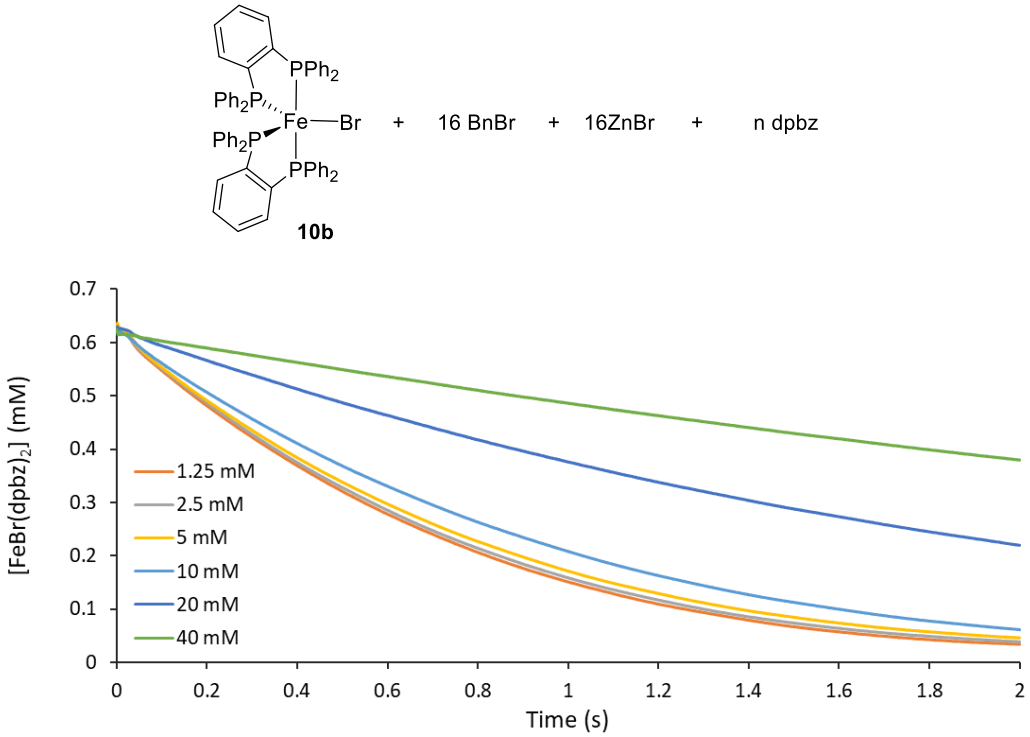

Figure 2. 24 Effect of a range of concentrations of dpbz in the rate of reaction between **6b** (0.625 mM), BnBr (10 mM) and ZnBr (10 mM)

In summary, the presence of Lewis bases reduces the rate of reaction between Fe(I) and BnBr, while the presence of Lewis acids accelerates the oxidation. $ZnBr_2$ has been shown to behave as both a Lewis base and acid, as it decelerates the decay of Fe(I) in the absence of BnBr but accelerates it when the nucleophile is in the mixture. Once the effect of these additives was tested, the order of reaction was determined to get insight into the mechanism of reaction and determine the rate-limiting step.

2.5 Order of reaction

Rates of reaction are the change in concentration of reactants or products over time. These rates are influenced by the order with respect to a given reactant, which is an exponent to which the concentration of said reactant is raised and indicates the interdependency between the components in a reaction, i.e. the portion of given matter which takes part in the reaction. A rate constant, k, is a value that quantifies the rate of a chemical reaction (Figure 2.25), which is a fixed value for a reaction at a specific temperature. The linearised form of the rate of the equation determines the order of reaction of a reagent when only the initial concentration of

that reactant is varied. A plot of the logarithm of the initial rate against the logarithm of the initial concentration of the reagent studied gives a straight line, the gradient is equal to the order of reaction with respect to that reagent.

$$r = -\frac{d[\mathrm{A}]}{dt} = k[\mathrm{A}]^x[\mathrm{B}]^y$$

$$\ln(r) = x\ln[A] + y\ln[B] + \ln k$$

Figure 2. 25 Rate equation (top) and linearised form of the rate equation (bottom)

Experiments were carried out between **6b**, BnBr and $ZnBr_2$ to determine the order of reaction with respect to each of the components. The data used in this section was recorded by Weightman as part of his MSci final project, and the author of this thesis reviewed and analysed the data accordingly, in some cases the data were re-recorded if necessary.

Due to the faster rates of reaction in the presence of $ZnBr_2$, the oxidative reaction of **6b** and BnBr in the absence of $ZnBr_2$ was monitored in a range of electrophile concentrations (0 – 16 equivalents relative to Fe(I)) (Figure 2.26). The order of reaction of a reagent was established by acquiring the maximum rates of reaction of the different variations of concentration of the reagent being studied. Maximum rates of a reaction are determined using the steepest gradient of the curve, which are shown in table 2.4.

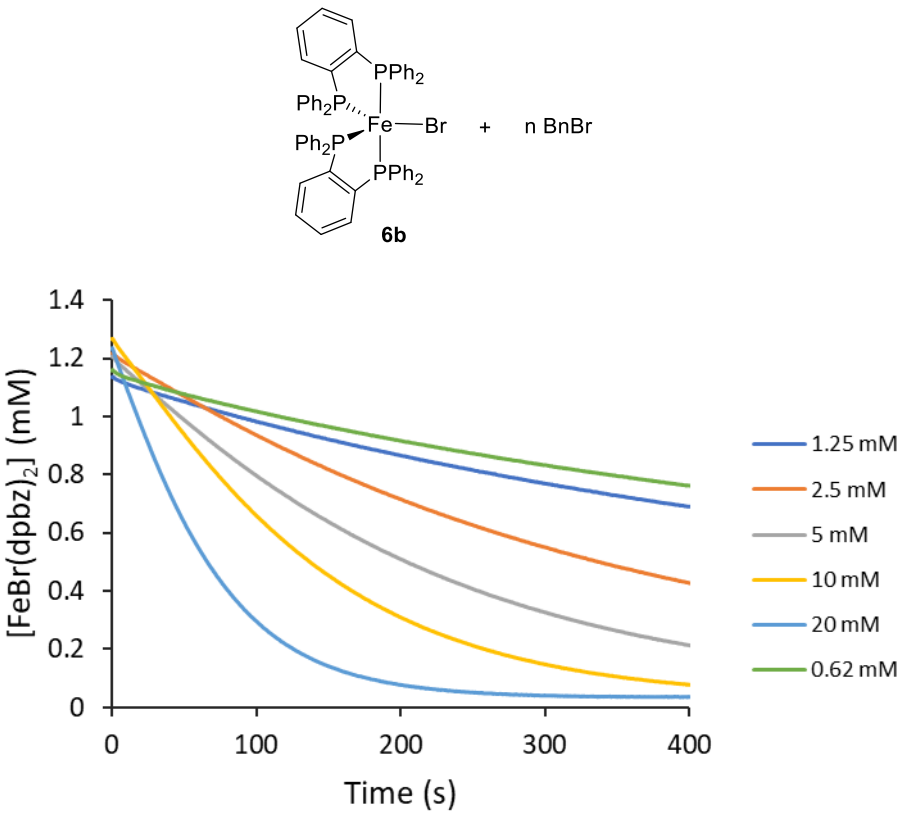

Figure 2. 26 Concentration-time plots for reaction of **6b** (1.25 mM) with BnBr (0 – 8 eq) at 40 °C

Table 2. 4 Initial rates from the time profiles in figure 2.26 at 40 °C

Entry	Added BnBr (equivalents)	Initial rate, v (10^{-3} mol dm^{-3} s^{-1})
1	0.5	-0.00117
2	1	-0.00136
3	2	-0.00281
4	4	-0.00427
5	8	-0.00661
6	16	-0.01330

In Figure 2.27, the values of the logarithm of the initial rate are plotted against the logarithm of the concentration of BnBr, the gradient of the best fit line will provide the reaction order with respect to BnBr. The estimated value for the reaction order respect to BnBr is 0.7137 $\pm$ 0.01.

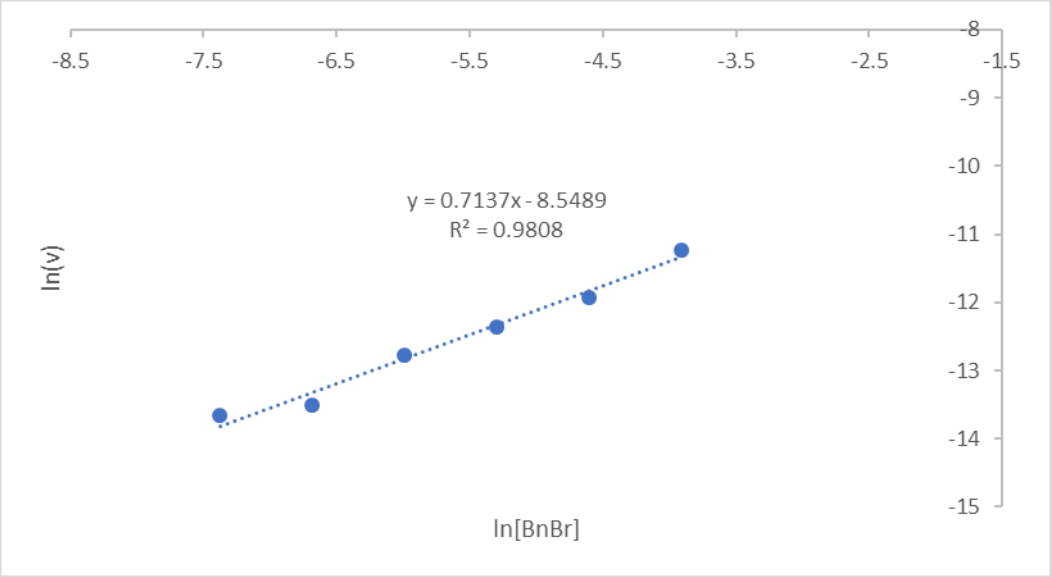

Figure 2. 27 Plot of the logarithm of the initial rate against the logarithm of the BnBr concentration in the reaction of **6b** with BnBr at 40 °C

The order of reaction with respect to **6b** was also determined by varying the initial concentration of **6b** in excess of BnBr (20 mM) at 40 °C (Figure 2.28). After obtaining the initial rates from these runs (Table 2.5), the logarithm of the initial rate against the logarithm of the initial concentrations was plotted.

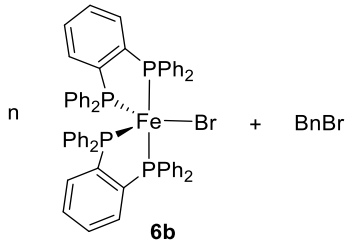

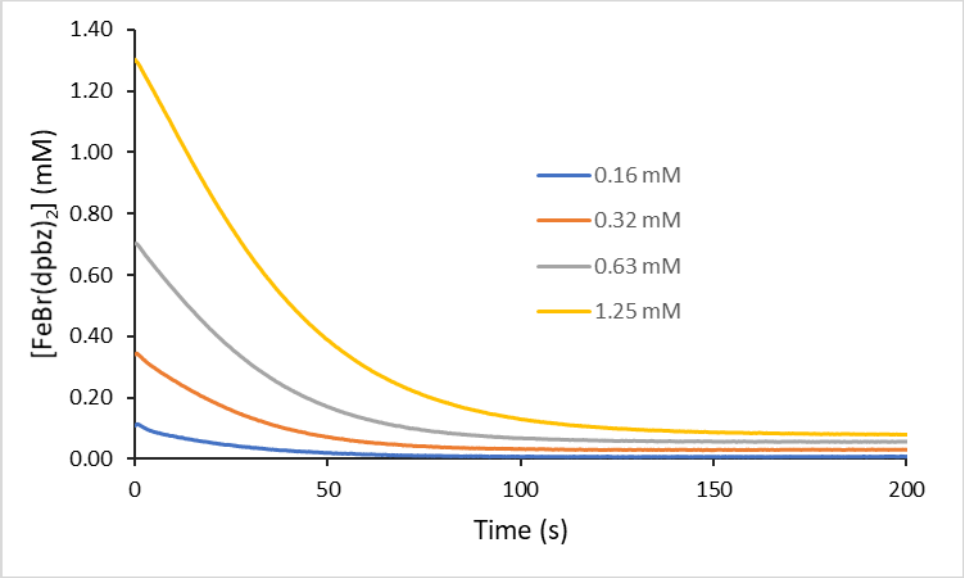

Figure 2.28 Concentration-time plots for reaction of **6b** (0.16-1.25 mM) with BnBr (20 mM) at 40 °C.

Table 2. 5 Initial rates from the time profiles in 2.28

Entry	Added Fe(I) (mM)	Initial rate, v (10^{-3} mol dm^{-3} s^{-1})
1	0.16 mM	-0.0065
2	0.32 mM	-0.0086
3	0.625 mM	-0.0159
4	1.25 mM	-0.0228

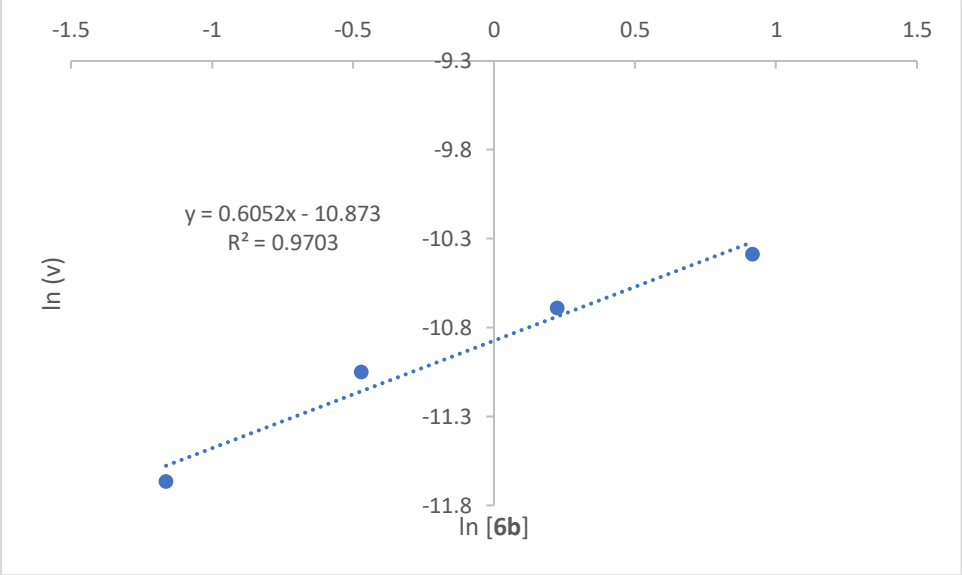

Figure 2. 29 Plot of the logarithm of the initial rate against the logarithm of the **6b** concentration in the reaction of **6b** with BnBr at 40 °C

The fitting line gave a gradient of 0.6052 ± 0.1497 (Figure 2.29). Orders of reactions of this nature are usually found in reactions that proceed in several elementary steps. If the order of reaction is 1/2,[128] the reaction can be interpreted as an indication that free atoms or radicals are taking part in the reaction. In the case of these reactions, the order in Fe(I) could be considered close to order 1. The fractional order of reaction obtained for the BnBr also indicates its involvement in a complex mechanism of reaction where elementary steps of reaction take place before the rate-limiting reaction.

The kinetic studies reported so far exclude the involvement of $ZnBr_2$, which have been shown to increase the rate of reaction to a more catalytic relevant rapidity. It was necessary to analyse the oxidation system with timeframes in agreement with the catalytic reaction to establish a better model for the catalytic Negishi reaction; It was reported that the Negishi reaction at 40 °C was 60% completed after 20 seconds of the reaction start (see section 2.2).[124] The timeframes of the reaction in the absence of $ZnBr_2$ are not in accordance with this, whereas the use of $ZnBr_2$ makes the reaction fast enough to be in congruence with the catalytic reaction timeframes. For that reason, the reaction between **6b**, BnBr and $ZnBr_2$ was studied to get the order of reaction of these reactants. The first set of experiments were to determine the order with respect to $FeBr(dpbz)_2$. The concentration of $ZnBr_2$ and BnBr was

kept constant (both at 20 mM) and the concentration of **6b** was varied. As the concentration of **6b** increased, the rate was increased. Table 2.6 shows the initial rates determined in these experiments. The gradient of the best fit line was found to be 0.8851 ± 0.0620 (Figure 2.30), which indicates that the reaction is close to first order with respect to Fe(I).

Table 2. 6 Initial rates from the reaction of a range of **6b** concentrations with BnBr and $ZnBr_2$ (both 20 mM) at 40 °C.

Entry	Added Fe(I) (mM)	Initial rate, v (10^{-3} mol dm^{-3} s^{-1})
1	1 mM	-3.58
2	0.5 mM	-2.03
3	0.25 mM	-1.13
4	0.125 mM	-0.56

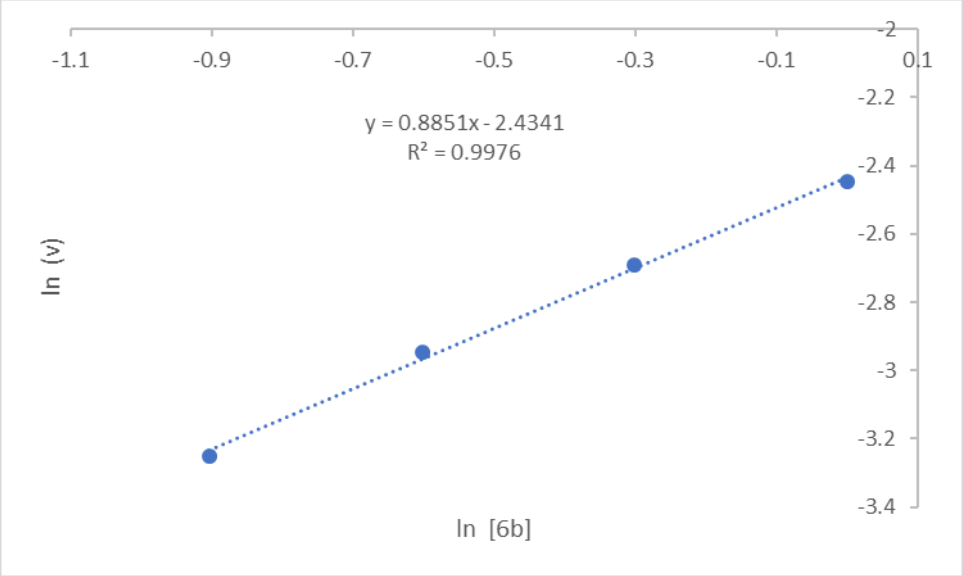

Figure 2. 30 Plot of the logarithm of the initial rate against the logarithm of the concentration of **6b** with a constant concentration for BnBr and $ZnBr_2$ at 40 °C

The order of reaction with respect to BnBr was determined using a range of concentrations of the electrophile with a fixed excess of $ZnBr_2$ (20 mM) and a fixed concentration of **6b** (0.625 mM). Table 2.7 shows the initial rates for the different concentrations. The best linear fit gave a slope of 0.9951 ± 0.0287 as shown in Figure 2.31.

Table 2. 7 Initial rates from the reaction of a range of concentrations of BnBr with constant concentrations of $ZnBr_2$ (20mM) and **6b** (0.625 mM) at 40 °C.

Entry	Added $BnBr_2$ (mM)	Initial rate, v (10^{-3} mol dm^{-3} s^{-1})
1	0.6	-0.0353
2	1.3	-0.0729
3	2.5	-0.1460
4	5.0	-0.2950
5	10.0	-0.5520

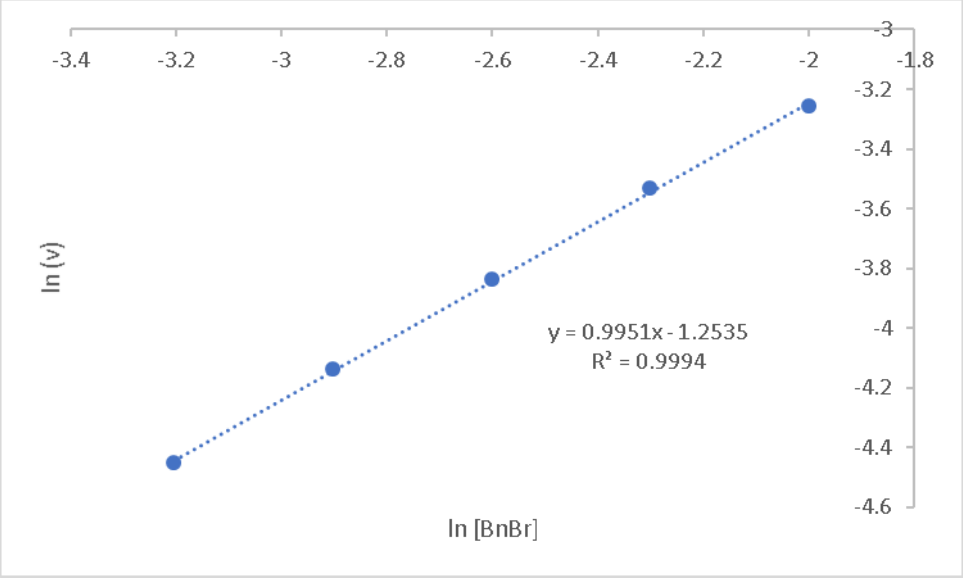

Figure 2. 31 Plot of the logarithm of the rate of reaction against the logarithm concentration of BnBr with constant concentrations of $ZnBr_2$ and **6b** at 40 °C

The final study determined the order of reaction with respect to zinc bromide; Table 2.8 shows the rates of reaction and the best fit linear line had a gradient of 0.6486 $\pm$ 0.0240 (Figure 2.32). The fractional number of this order of reaction suggests that there is a reaction between these two species before interaction with the BnBr or Fe. The lower value obtained for zinc bromide indicates that this salt is involved in more simple steps than **6b**. It is possible that the ability of $ZnBr_2$ as a dpbz abstractor and Br abstractor accounts for this behaviour.

Table 2. 8 Initial rates from the reaction of a range of concentrations of $ZnBr_2$ with constant concentrations of BnBr (20mM) and **6b** (0.625 mM) at 40 °C.

Entry	Added $ZnBr_2$ (mM)	Initial rate, v (10^{-3} mol dm^{-3} s^{-1})
1	0.6	-0.10
2	1.3	-0.15
3	2.5	-0.24
4	5.0	-0.38
5	10.0	-0.57

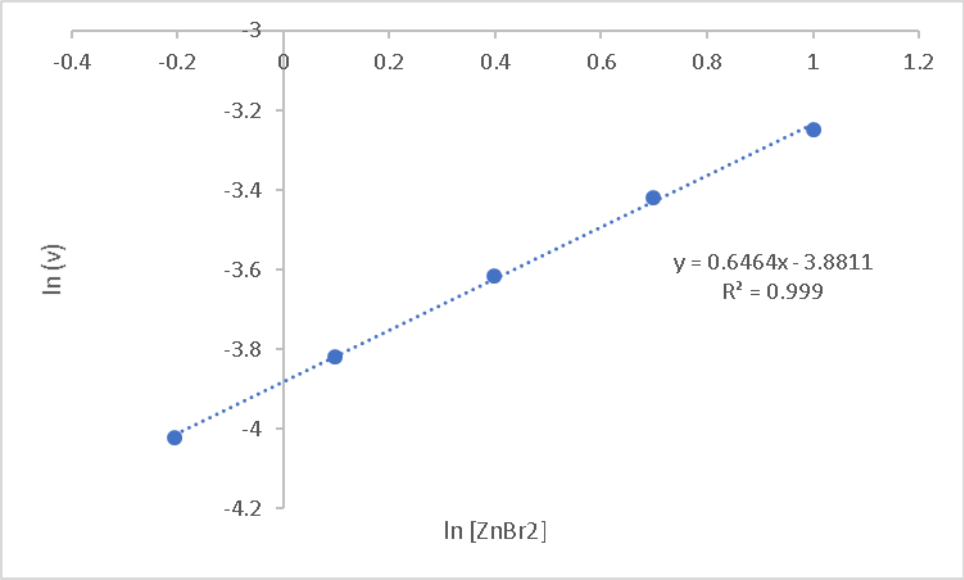

Figure 2.3228 Plot of the logarithm of the rate of reaction against the logarithm concentration of BnBr with constant concentrations of $ZnBr_2$ and **6b** at 40 °C

This kinetic study gives some suggestions about what is happening between the compounds tested here. The rate law for the reaction between **6b** and BnBr is

$$v=k[\mathbf{6b}]^{0.7}[BnBr]^{0.6} \quad (2)$$

and the rate law in the presence of $ZnBr_2$ is

$$v=k[\mathbf{6b}]^{0.89}[BnBr][ZnBr_2]^{0.65} \quad (3)$$

These results suggest that the reaction in the presence of $ZnBr_2$ have different elementary steps due to the difference in the order of reaction. Both reactions seem to involve a radical step or a very active intermediate that can undergo recombination disappearing from the mixture.[128]

2.6 Linear free energy relationship analysis using the Hammett equation.

The Hammett equation is a linear free energy relationship that determines a quantitative relationship between structure and activity in a given reaction where the reactant is changed systematically. This analysis uses a substitution constant (σ) which is a measure of the total polar effect exerted by a substituent on the reaction centre, with electron-withdrawing substituents having a positive value of sigma, and electron-donating having a negative one. These σ values are correlated in the Hammett Equation with the logarithm of the ratio of the rate constant of the substituted reagents and the non-substituted reagent. When the ratios and the σ are plotted, the sign of the gradient gives information about the inhibition or the activation of the reaction by electron-donating and electron-withdrawing substituents. This gradient is known as the reaction constant, or ρ. Equation 4[129] shows the Hammett equation, where k_0 is the rate constant of reaction for the unsubstituted compound, k_x is the rate constant of reaction with the substituted aromatic compound. A negative ρ means that the transition state develops a positive charge at the reaction centre in the rate-limiting step, and a positive value indicates a negative charge building up in the reaction centre in the rate-limiting step.[111]

$$\log\left(\frac{k_x}{k_o}\right) = \rho\sigma_x \qquad (4)$$

The reaction of **6b** with RBr, where R is a substituted benzyl bromide in the presence of $ZnBr_2$ (10 mM) was monitored having a constant concentration of **6b** (0.625 mM) and a varying concentration of the electrophile (0.625-10 mM) (Scheme 2.28). The maximum rates of reaction were obtained using the steepest section of the decay of Fe(I). Then the initial rates were plotted against the concentration of benzyl bromide to get the rate constant. The logarithm of the ratio of the rate constants of the different benzyl bromides was calculated.

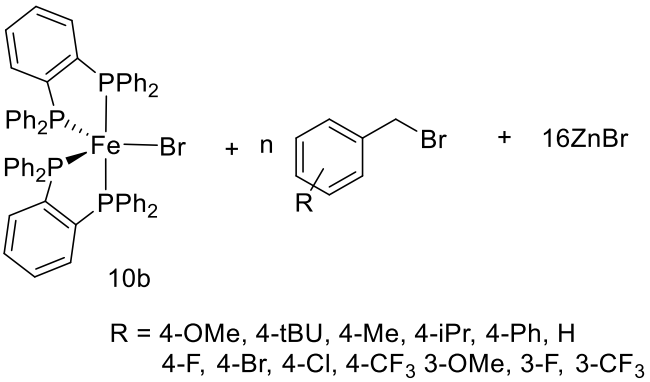

Scheme 2. 28 Reaction analyses with a Hammett study.

The apparent rate constants, the ratio of the rate constants and the sigma values are recorded in Table 2.9 below. The different types of sigma values consider the enhancement of resonance or inductive effects that the substrates have. σ^+ addresses the resonance effects of electron donor groups when a positive charge is built up; σ^- addresses the enhanced resonance effect for electron-withdrawing substituents when a negative charge is generated in the substrate, and $\sigma^\bullet$ relates to the formation of radical species and its stabilisation by the substituent. There are two scales of $\sigma^\bullet$ reported in the literature, the Creary[130] ($\sigma^\bullet_C$) which is based in the rearrangement of a radical, and the DAW[131] ($\sigma^\bullet_{DAW}$) which considers the stabilisation effects of a radical based on hyperfine coupling constants.[130]

Table 2. 9 Activation parameters for the reaction of **6b**, $ZnBr_2$ and a range of substituted benzyl bromides

Substituent	σ	σ^+	σ^-	$\sigma\bullet_C$	$\sigma\bullet_{DAW}$	log(kx/k0)
4-OMe	-0.27	-0.78	-0.26	0.24	0.034	0.104
4-tBu	-0.197	-0.26	-0.13	0.13	0.008	0.165
4-Me	-0.17	-0.31	-0.17	0.11	0.015	0.180
4-iPr	-0.151	-0.28				0.092
4-Ph	-0.01	-0.18	-0.02	0.46		0.127
H	0	0	0	0	0	0.000
4-F	0.06	-0.07	-0.03	-0.08	-0.011	-0.051
4-Br	0.23	0.15	0.25	0.13		0.146
4-Cl	0.23	0.11	0.19	0.12	0.017	0.150
4-CF_3	0.54	0.61	0.65	0.08	0.001	0.079
3-OMe	0.12	0.158		0.03	-0.001	0.002
3-F	0.34	0.352		-0.05	-0.018	0.067
3-CF_3	0.43	0.52		-0.07	-0.014	-0.157

The logarithm of the ratio of rate constants was plotted against the different values of sigma values. The plot for σ is shown in Figure 2.33. Most of the substituents increase the rate of reaction compared to the unsubstituted benzyl bromide. Although there is no trend in this plot, the pattern showed is consistent with a neutral radical intermediate.[132]

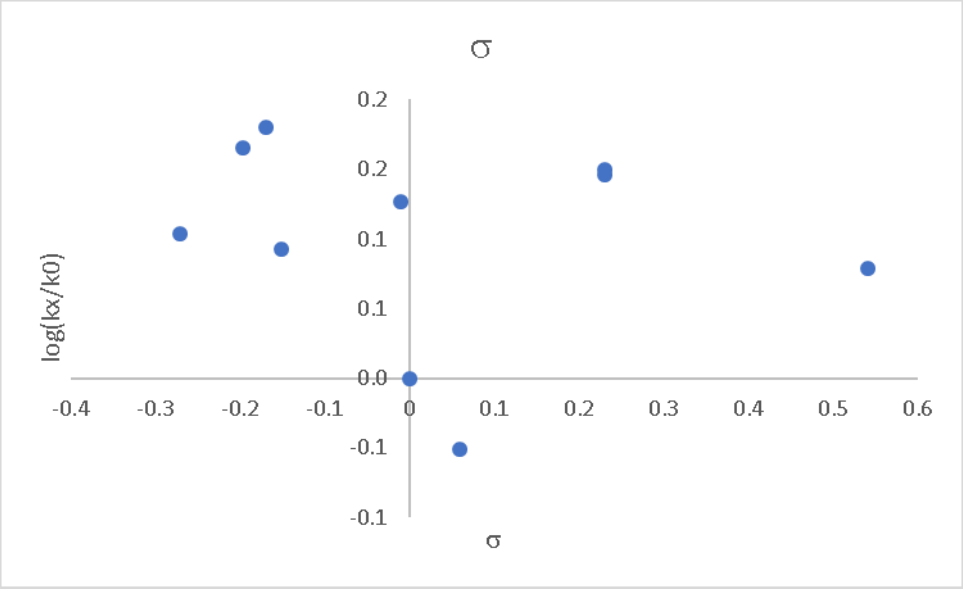

Figure 2. 293 Plot of $\log(k_x/k_0)$ against σ

It is evident that there is no correlation in the case of σ^+, σ^- (Figure 2.34). This behaviour indicates the lack of a cationic or anionic character in the transition state of the reaction.

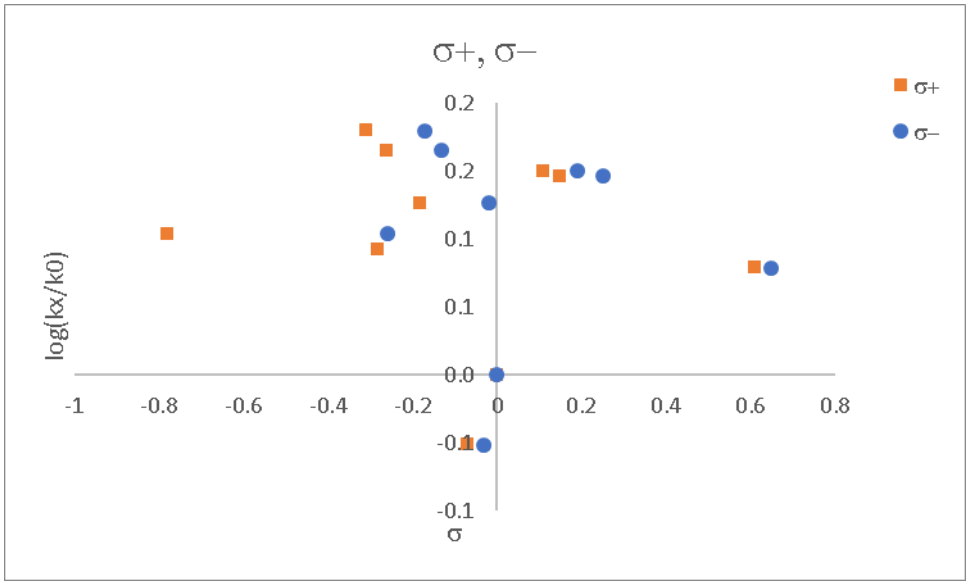

Figure 2.304 Plot of $\log(k_x/k_0)$ against σ^+ and σ^-

Finally, the use of both σ• for para-substituted benzyl bromides is presented in Figure 2.35 where a good correlation is found with both scales. The ρ was better in the case of $\sigma\bullet_c$, with

an R^2=0.9314 compared to 0.8458 of the DAW value. It is possible that this is because the rearrangement influence is stronger than the hyperfine splitting. When the meta-substituted BnBr are studied (Figure 2.36), the rearrangement appears to be irrelevant, and the only correlation observable is with $\sigma^{\bullet}_{DAW.}$

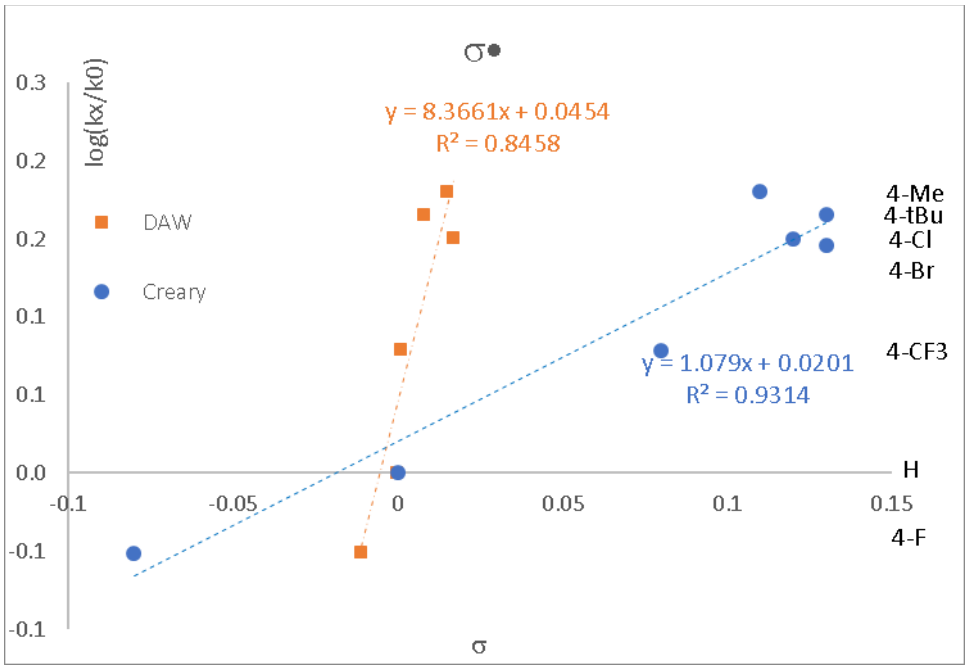

Figure 2. 315 Plot of $\log(k_x/k_0)$ against $\sigma^{\bullet}_{c}$ and $\sigma^{\bullet}_{DAW}$ for para-substituted benzyl bromides

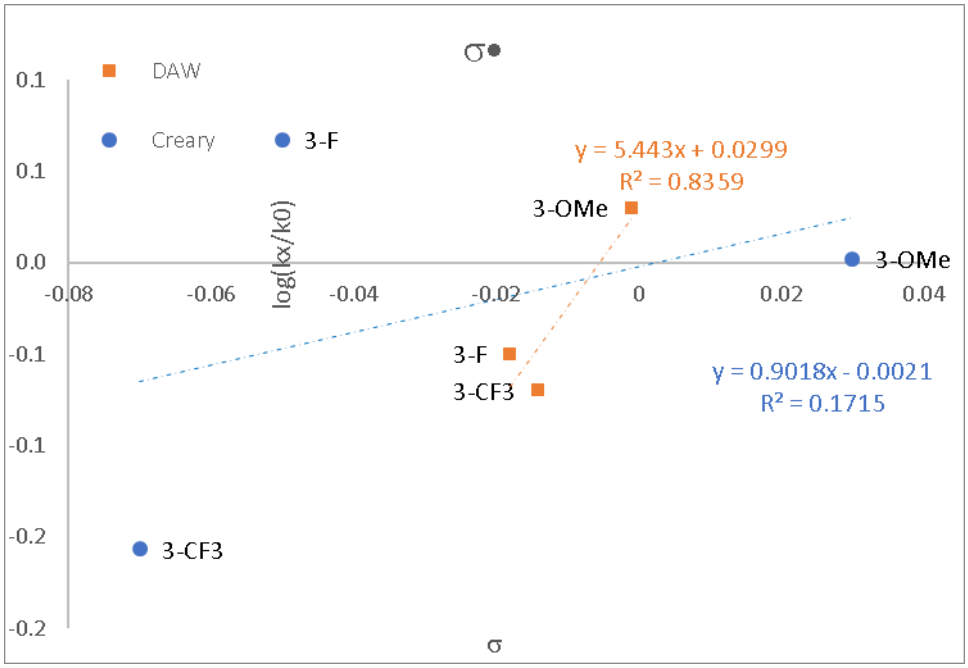

Figure 2.36 Plot of $\log(k_x/k_0)$ against $\sigma^{\bullet}_c$ and $\sigma^{\bullet}_{DAW}$ for meta-substituted benzyl bromides.

This Hammett analysis indicates that the reaction studied has a free radical nature, in accordance with the order of reaction calculated in the past section. Most of the $\sigma^{\bullet}$ values are positive, and in accordance with this, the substitution accelerates the reaction in most of the cases meaning that the presence of most substituents will stabilise the formation of a free radical transition state. Correlations between the ratios of reactions with a $\sigma^{-} + \sigma^{\cdot}$ or $\sigma^{+} + \sigma^{\cdot}$ were attempted with no success, which indicates that in the rate-limiting step, an increase of charge is not developed in the transition state. The good fit of using the Creary scale, which is derived using a radical reaction with very low polar character,[118] supports the hypothesis of a transition state with little polarity.

2.7 Activation parameters of the reaction of $[FeBr(dpbz)_2]$ and BnBr in the presence of $ZnBr_2$

The Eyring equation is used to calculate the common thermodynamic parameters of Gibbs free energy, enthalpy and entropy ($\Delta G^{\ddagger}$, $\Delta H^{\ddagger}$, $\Delta S^{\ddagger}$). This information gives insight on how a transformation to the activation complex happens and provides understanding about the changes in structure and energy states.

The activation parameters were calculated to get more information about the oxidation reaction. The initial rates of the reaction between **6b**, $ZnBr_2$ and benzyl bromide with different substituents (3-MeO, 4-t-Bu, H, 4-Br, 4-F and 4-CF_3) were measured at different temperatures (10, 20, 30, and 50 °C). The concentration against time profile of a 4-Bromobenzyl Bromide at different temperatures is shown in Figure 2.37.

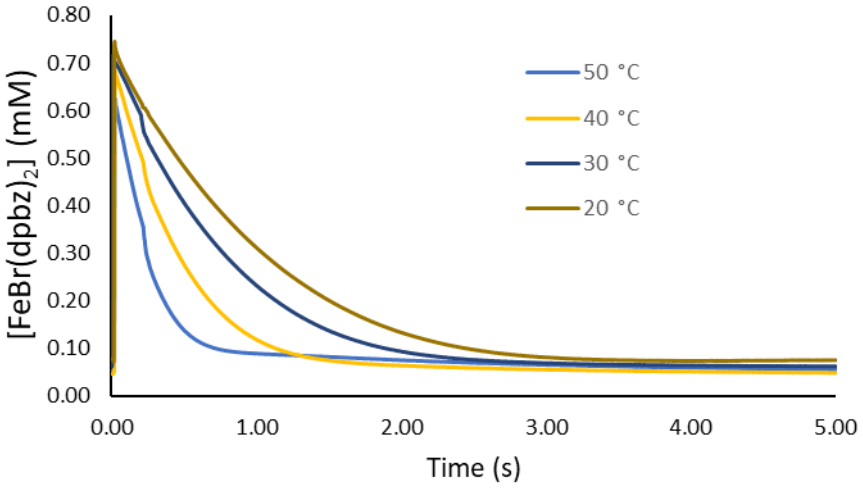

Figure 2.37 Temperature profiles of the reaction of **6b** with 4-BrBnBr and $ZnBr_2$

The initial rate at each temperature was obtained and then used in the linearised Eyring equation (equation 6), where k is the rate constant, k_B is the Boltzmann constant, T is the absolute temperature, h is Planck's constant, R is the gas constant, ΔG is the free energy of activation, $\Delta H^{\ddagger}$ is the enthalpy of activation, and $\Delta S^{\ddagger}$ is the entropy of activation.

$$k = \frac{k_B T}{h} exp\left(-\frac{\Delta G^{\ddagger}}{RT}\right) = \frac{k_B T}{h} exp\left(-\frac{\Delta H^{\ddagger}}{RT} + \frac{\Delta S^{\ddagger}}{R}\right) \quad (5)$$

$$\ln\frac{k}{T} = -\frac{\Delta H^{\ddagger}}{RT} + \frac{\Delta S^{\ddagger}}{R} + \ln\frac{k_B}{h} \quad (6)$$

The enthalpy and entropy of activation were obtained from the gradient (Figure 2.38). Plotting the ln(k/T) against 1/T, $\Delta H^{\ddagger}$ is obtained from the gradient and $\Delta S^{\ddagger}$ from the intercept.

Using the equation of state $\Delta G^{\ddagger} = \Delta H^{\ddagger} - T\Delta S^{\ddagger}$, the free energy of activation was calculated. A good linear correlation was obtained for all the reagents. Calculated values of enthalpy and entropy of activation for the reaction of BnBr with Fe(I) and $ZnBr_2$ and its free energy of activation is shown in Table 2.10.

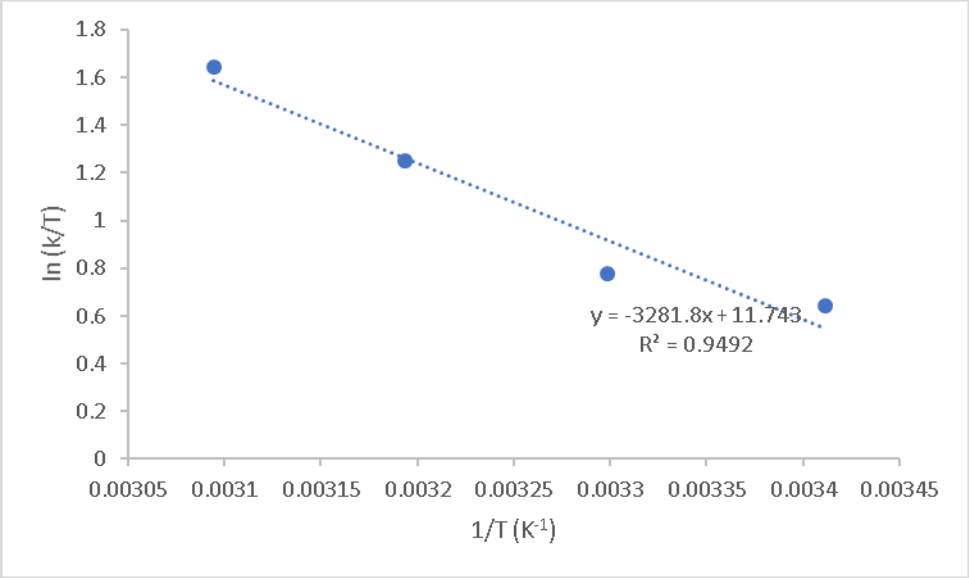

Figure 2.38 ln(k/T) against 1/T for the reaction 4-Bromobenzyl bromide with $ZnBr_2$ and **6b**

Table 2. 10 Activation parameters for the reaction of a range of substituted benzyl bromides with $ZnBr_2$ and **6b** at 298 K

	k 298	±	$\Delta G^{\ddagger}_{298}$ (kcal/mol)	±	$\Delta H^{\ddagger}$ (kcal/mol)	±	$\Delta S^{\ddagger}$ (kcal/mol K)	±
3-OMe	330.13	5.1007	13.65	0.0188	9.08	0.0253	-0.0165	0.0001
4-tBu	600.34	19.1931	14.01	0.0091	7.08	0.0933	-0.0221	0.0003
H	446.68	19.2711	13.83	0.0253	5.15	0.8424	-0.0291	0.0027
4-Br	620.98	2.6338	13.63	0.0025	6.14	0.4987	-0.0252	0.0017
4-F	329.14	24.6692	14.01	0.0435	9.39	1.3999	-0.0155	0.0046
4-CF_3	391.58	30.3609	13.91	0.0469	7.11	1.5458	-0.0228	0.0050

All the reagents showed a negative value for the entropy of activation for the reaction, which signifies that the transition states involve an associative step.[133] This result provides evidence

that the reaction between the BnBr and the active species form an adduct in the transition state. An endothermic reaction is expected for the formation of the transition state, as energy is needed to bring both species together. An atom transfer is a good possibility for the associating transition state.

2.8 Mechanism of reaction.

The use of the complexes [Fe(4-tolyl)$(dpbz)_2$] and [FeCl$(dpbz)_2$] as pre-catalyst showed that they were less active than complex **6b**. Benzyl bromide reacts faster with **6b** in the presence of Lewis acidic additive, while magnesium and lithium salts, and excess diphosphine ligand retarded the rate of reaction. The activation parameters point to an associative reaction, and the Hammett study showed that the reaction with a range of benzyl bromides substituted with electron-withdrawing and electron-donating had a good fit with the Creary σ scale, which correlates to a free radical transition state that is promoted by both EWG and EDG.

Two catalytic cycles are proposed for the Negishi cross-coupling reaction catalysed by FeBr$(dpbz)_2$. The first cycle is shown in Scheme 2.29 and involves a Fe(I)/Fe(III) process: complex **6b** loses a bromide through reaction with $ZnBr_2$ to form the cationic Fe(I) intermediate **8**. This step would be inhibited by the presence of any bromide donating salt, like LiBr or $MgBr_2$. Complex **8** then abstracts a bromide from the electrophile benzyl bromide via an atom transfer step forming the cationic species **10** which in the presence of $ZnBr_2$ loses a dpbz ligand to form **11** Recombination with the benzyl radical forms the intermediate **12** which transmetallates Zn(4-tolyl)$_2$ forming **13**. Finally, reductive elimination and coordination with dpbz regenerate **8**.

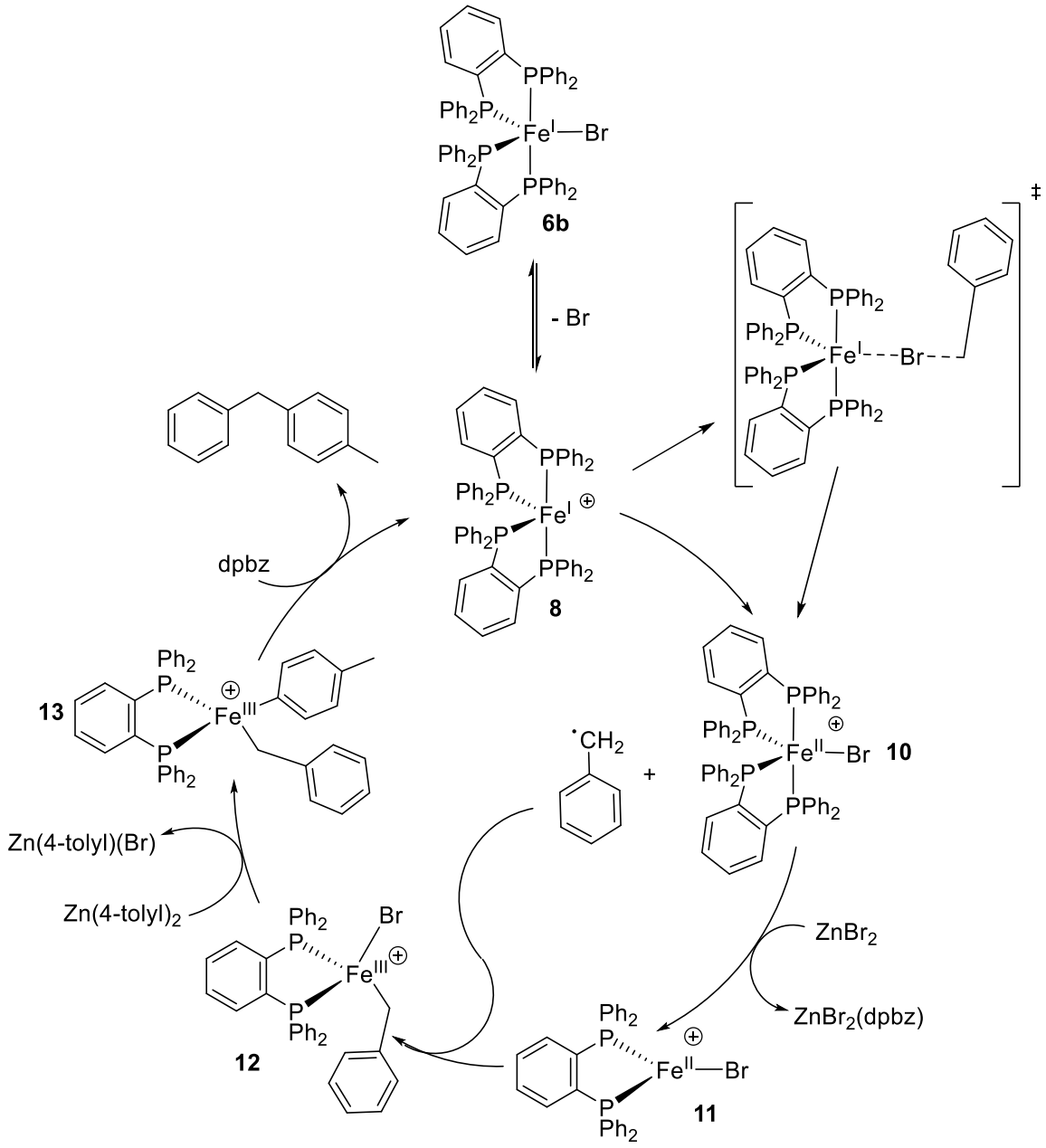

Scheme 2. 29 Catalytic cycle proposed for the Fe(I) Negishi cross-coupling with halide abstraction as the first step of the reaction.

The other mechanism shown in Scheme 2.30 starts with the complex **6b** losing a ligand dpbz to form **7**, leaving a coordination site available for abstraction of bromide from the electrophile via an atom transfer step forming **14** which collapses with a benzyl radical forming **15.** $Zn(tolyl)_2$ then reacts with **15** in a transmetallation step producing complex **16**,

which follows reductive elimination and regenerates complex **7** along with the cross-coupling product.

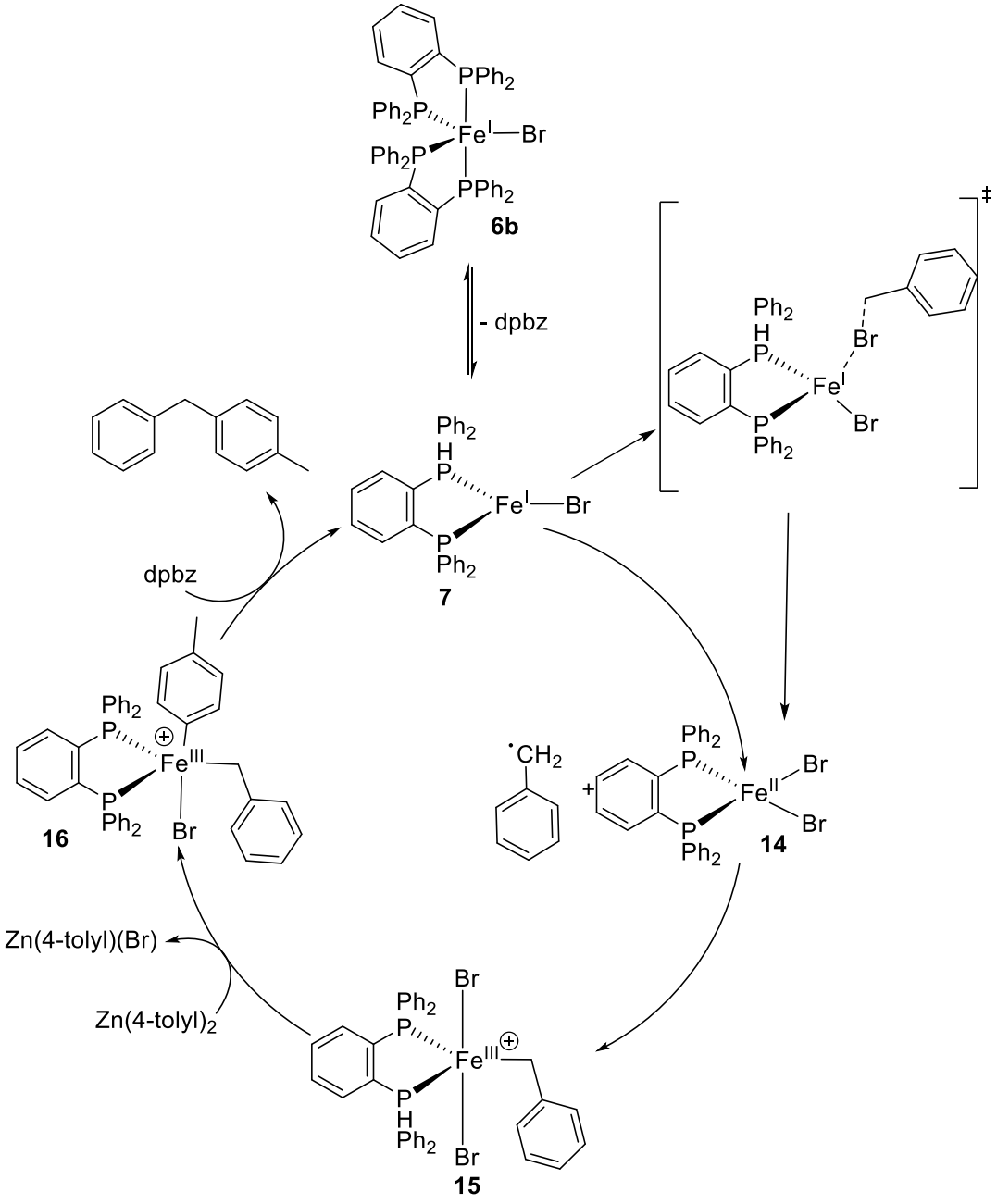

Scheme 2. 30 Catalytic cycle proposed for the Fe(I) Negishi cross-coupling with dpbz abstraction as the first step of the reaction.

Bedford has performed DFT calculations for abstraction of either bromide or ligand (Figure 2.39). Both abstractions were found to be energetically viable. The energies obtained in the modelling do not match the experimental energies obtained in this work, but it shows that

the formations of species **7** and **8** are favoured by similar energies of reaction, and it also shows that the initial abstraction of dpbz or Br is favourable in energy. The atomic transfer with BnBr was found to be the rate-limiting step, having higher energy of activation.

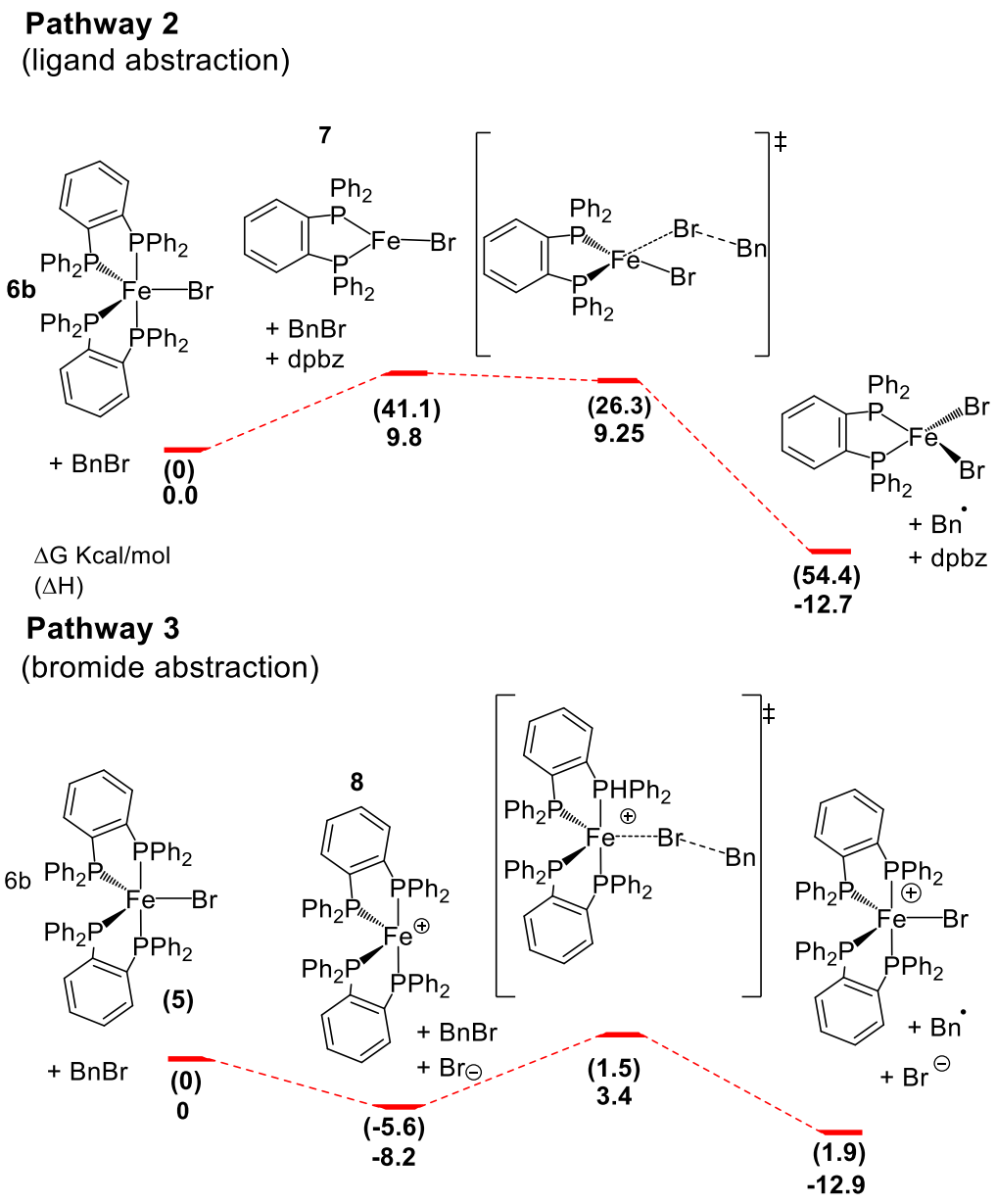

Figure 2. 32 Energies of reaction for the halide and dpbz abstraction obtained with DFT calculations by Robin Bedford.

2.9 Conclusions and Future Work

Iron(I) complex **6b** has shown to be active in the Negishi cross-coupling. This has been identified in situ in the Negishi cross-coupling from catalytic reaction mixtures using different spectroscopic techniques. Preliminary kinetic experiments demonstrated that iron(I) is the lowest relevant oxidations state under the reaction conditions of the catalysis. Iron(I) has been isolated and shown to be stable throughout the cross-coupling reaction.

It has been observed that the presence of Lewis acids in the reaction increases the rate of oxidation of **6b**. Additionally, an increasing concentration of dpbz inhibits the oxidative reaction with the electrophile. The order of reaction of $ZnBr_2$ and Fe(I) are fractional, which most likely indicates a reversible reaction step before the interaction with BnBr. The addition of $Li[B(Ar_f)_4]$ to the mixture accelerates the reaction, making the bromide abstraction a good candidate for the step before the oxidative addition. The ligand abstraction cannot be excluded because an excess of dpbz slows the reaction. The experimental data provided in this work does not allow us to discriminate between the possibilities.

The orders of reaction determined in this work give evidence of the complexity of this apparently simple process. The fractional order of reactions suggests that $Zn(tolyl)_2$ is involved in more elemental steps of reaction prior to the rate-limiting step. The order with respect to the electrophile was first order. The evidence for the formation of a benzyl radical is in accordance with the order of reaction different from 1 due to the number of reactions that a radical can undergo.

The Hammett analysis has shown that the reaction is likely happening in a free radical fashion. Negative entropies of activation suggest that if a radical is formed it must be via an atom transfer because a single-electron transfer would involve a dissociating transition step. Also, a SET step would show an increase in the electron density of the transition state, which would show a good correlation with σ^- values or a combination of σ^- and $\sigma\bullet$.

Further work on Fe(I) should determine if the halide abstraction or the dpbz abstraction is the elemental step that precedes the oxidation with BnBr. The Negishi cross-coupling reaction occurs with a mixture of Zn(4-tolyl)$_2$, BnBr and FeBr(dpbz)2 in the presence of $MgBr_2$. The mixture of Zn(4-tolyl)$_2$ and $MgBr_2$ must be in a Schlenk equilibrium which would make $ZnBr_2$ available in the mixture. A determination of the effect of this equilibrium would be interesting in order to associate it with the rate of reactions.

The study covered in this thesis addresses the oxidation step of the cross-coupling. It is necessary to undertake a kinetic analysis of the reaction with the nucleophile in order to understand further the transmetallation step of the reaction.

Chapter 3. Further studies on the iron-catalysed cross-coupling

3.1 Introduction

Determination of the of the lowest oxidation state of the metal in a mechanism is an aspect of crucial importance, as it provides a foundation upon which build suggestions of elemental steps of the catalytic manifold, exploring the possible redox processes that can arise in the system of study.

Mechanistic studies on iron catalysed cross-coupling reactions have provided insight on the different oxidation states of the species in the cycle, with proposals that range from Fe(-II) to Fe(II) as the lowest oxidation state in the cycle.

Although there are reports where iron complexes with oxidation states below zero have been found to have activity as pre-catalysts, this does not provide evidence of the direct activity of these species, merely that they are competent pre-catalysts.

In cross-coupling reactions, due to the characteristics of the electrophilic substrate, it is safe to say that they have an oxidative nature, while the nucleophile possesses a reducing one. In the reaction mixtures, the pre-catalyst is in contact with these reagents, and it is expected that the interaction between them, irrespective of the cross-coupling reaction, will generate Fe species that can be participating as on-cycle intermediates or they can be off-cycle species.

When a cross-coupling reaction is conducted, the reaction is started by an initial compound that may or not may be the active catalyst. If this initial compound is converted under reaction conditions to a different compound which shows a better activity for the catalysis, the initial compound must be called a pre-catalyst (Fe_{pre}) (Scheme 3.1). This Fe_{pre} is then said to be activated in the reaction mixture, in this case, most likely through a reduction producing the active species (Fe_{act}). Fe_{act} is expected to go through consecutive transformations with the coupling partners such as oxidative addition, transmetallation, reductive elimination and single electron transfer, which result in the formation of the product of catalysis. Each of these transformations will form different on-cycle species (Fe_{on})

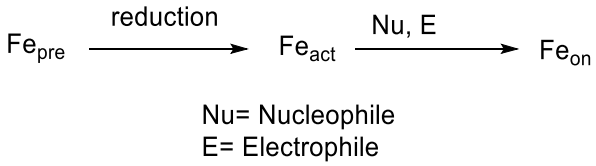

Scheme 3. 1 Consecutive transformations of Fe in a cross-coupling reaction

When a reaction is being monitored, it is possible to detect some complexes in the course of the reaction. It is crucial to be cautionary that the detection of a complex does not translate to the activity of the said species. In fact, they can be off-cycle resting states (Fe_{off}) which, upon interaction with the coupling partners, could undergo a redox process that activates them and incorporates them back into the cycle. Another possibility of the presence of this detectable species is that they can merely be a side product which is stable enough not to get activated and reintroduced in the cycle (Fe_{out}). Scheme 3.2 summarise the transformations that the metal centre can get through.[134]

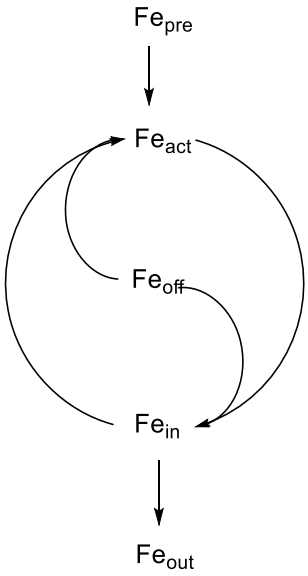

Scheme 3. 2 Possible precatalyst-derivated species present in a cross-coupling reaction

Complex [FeBr(dpbz)$_2$] (**6b**) has been found to be a good pre-catalyst in the Negishi cross-coupling, the studies on chapter 2 were envisioned due to the observed activity in the cross-coupling processes with Zn(4-tolyl)$_2$. Reactions using **6b** gave yields and rates of reactions

comparable to those of the equivalent Fe(II) pre-catalysts [FeBr2(dpbz)$_2$]. (**6b**).[99] It was then assumed that **6b** is the active species or is in equilibrium with the active species, as it was shown in chapter 2. Also, the detection of **6b** in EPR spectra of the catalytic reaction mixtures gave more evidence to suggest that Fe(I) complex **6b** is a good candidate of the lowest-oxidation state, and as such, the active species. [99]

A series of experiments using X-ray absorption spectroscopy were undertaken in order to detect the Fe species that are present in the catalytic reaction. Kinetic experiments performed by Messinis showed that the lowest oxidation in the cycle could not be the complex [FeBr(dpbz)$_2$]. (see below, Section 3.3).

3.2 Results and discussion

This work is a follow up to the previous experimental and mechanistic work on the iron catalysed Negishi cross-coupling reaction. This work is a collaborative effort between the postdoctoral researchers Messinis, Elorriaga, Luckham and the author of this work.

3.2.1 X-ray absorption spectroscopy

A collaborative work with Wells of the Diamond laboratory in Harwell, exploring the differences in the spectra of the Fe species found in the Negishi reactions was conducted in order to get a better understanding of the mechanism of this reaction.

3.2.1.1 Introduction to XAS

X-ray absorption spectroscopy (XAS) is the study of how X-rays are absorbed by an atom. Specifically, it measures the energies near and above the core-level binding energies of the atom.

The formal oxidation state, the coordination environment, distances and the nature of the species surrounding the element being study are properties and characteristics that can be

detectable with XAS, making it an excellent technique to determine the properties of complexes and intermediates of reaction.[135]

XAS is divided into two types of measurement: X-ray absorption near-edge spectroscopy (XANES) and extended X-ray absorption fine-structure spectroscopy (EXAFS) (Figure 3.1). From XANES it is possible to extract information about the oxidation state and coordination chemistry. XAS measures the energy of the absorption coefficient, which is the probability of x-rays being absorbed. μ is dependent on the atomic number, the atomic mass, the density of the sample and the X-ray energy. In an experiment, absorption will be observed when the incident X-ray has the same energy as the energy binding of a core-level electron, an absorption edge, showing a sharp rise in absorption. The instrument is tuned to the x-ray absorption energies of a specific element, in other words, XAS is element-specific. After the absorption, the atom is in an excited state, where one electron left its core level and then decays. (Figure 3.2) Upon the decay, an X-ray photon is emitted as fluorescence. The XAS is measured either with the fluorescence or the transmission.

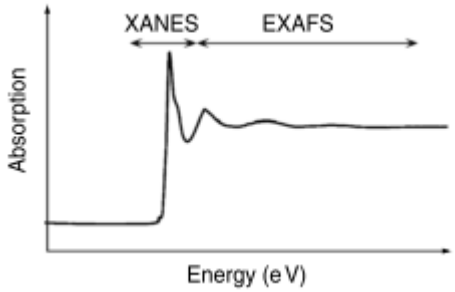

Figure 3. 1 Example of an X-ray spectroscopy. It is shown its division in XANES and EXAFS

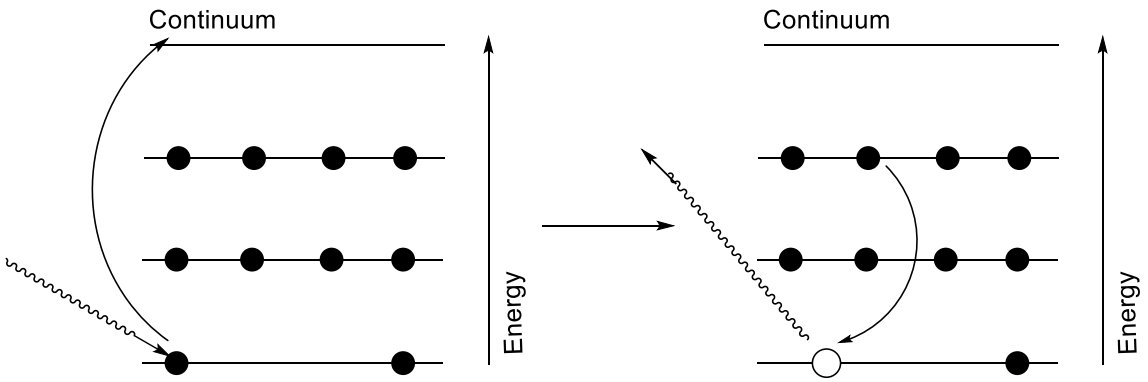

Figure 3. 2 Absorption of X-ray by a core electron (left) and X-ray fluorescence

A typical XAS spectrum has a sharp rise in E and oscillations in what is called the XANES region. When there is a neighbouring atom, the electron emitted is scattered, altering the absorption coefficient, which is the main characteristic of XAS and generates the oscillations observed in the EXAFS section.

3.2.1.2 Qualitative analysis of XAFS of Fe species active in the cross-coupling reaction.

The spectra of different Fe species that have been reported to be involved in the cross-coupling reaction were recorded to compare them and be able to interpret what is the mechanism of reaction and the different states in which the Fe can be found. These comparisons are qualitative in the sense that the spectra are superimposed, and the differences are observed. The data in this section were processed by Messinis.

The spectra of $FeBr_2$, $[FeBr_2(dpbz)_2]$ and $[FeBr(dpbz)_2]$ were obtained (Figure 3.3-3.5). The first derivative was obtained because it is easier to compare the different traits of the spectra.

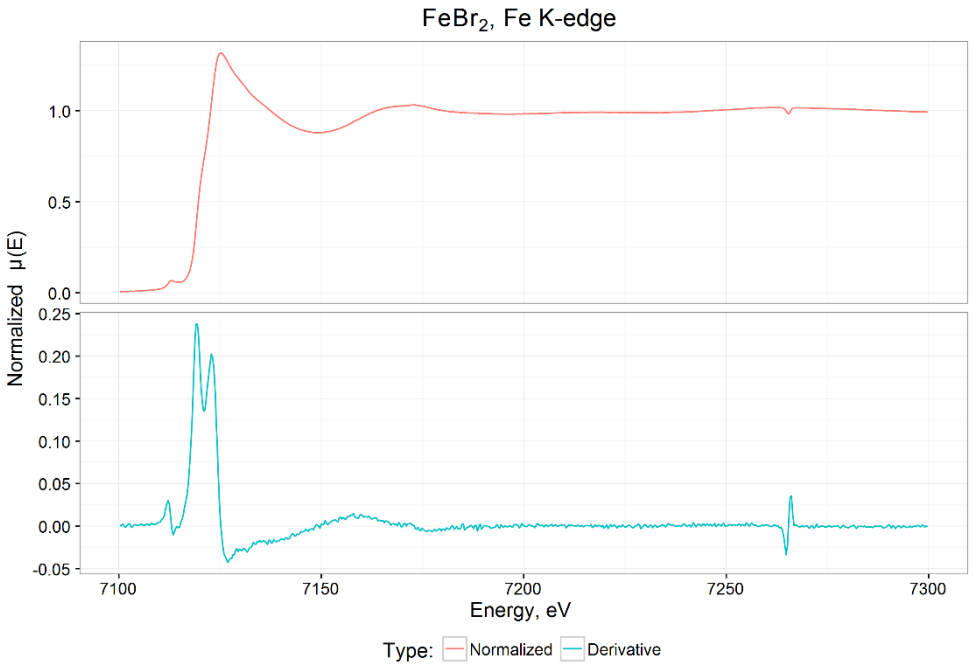

Figure 3. 3 XAS of a $FeBr_2$ (40 mM) solution in THF

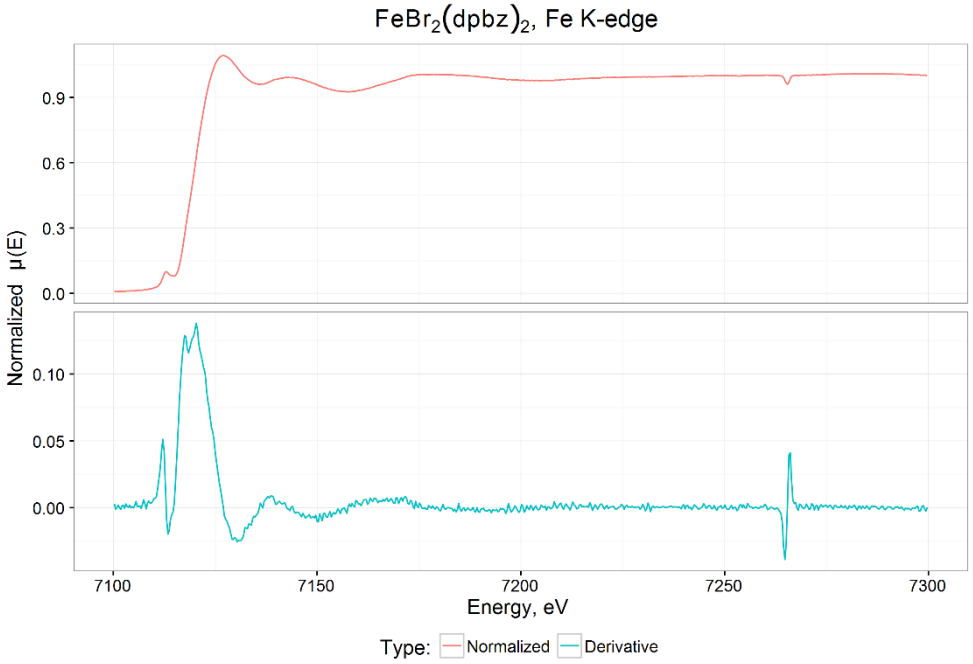

Figure 3. 4 Fe XAS of $[FeBr_2(dpbz)_2]$ 40 mM solution in THF

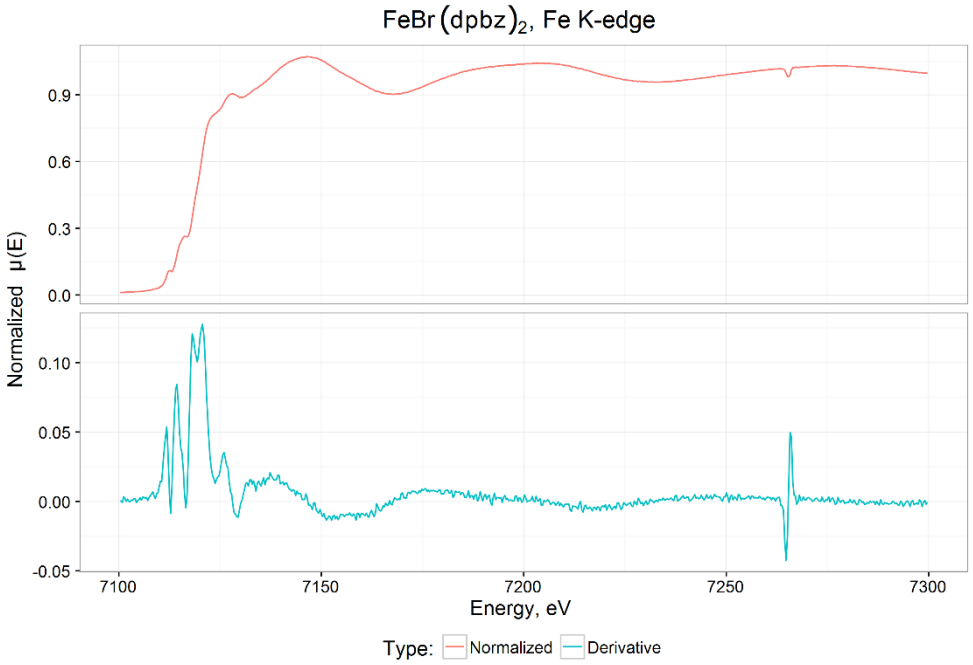

Figure 3. 5 XAS of [$FeBr(dpbz)_2$] 20 mM solution in THF

A comparison of the spectra of $FeBr_2$ and [$FeBr_2(dpbz)_2$] show a similar profile (Figure 3.6), with a difference in intensity due to the presence of dpbz. This was expected as both complexes have the same oxidation state, and the ligand atoms scatter the electrons.

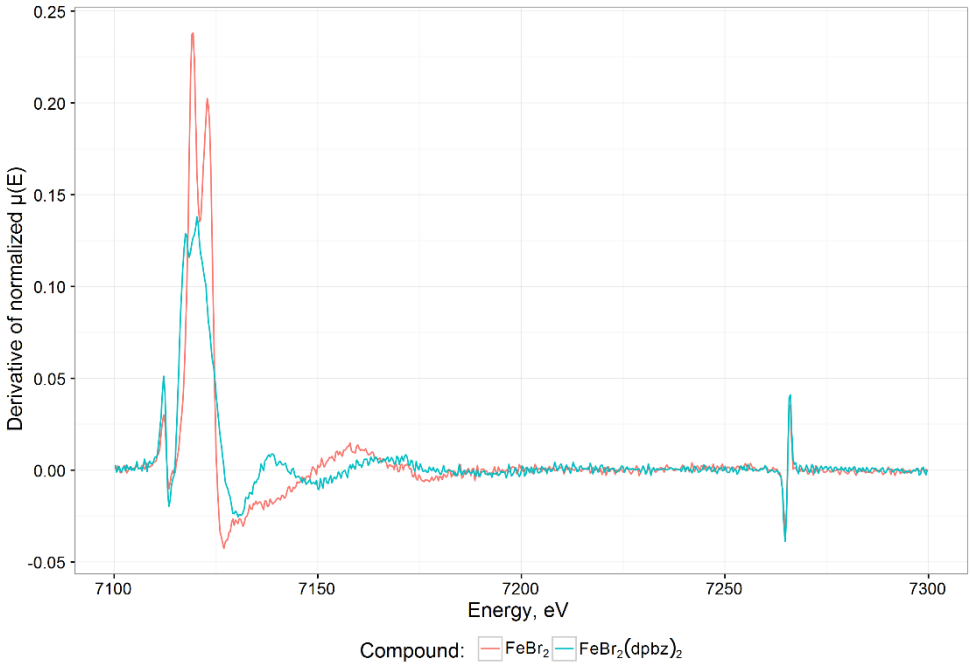

Figure 3. 6 First derivative comparison of the XAS of $FeBr_2$ and $[FeBr_2(dpbz)_2]$ in THF

A comparison between the complexes [FeBr(dpbz)] and $[FeBr_2(dpbz)_2]$, as expected, show a very different profile due to the difference in oxidation state. Also, the difference is a consequence of the geometry that these complexes have, with **1b** being octahedral and **6b** being trigonal bipyramidal. (Figure 3.7)

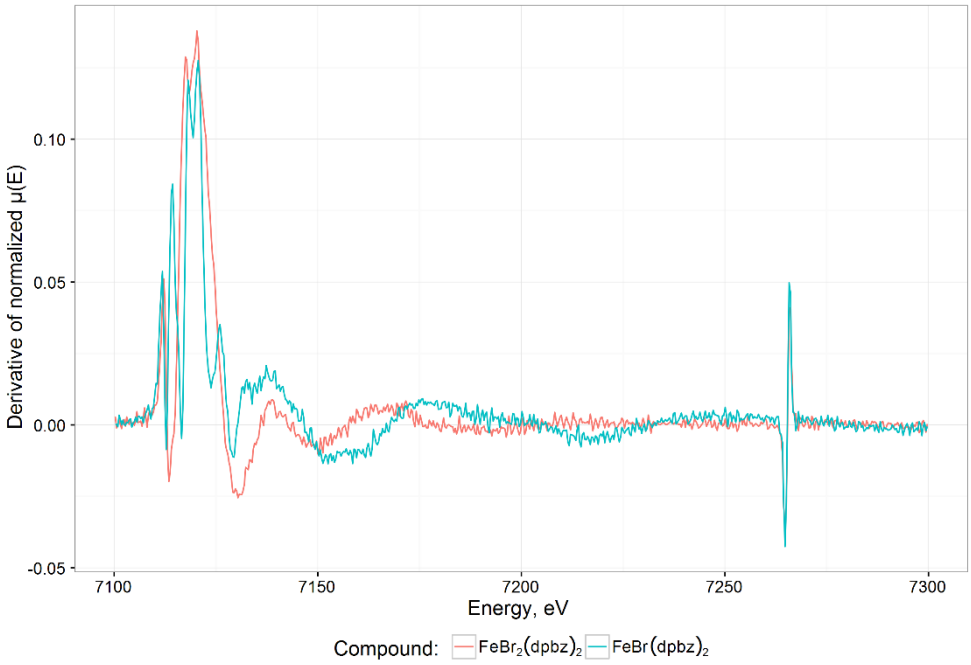

Figure 3. 7 Comparison of the first derivative of the XAS of [FeBr(dpbz)$_2$] and [FeBr$_2$(dpbz)$_2$] in THF.

3.2.1.3. XAS spectra of the catalysis reaction mixtures at the end-point.

Reactions that represent the catalysis were conducted, and the XAS was collected to reaction mixtures at the end of the reaction in order to identify the presence and nature of the Fe species at this point.

A mixture of FeBr$_2$(dpbz)$_2$ **1b** band Zn(tolyl)$_2$ was done to detect the formation of Fe(I) in the presence of this nucleophile. Comparison of this spectrum with the spectrum of isolated FeBr(dpbz)$_2$ showed identical features (Figure 3.8), in accordance with the experiments of formation of the complex **6b** in excess of nucleophile as it has been reported by the Bedford group.[99] The subtle differences may be due to the formation of the complex Fe(4-tolyl)(dpbz)$_2$

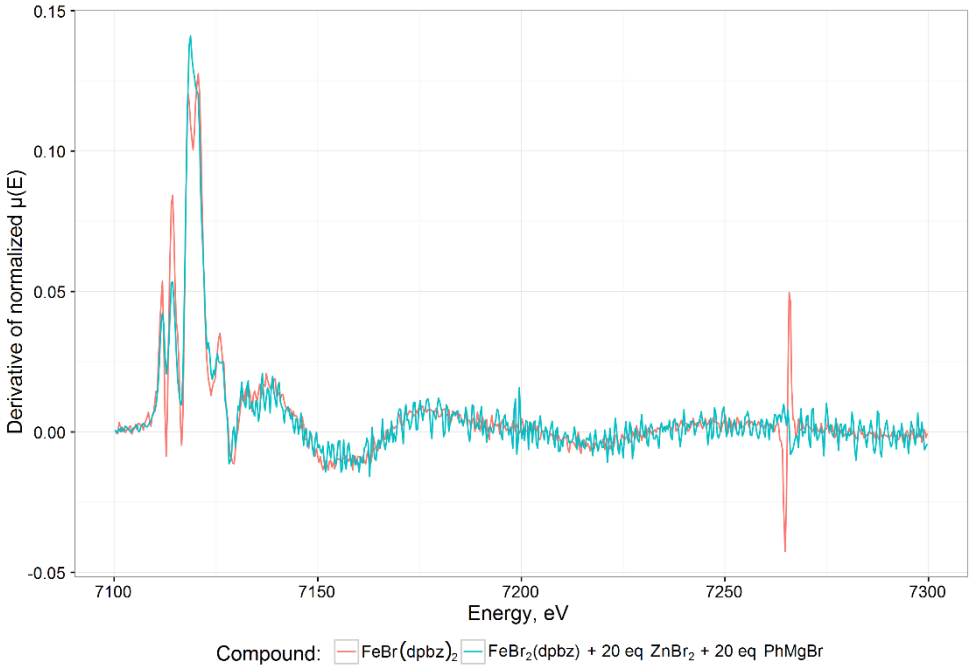

Figure 3. 8 Comparison of the XAS of $FeBr(dpbz)_2$ and $FeBr_2(dpbz)$ + 20 $Zn(4\text{-tolyl})_2$ solution in THF

As discussed in Chapter 2, the complex **6b** is oxidised in the presence of BnBr. It was of interest to see the final state of Fe after the reaction of these reagents. The compared spectra of the end-point with $FeBr_2(dpbz)_2$ matches perfectly, signifying a complete conversion of **1b** to **6b** (Figure 3.9).

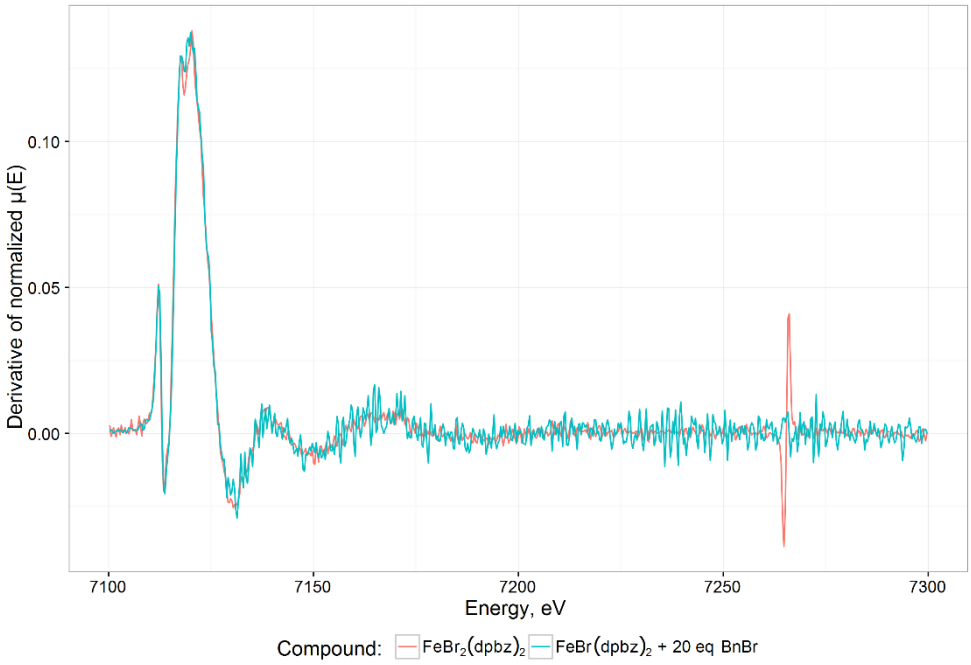

Figure 3. 9 Comparison of the XAS of the Negishi reaction between BnBr + $FeBr(dpbz)_2$ in THF and $FeBr_2(dpbz)_2$

3.3 Monitoring the catalysis using $FeBr_2(dpbz)_2$

To identify the different species of Fe present in the catalytic reaction, a flow experiment was devised in which the reaction progress will be monitored at different distances. In this experiment, collecting at a certain distance in the flow cell correlates to directly proportional reaction time, and different ratios of the concentration of Fe species will be expected to be detectable, which will be shown as the overall oxidation state of Fe. The catalytic reaction was conducted in the flow experiment. The results of this experiment are still being analysed. A preliminary analysis showed that there exist different distributions of Fe species through the time of reaction.

3.3.1 Kinetic exploration of the Negishi cross-coupling reaction catalysed by $FeBr_2(dpbz)_2$ vs $FeBr(dpbz)_2$

A kinetic study was undertaken by Messinis using a ReactIR. The speed of reaction of the cross-coupling of benzyl bromide and $Zn(4\text{-tolyl})_2$ using $FeBr_2(dpbz)_2$ (**1b**) and $FeBr(dpbz)_2$ (**6b)**

were compared. This experiment showed that the reaction using **1b** proceed faster than with **6b**. (Figure 3.10). Also, an induction period was observed when **6b** is used as the pre-catalyst, indicating an activation period in which the pre-catalyst is transformed into the active species. Therefore, **6b** cannot be an active intermediate in the catalytic cycle.

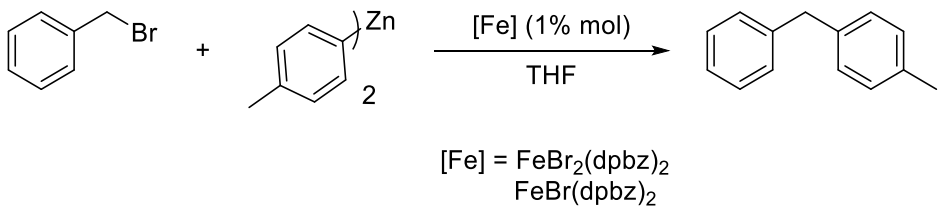

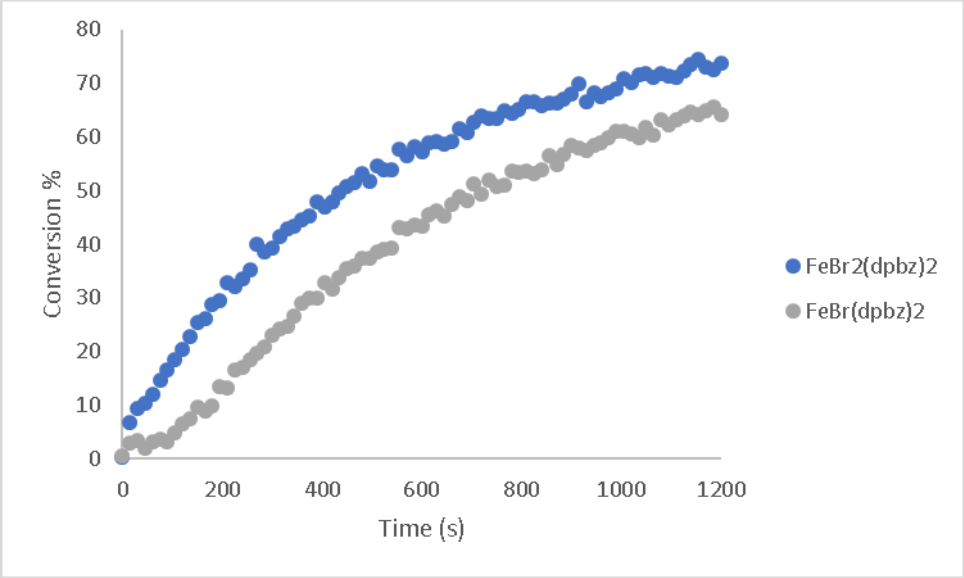

Figure 3. 10 Reaction profiles of the production of the cross-coupled product in the standard Fe catalysed Negishi reaction exploiting $FeBr_2(dpbz)_2$ and FeBr(dpbz) as the catalyst.

What is the role of Fe(I)? A plausible answer is that the complex **6b** is a stable product of the reaction of **1b** with Zn(4-tolyl)$_2$. Even though there is an excess of nucleophile in the catalytic conditions, the slower reaction using $FeBr(dpbz)_2$ demonstrates that this species must be a pre-catalyst which transforms to the active catalyst, producing an induction time in which the activation is taking place. The lack of induction time in the case of the Fe(II) species is showing that this complex could be the active catalyst, or a quick transformation produces the active species faster than Fe(I).

Having eliminated Fe(I) as the active catalyst, it was of interest understand more the mechanism of the cross-coupling using **1b** as the catalyst. A kinetic study was undertaken to get more insight into the reaction.

3.3.2 Kinetic analysis of the Negishi cross-coupling catalysed by $FeBr_2(dpbz)_2$

Messinis performed kinetic studies to get the order of reaction for the different reagents involved in the catalysis. The rate law is shown in equation 7

$$V = [FeBr_2(dpbz)_2]^2[Zn(4\text{-tolyl})_2]^0[BnBr]^0 \quad (7)$$

It was then analysed to what extent the dpbz affects the order of reaction. The reaction was conducted using **6b** as the precatalyst, showing a zeroth order of reaction. If instead of **6b** the salt $FeBr_2$ was used in the reaction, with an excess of dpbz, the second order of reaction with respect to $FeBr_2$ was calculated. The order of reaction of dpbz using $FeBr_2$ as pre-catalyst was first order when the ratio dpbz: Fe was below 2:1 (equation 8); at bigger dpbz:Fe ratios a zeroth order in dpbz was obtained (equation 9) with

$$v=k[FeBr_2]^2[dpbz][Zn(4\text{-tolyl})_2]^0[BnBr]^0 \quad (8)$$

$$v=k[FeBr_2]^2[dpbz]^0[Zn(4\text{-tolyl})_2]^0[BnBr]^0 \quad (9)$$

In summary, the reaction does not have a dependence on the concentration of BnBr or $Zn(tolyl)_2$. Ligand dpbz showed a first-order dependence with ratios of concentration Fe:Zn below 2:1, becoming order zero at higher ratios. A second-order dependence of reaction on the Fe was found.

3.4 Conclusion and future work

The slower speed of the catalysis using Fe(I) compared to the use of Fe(II), has excluded **6b** from being the active species of the reaction. In the oxidative addition experiments of **1b**, it

was shown that the reaction had a complex mechanism of reaction with fractional orders of reaction. The nature of the overall order of the oxidative addition may account for the induction time observed when **6b** is used as the pre-catalyst, with the oxidation of Fe(I) to the active catalyst delaying the reaction. It is suggested that under catalytic conditions, **6b** is oxidised to an active Fe(II) species. This putative Fe(II) must be more readily available using complex **6b**, demonstrated by the lack of induction period and a faster speed of reaction.

Although the experimental results indicate that **6b** is the active species, its formation under catalytic conditions is not completely excluded. The order of reaction concerning $FeBr_2(dpbz)_2$ indicates a bimolecular reaction. It is probable that two distinct Fe centres are at play in the reaction. After the speciation of Fe, the interaction between them could be the rate-limiting step of the reaction, explaining the second order found with the experiments. Formation of **6b** could be happening and consumed immediately upon contact with a Fe(II) complex and benzyl bromide, thus explaining the null concentration of Fe(I) over the reaction. A mechanism of the reaction is proposed in Scheme 3.3, where a Fe(II) complex transmetallates with the zinc reagent. At the same time, Fe(I) is produced, and upon losing a ligand dpbz, reacts fast with benzyl bromide producing a benzyl radical and a bimetallic adduct that regenerates the active species.

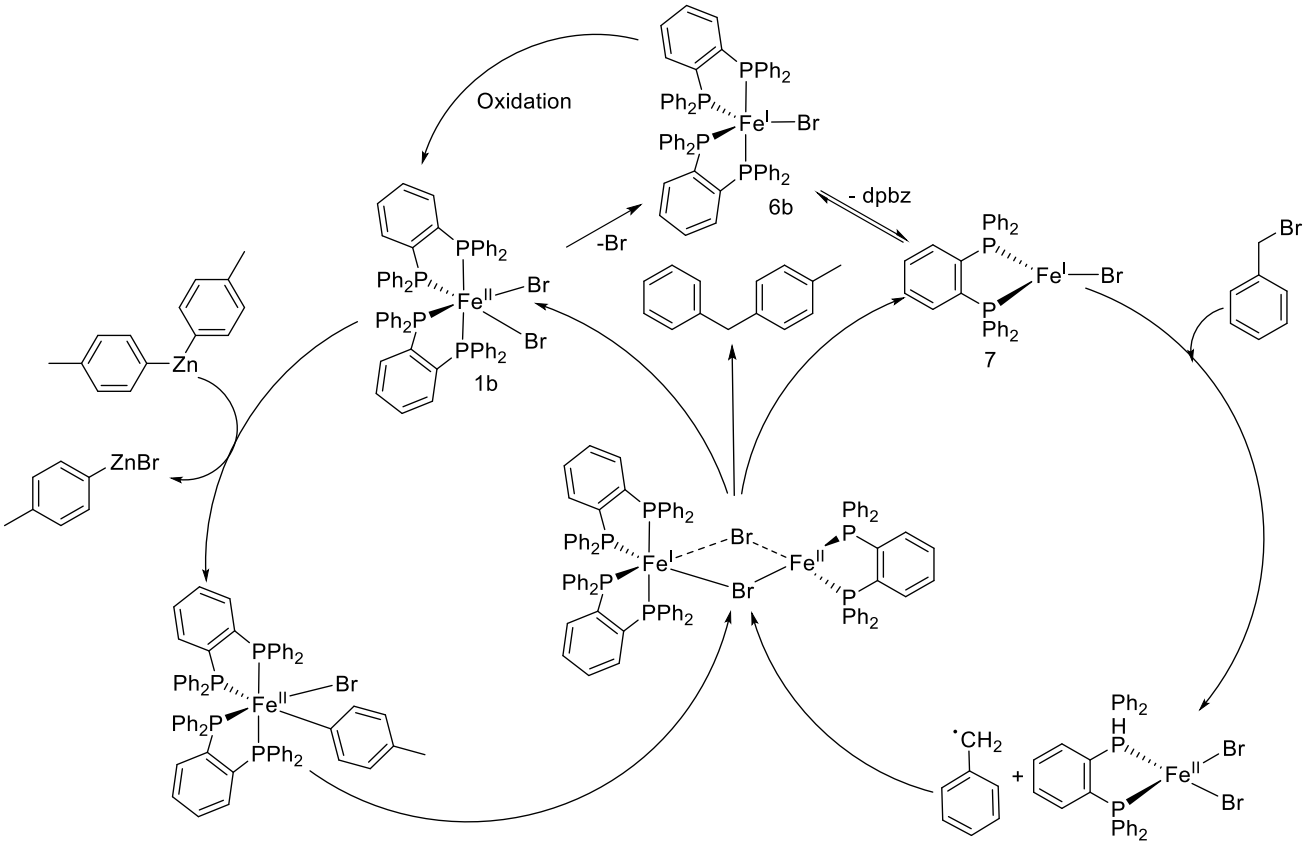

Scheme 3.3 Mechanism of the reaction involving a bimolecular reductive elimination of two different Fe species where the bimolecular reductive elimination is the rate-limiting step

The orders of the reaction in the catalysis using **6b** as the catalyst will provide evidence of the validity of this mechanism.

The X-ray spectroscopy is a technique that provides information about the oxidation state of an atom, the ligands surrounding it and the geometry. In the recordings conducted in this study, it was confirmed the transformation of 1**b** into **6b** with an excess of $Zn(4\text{-tolyl})_2$. Also, the reaction of BnBr with complex **6b** generated a species with the same profile as the one of **1b**.

The flow experiment results will provide evidence of the overall oxidation state of the ligand at different times in the reaction, providing more evidence of the validity of the mechanism, or provide enough evidence to propose other more consistent with the results obtained.

Chapter 4. Developing a novel Manganese-catalysed Negishi cross-coupling system.

4.1 Introduction

Manganese is an excellent candidate for catalysis due it being an inexpensive, non-toxic, abundant metal. Economically and environmentally speaking, manganese has similarities to iron, making it a promising alternative.[136] Despite this, manganese-based catalysis has not had the same attention as other earth-abundant metals like iron and cobalt.

Manganese is a unique element as it can exist in ten oxidation states (ranging from -3 to +7), which means an excellent potential for redox activity. It can also form compounds with a coordination number of up to 7 which is atypical for 1st row metals. [137] It is well known in oxidation chemistry, like $KMnO_4$. The chemistry of some manganese compounds can show similarities to main group compounds (for example, RMnX behave similarly to Grignard reagents).[138] In the last 5-10 years, reports for new applications of manganese compounds have been revealed, such as oxidation of organic compounds, hydrosilylation, chlorination, and cross-coupling reactions. Following some of the advances in manganese chemistry are summarised here.

4.1.1 Manganese Catalysis

The conversion of alkenes to diazides was reported by Fristad and co-workers using stoichiometric amounts of Mn^{III} acetate as a radical initiator, and NaN_3 as the azide source (Scheme 4.1).[139] Other reports of azidation are hydroxyazidation of alkenes using $MnBr_2$ as catalyst,[140] and azidation of cylclobutanol by C-C bond cleavage catalysed by $Mn(OAc)_3$.[141]

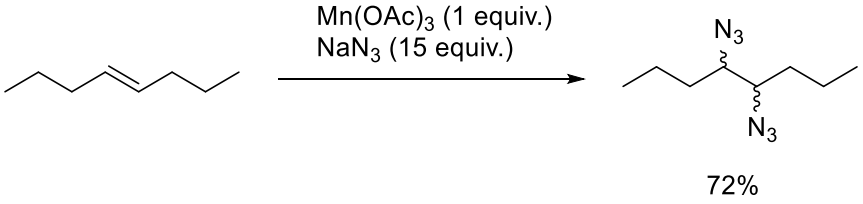

Scheme 4. 1 Diazidation of alkenes

$Mn(dmp)_3$ has been reported to catalyse the alkene reduction of α,β-unsaturated ketones.[142] This compound has also been used in the hydrogenation of cyclic alkenes to give a *trans*-diastereomer. Compared to the Pd/C systems, manganese showed more diastereoselectivity (Scheme 4.2).[143]

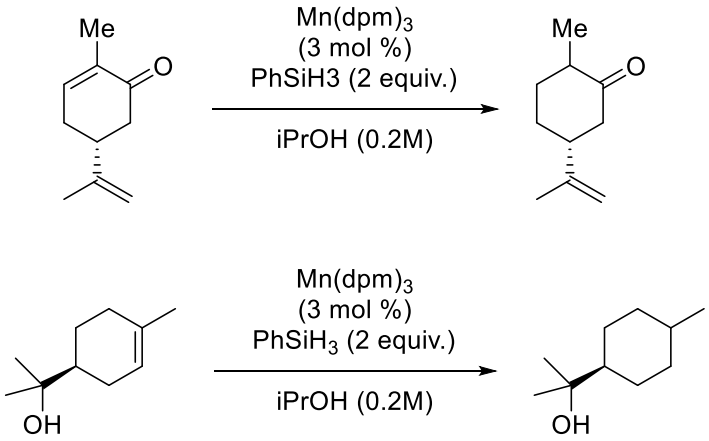

Scheme 4. 2 Hydrogenation of alkenes

C-H activation is a significant field of chemistry because it allows for an increase in atom economy by removing the need for pre-functionalised substrates; therefore, many reaction steps can be avoided which translates to a decrease in waste. Groves and co-workers reported the oxidation of hydrocarbons via hydroxylation of inactive C-H bonds by metalloporphyrin compounds (Scheme 4.3). [144]

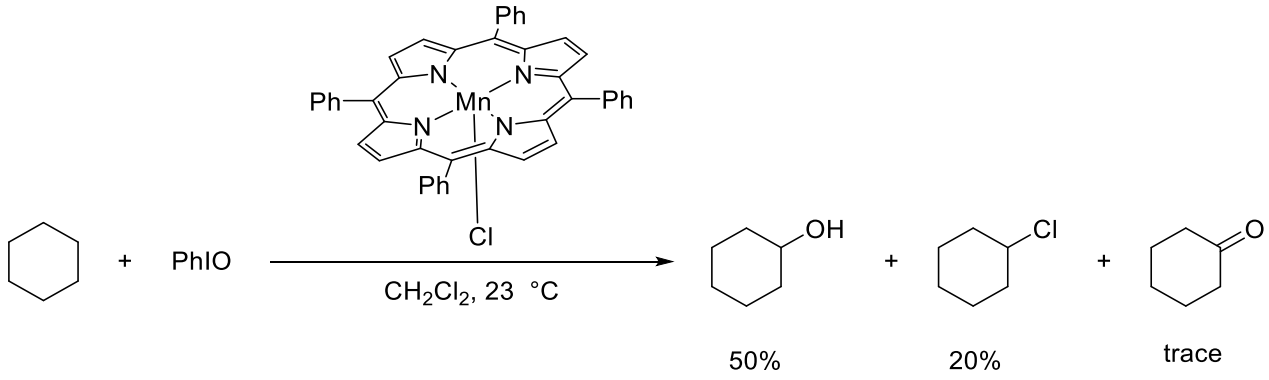

Scheme 4. 3 Oxidation or chlorination of cyclohexane mediated by manganese-Porphyrin

The oxidation of C-H bonds was also reported with tetradentate amine ligands on Mn^{II} centres. Nam and co-workers described the oxidation of alkanes using a manganese oxo complex [145]. Other successful manganese compounds that showed activity for C-H oxidation are tetraamino complexes,[146] and tetracyano pyramidal complexes of Mn^{V}. [147]

The halogenation of C-H bonds happens as a side-reaction in C-H oxidation reaction. Efforts were made to understanding more about this reaction in order to see if it could, in fact, become a useful reaction. Groves improved the selectivity of the halogenation by changing the axial ligand to a stronger donor (Scheme 4.4).[148] This methodology was later expanded to the fluorination of C-H bonds.

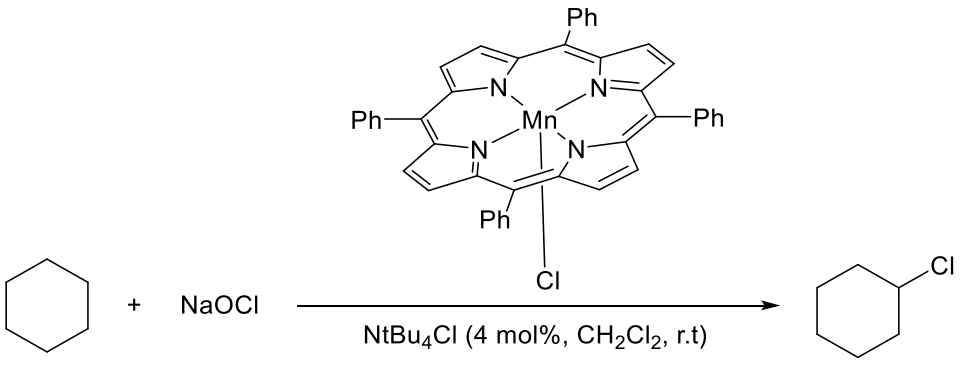

Scheme 4. 4 Chlorination of C-H bonds of simple hydrocarbons.

Hartwig reported the borylation of benzene and pentane through photoirradiation of manganese(I) carbonyl compounds (Scheme 4.5).[149]

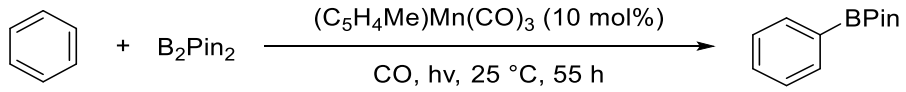

Scheme 4. 5Borylation of C-H bonds using a manganese carbonyl compound

Acyl manganese species can be hydrosilylated using Ph_2SiH_2. Hydro-silylation of ketones and esters was also achieved, yielding the silyl ether[150] and ether products respectively[151] (Scheme 4.6).

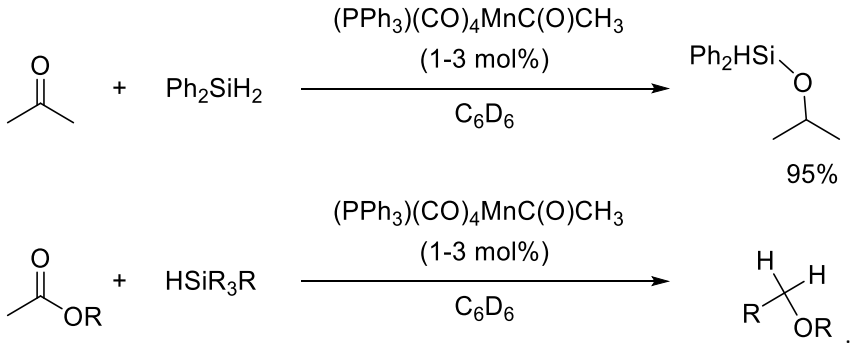

Scheme 4. 6Reduction of ketones and esters to ethers using manganese compounds.

Reduction of dimethylformamide was reported using manganese carbonyl compounds under irradiation of light. Carboxylic acids could be reduced to aldehydes using the same methodology.[152] Lavigne and co-workers reported the reduction of a variety of aryl and aliphatic aldehydes and ketones under UV irradiation using an N-heterocyclic carbene manganese complex (Scheme 4.7).[153]

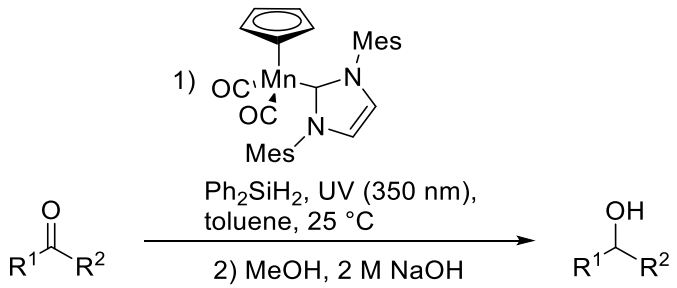

Scheme 4. 7 Hydrosilylation of carbonyls

Carbon-carbon and carbon-heteroatom bonds can be formed via carbometallation of olefins. Oshima and co-workers performed some transformations of alkynes to a range of products using an allylmagnesium bromide and manganese salts. Generation of an alkenyl Grignard reagent is followed by reaction with an electrophile. Where the electrophile is a vinyl ether, rearrangement to a diene product takes place (Scheme 4.8).[154]

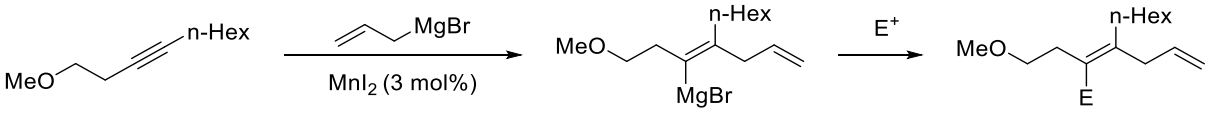

Scheme 4. 8 Carbometallation of alkynes

Takayi and co-workers studied the C-H activation of aryls in the presence of $HSiEt_3$, inserting aldehydes to produce benzylic silyl ethers. In this reaction, an imidazole would function as a directing group to give the ortho product (Scheme 4.9).[155]

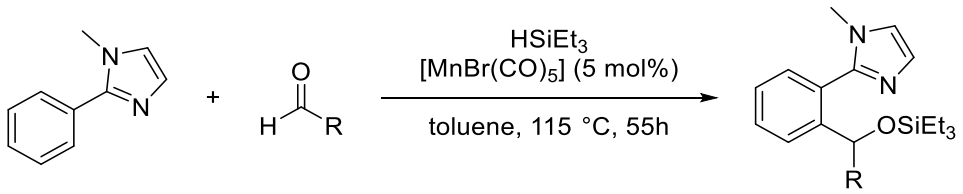

Scheme 4. 9 Mn catalysed insertion of an aldehyde to a C-H bond.

If the silane is replaced with a Lewis acid, the benzyl alcohol is obtained (Scheme 4.10).[156]

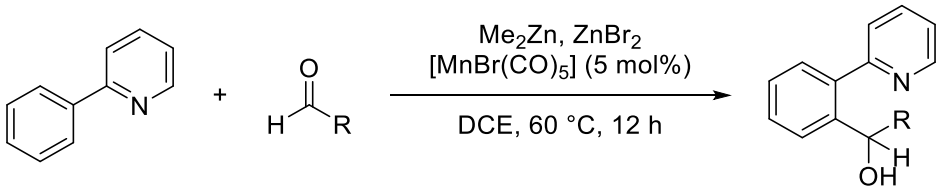

Scheme 4. 10 Mn catalysed insertion of aldehyde into an aryl C-H bond.

Wang expanded this methodology to the insertion of an alkyne to give styrenes (Scheme 4.11). The presence of a nitrogen-based directing group is necessary, suggesting deprotonation of the arene and then the formation of a manganacycle (Scheme 4.11, A).[157] The corresponding system using a benzylic imine group instead of the pyridine directing group yielded the [4+2] annulation takes place bearing an isoquinoline (Scheme 4.11, B).[158] Protection of the imine with a phenyl and using alkenes with an ester substituent as the substrate produced a cyclic cis-β-amino acid (Scheme 4.11, C).[159]

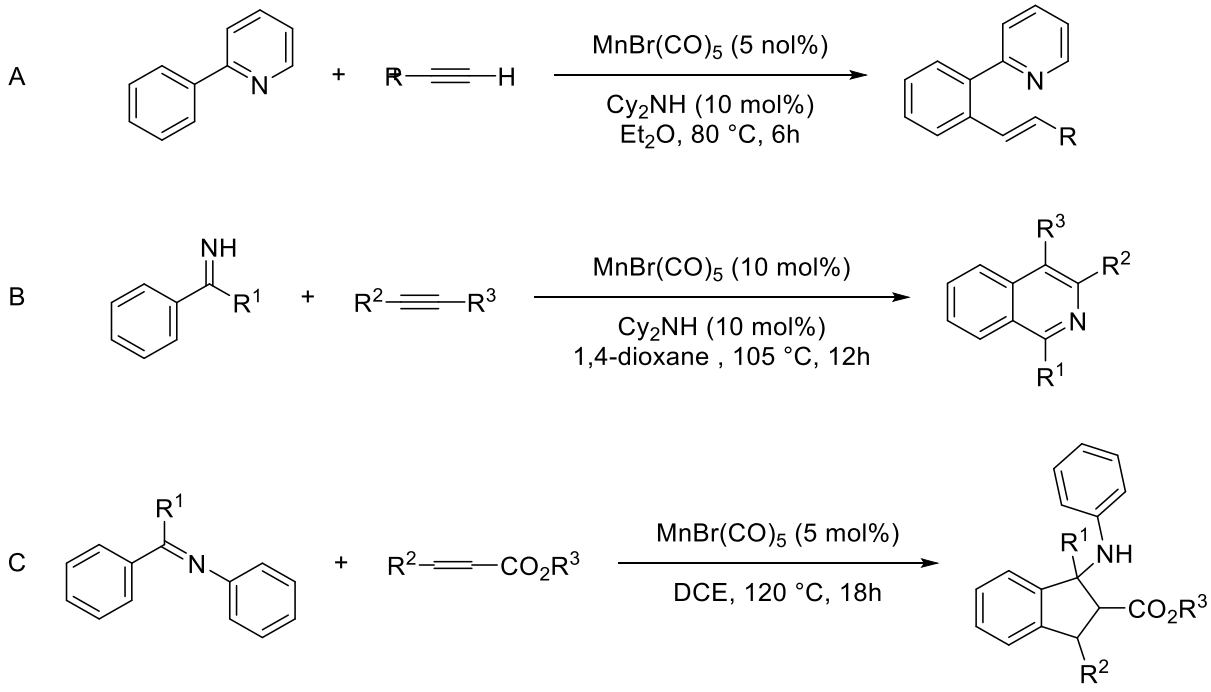

Scheme 4. 11 C-H activation of arenes A) alkyne partner, B) annulation of imines, C) annulation of protected imines.

4.1.2 Manganese catalysed cross-coupling

Manganese has been used as a catalyst for the Stille cross-coupling reactions for sp^2-sp^2 bond formation. NaCl was required as an additive, and not many substrates were suitable as electrophiles, being limited to just aryl- and alkynyl-iodine reagents. Aryl and alkenyl stannanes were optimal candidates as nucleophiles.[160] This reaction needed harsher conditions than the analogous palladium catalysed reaction (Scheme 4.12).

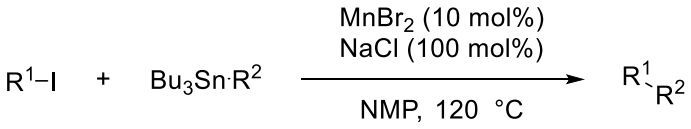

Scheme 4. 12 Stille cross-coupling with manganese salt.

Cahiez and co-workers developed the formation of aryl-aryl bond from an aryl chloride and Grignard reagents catalysed by a simple manganese salt.[161] This reaction was able to tolerate ketones when simple PhMgBr was used, but the aryl halide electrophiles required an electron withdrawing substituent in order for the reaction to proceed. The methodology was expanded by Rueping to include heterocycles containing nitrogen with aryl- and alkyl Grignard reagents (Scheme 4.13).[162] Later Cahiez reported the use of alkenyl halides as coupling partners for the reaction.[163]

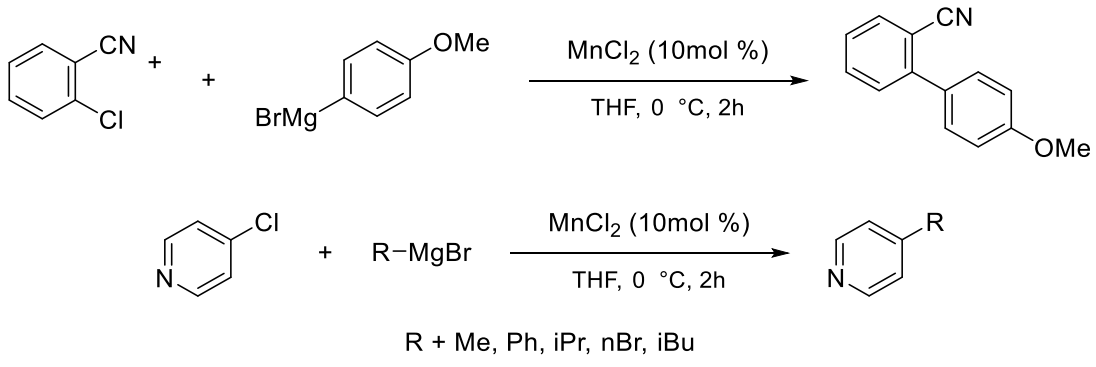

Scheme 4. 13 Coupling of aryl Grignard reagents with aryl chlorides with electron-withdrawing functionalities and nitrogen-containing heterocycles as electrophiles.

$MnCl_2$ was shown to be competent for the coupling of Grignard reagents to *gem*-dibromocyclopropanes; the addition of an electrophile functionalises further the substrate (Scheme 4.14).[164]

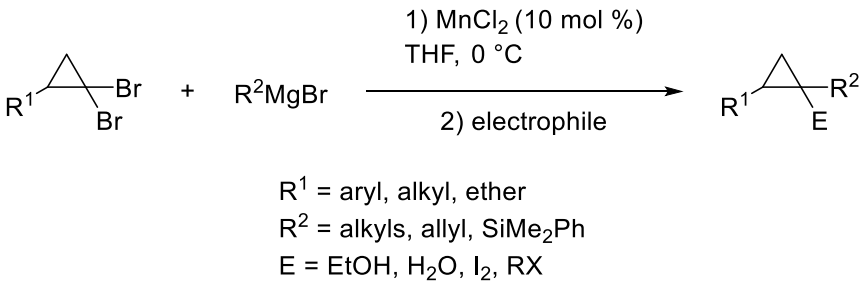

Scheme 4. 14 gem-dibromo cyclopropane cross-coupling

The homocoupling of Grignard reagents has been developed using $MnCl_2$, as the pre-catalyst where oxygen or dichloroethane serves as the oxidant. Heteroaromatic substrates did not react using this methodology. Alkyl chlorides were successfully homocoupled with good results (Scheme 4.15).[165,166]

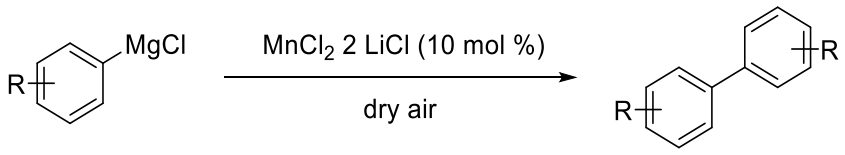

Scheme 4. 15 Manganese homocoupling using DCE as an oxidant.

Teo and co-workers reported the cross-coupling reaction of a range of nitrogen-containing heterocycles with aryl iodides. This reaction requires trans-1,2-diaminocyclohexane and K_3PO_4 H_2O. (Scheme 4.16). This methodology was screened successfully for a number of aryl iodides, tuning the electronic character of the substituents in the aryl group. However, *ortho*-substitution did now work in any case.[72] This method was tested with good results on aliphatic amines using L-proline as ligand and NaOtBu as the base.[167]

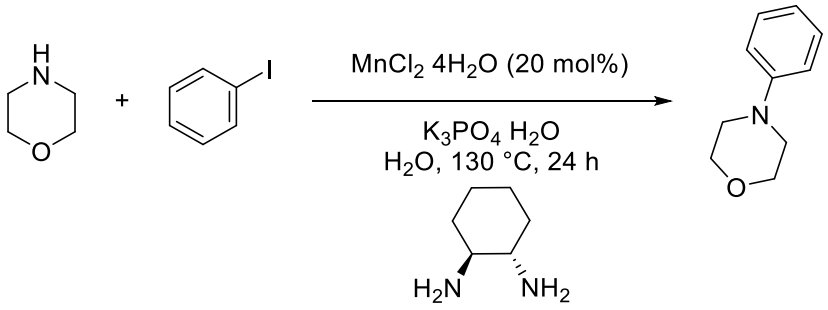

Scheme 4. 16Cross-coupling with heteroaromatic nitrogen nucleophiles and aryl iodides.

Liu and co-workers studied the use of $MnCl_2$ and phenanthroline ligand to cross-couple thiols and aryl iodides to form a variety of thioethers (Scheme 4.17).[168]

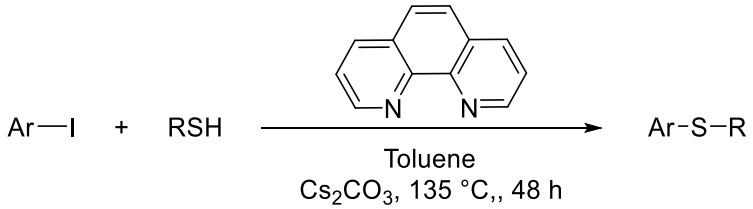

Scheme 4. 17 Cross-coupling of sulphur nucleophiles with aryl iodides.

Manganese compounds have been shown to catalyse various homocoupling and cross-coupling reactions. Both $MnCl_2$ and $MnBr_2$ are competent for the homo-coupling of organotin compounds. However, to this date, there have been no reports of cross-coupling reactions using Zinc reagents or boron complexes. Initial studies were undertaken on the cross-coupling reaction of ditolylzinc and benzyl bromide. Benzyl bromide was chosen because it is shown to be more active than its chloride in the corresponding iron-catalysed reaction, and ditolylzinc was chosen as it has been reported that the cross-coupling of aryl Grignards is more efficient than that of alkyl derivatives.[169] A range of manganese sources and ligands were tested, as well as different conditions for the reaction to obtain a new catalytic system for Negishi cross-coupling.

4.2 Results and discussion

Different manganese compounds were screened in order to see if they have any catalytic activity. Surprisingly, $MnCl_2$ had an almost non-existent activity compared to the other precursors (Table 4.1, entry 1); a higher activity was expected due to its previously reported activity in Grignard reagents cross-coupling reactions.[62,162,170,171] $Mn_2(CO)_{10}$ and $Mn(acac)_3$ showed little activity as well (Table 4.1, entry 3 and 4). $MnBr_2$, displayed the highest activity, although little selectivity as most of the products were homocoupling products.

Table 4. 1: Manganese salts test for Negishi cross-coupling

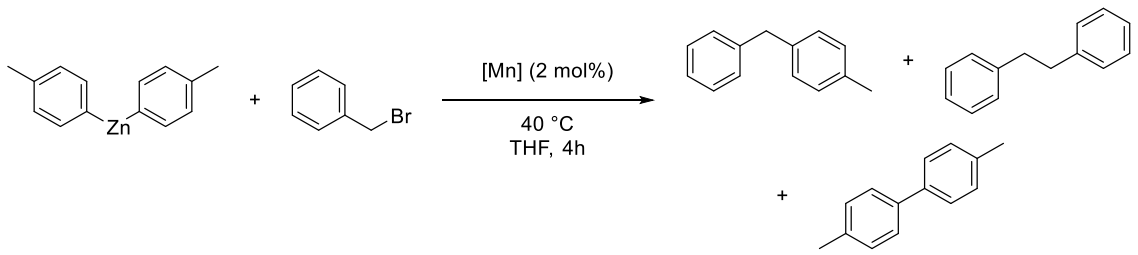

Entry	Manganese salt	Cross-coupling product (%)	Homocoupling electrophile (%)	Homocoupling nucleophile (%)
1	$MnCl_2$	0.01	0	1.4
2	$MnBr_2$	3.8	30.3	37
3	$Mn_2(CO)_{10}$	0.3	8.8	1.6
4	$Mn(acac)_3$	1.88	5.1	7
5	No metal	1.3	1.5	2.1

Iron catalysed Negishi cross-coupling has been conducted using chelating diphosphine ligands with great success.[99] With this antecedent, it was decided to test the influence of the ligand dpbz. Incremental amounts of the ligand were tested (Table 4.2)

Table 4. 2 Effect of dpbz ligand concentration.

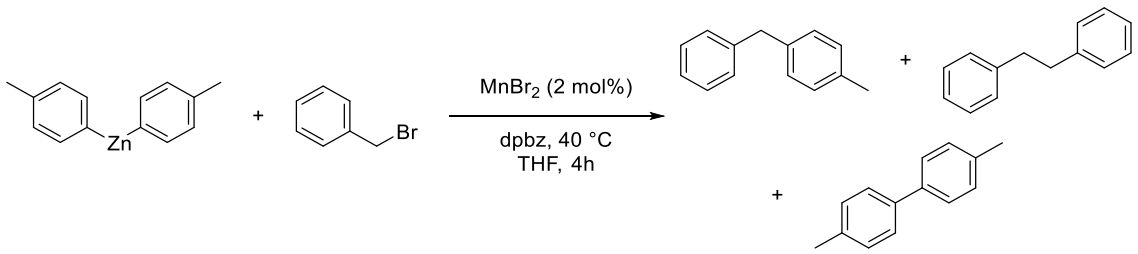

Entry	Amount of Ligand (%)	Cross-coupling product (%)	Homocoupling electrophile (%)	Homocoupling nucleophile (%)
1	2	6.9	9.6	10.9
2	4	9.9	16.2	19.1
3	8	6.7	13.9	16.8
4	16	4.2	5.8	6.5

When the ligand dpbz is added, the homocoupling seems to be slightly inhibited compared to the absence of ligand (Table 4.2, entry 5), and the proportion of cross-coupling reaction increases. Nevertheless, the conversion to homocoupling side-products is favoured. This result could be due to the ligand over-protecting the catalyst, inhibiting its activity. Addition of 2 equivalents of the ligand with respect to the Mn gives the highest yield of cross-coupled product (Table 4.2, entry 3), although the presence of side-products is still noticeably higher. Based on these findings, these conditions were chosen as the standard for the rest of the study.

It was suggested that an increase in the amount of catalyst loading could result in a positive change to the conversion of substrates (Table 4.3). However, using 5 % and 10% of the salt proved to have a detrimental effect on the conversion to any product.

Table 4. 3 Effect of concentration of $MnBr_2$

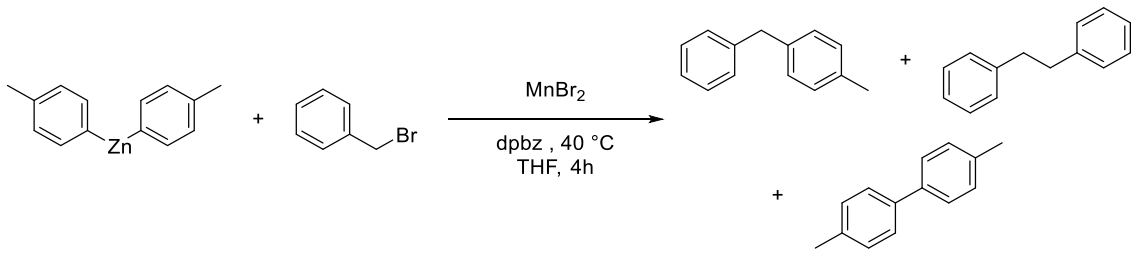

Entry	Amount of $MnBr_2$ (%)	Cross-coupling product (%)	Homocoupling electrophile (%)	Homocoupling nucleophile (%)
1	5	6.5	8.1	8.9
2	10	3.8	6.9	9.1

It was then decided that the suppression of the homocoupling reactions was the first course of action in order to improve the selectivity of the cross-coupling reaction. In order to try and improve the selectivity of the reaction, the reaction temperature was reduced to 0 °C (Table 4.4, entry 1) and 20 °C (Table4.4, entry 2). In both cases, the change in temperature did not suppress the homocoupling reaction, leading only to reduced activity of the catalyst. Alternatively, the reaction temperature was increased. An increase in the reaction temperature was also attempted, again with detrimental results, without any sign of the homocoupling products diminishing.

Table 4. 4 Temperature trial

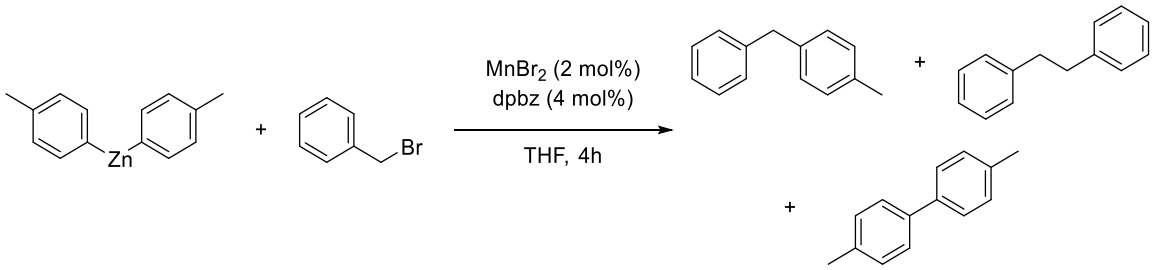

Entry	Temperature (°C)	Cross-coupling product (%)	Homocoupling electrophile (%)	Homocoupling nucleophile (%)
1	0	1.8	2.8	3.1
2	20	4.7	7.5	8.0
3	40	7.8	12.1	18.0
4	60	4.2	5.9	8.0

It has been reported that the presence of oxidising agents such as aryl halides catalyse the homocoupling of Grignard reagents with Fe catalyst.[172] Similarly, the presence of reducing agents promote the homocoupling of benzyl halides;[173,174] nucleophilic reagents, like zinc reagents used in this reaction, are considered to have a reducing nature.[134] It was suggested that a stepwise addition of the nucleophile or the electrophile would provide a more controlled environment, where the nucleophile would be pre-activated by a transmetallation, or an oxidative addition of the electrophile. Subsequent addition of the second coupling partner would initiate the cross-coupling reaction. This reaction was set up, and the addition of the second substrate was done after 10 minutes of the addition of the first one. (table 2.5). Little difference was seen from the standard conditions (Table 4.5).

Table 4. 5 Stepwise addition of substrates

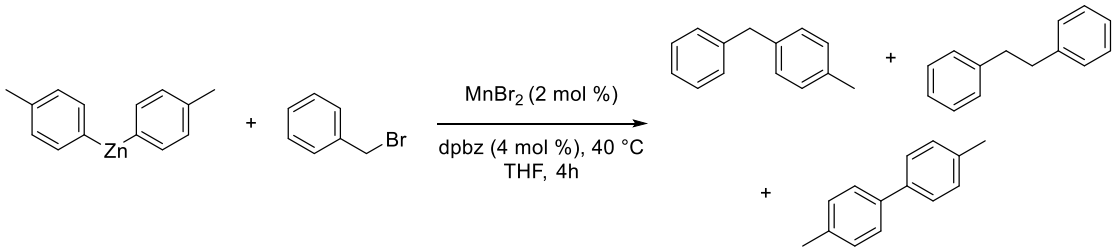

Entry	Condition	Cross-coupling product (%)	Homocoupling electrophile (%)	Homocoupling nucleophile (%)
1	Activation with Electrophile	6.5	9.6	10.7
2	Activation with nucleophile	7.5	10.8	12.2

The use of additives has been reported as a method for promoting or suppressing of homocoupling reactions and facilitate the conversion to the cross-coupling product. [72] For example, NMP has been shown to improve the homocoupling of alkyl halides.[1] Potassium formate inhibits the homocoupling in palladium-mediated homocoupling in Suzuki cross-coupling.[175] Potassium fluoride has been used to suppress the homocoupling in the iron-catalysed biaryl coupling.[71,84,176] Considering the effect that some organic additives and salts have, a range of reagents were tested to observe their influence on the reaction studied. The amount of additive used was 10% mol (Table 4.6). In all cases, the use of the additive diminished the conversion to all products without promoting the cross-coupling. Use of dmpu, NaCl and KCl (Table 4.6, entries 1, 4 and 5) seem to be detrimental to the yield of cross-coupled product.

Table 4. 6: Effect of additives

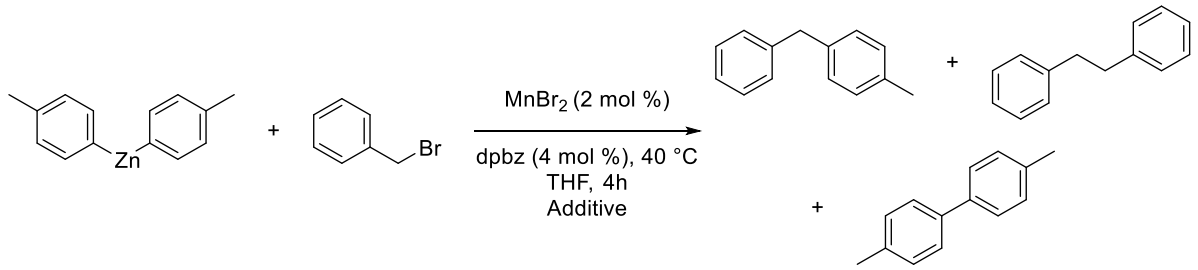

Entry	Additive	Conversion to Cross-coupling product (%)	Conversion to Homocoupling product of electrophile (%)	Homocoupling nucleophile (%)
1	dmpu	3.4	7.2	8.5
2	nmp	7.1	11.3	13
3	KF	7.4	9.8	11
4	NaCl	3.3	7.5	9.1
5	KCl	2.6	6.4	8.1

Some ligands have shown to suppress homocoupling. The use of pybox-type ligand has been shown to promote cross-coupling and inhibit homocoupling in the alkyl-alkyl reductive cross-coupling.[174] In the direct iron-catalysed cross-coupling of aryl bromides with alkyl halides in the presence of stoichiometric amounts of magnesium turnings, TMEDA was competent at inhibiting the conversion to undesired side-products.[177] Adducts of Fe dppp or dpbz ligands have shown to suppress homocoupling in the iron-catalysed Negishi coupling of benzyl halides and phosphates.[97] Terpyridine ligands suppressed the formation of homocoupling product entirely in the nickel-catalysed Negishi cross-coupling of secondary alkylzinc halides and aryl iodides.[178] For this reason, the use of different ligands was addressed with the aim of improving the selectivity of the reaction. (Table 4.7). In most cases, a reduction in the conversion to any product except when bathophenanthroline was used (Table 4.7, entry 21), which reduced the cross-coupling product yield in comparison to the homocoupling products.

Table 4. 7 ligand screening

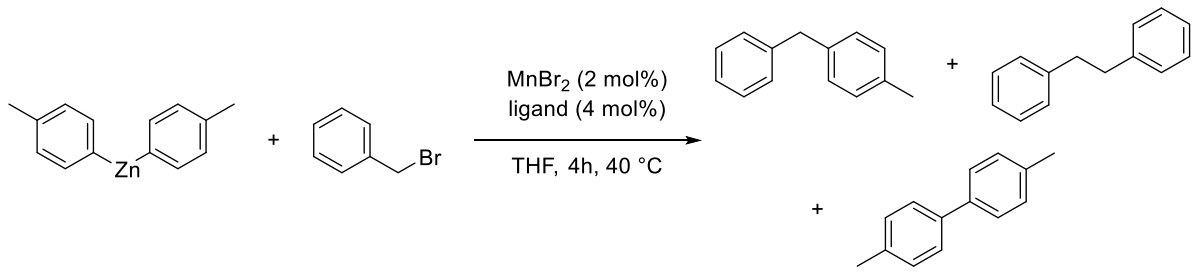

Entry	Ligand	Conversion to Cross-coupling product (%)	Conversion to Homocoupling product of electrophile (%)	Homocoupling nucleophile (%)
1	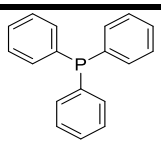	0	0	0
2	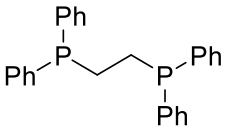	1.63	4.1	4.9
3	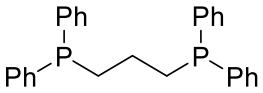	3.2	5.5	6.8
4	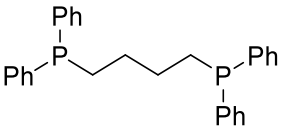	1.8	3.1	4.1
5	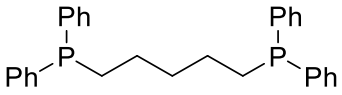	1.8	2.8	3.6
6	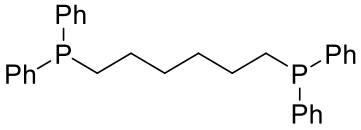	6.9	2	15.2
7	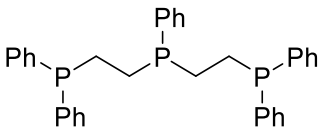	0	1.0	0

8	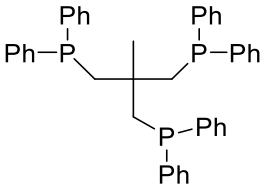	2.3	4.0	5.0
9	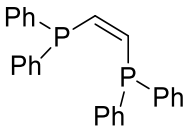	0	0	0
10	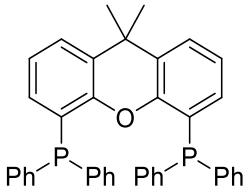	1.8	1.4	1.9
11	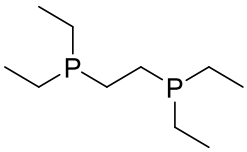	2.2	4.0	4.9
12	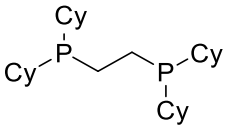	1.6	1.0	1.6
13	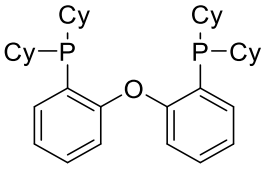	1.7	1.0	1.4
14	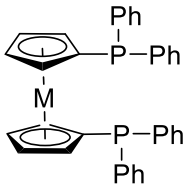	6.7	3.4	5.6
15	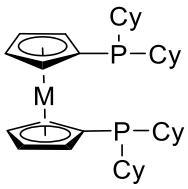	13.3	7.0	10.6
16	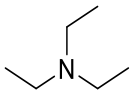	2.3	1.2	1.9

17	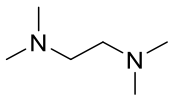	2.3	2.1	2.7
18	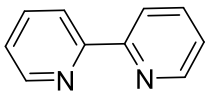	2.4	1.9	3.1
19	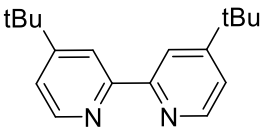	3.6	4.7	6.2
20	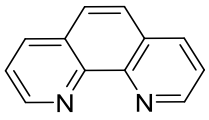	2.5	2.0	3.3
21	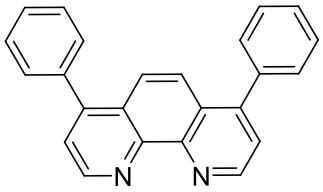	3.1	10.9	13.7
22	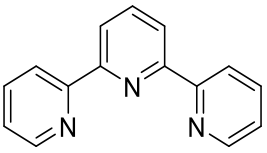	2.3	2.1	2.7

Changes in reaction solvent have been shown to have a profound influence on the results of the reaction; accordingly, a solvent screen was carried out (Table 4.8). Although there are some differences between the results obtained in these reactions, they are not noteworthy. There does not seem to be any consistent trend derived from polarity or chemistry aside from the high polarity of acetone seeming to act as a quench of reaction or addition of Zn(4-tolyl)$_2$ to the ketone group in acetone which has been reported by Takai[155] (Table 4.8, entry 5). No improvement to selectivity was reached with any of the solvents tested, with most of cross-coupling and homocoupling ratios staying similar.

Table 4. 8 Solvent screening

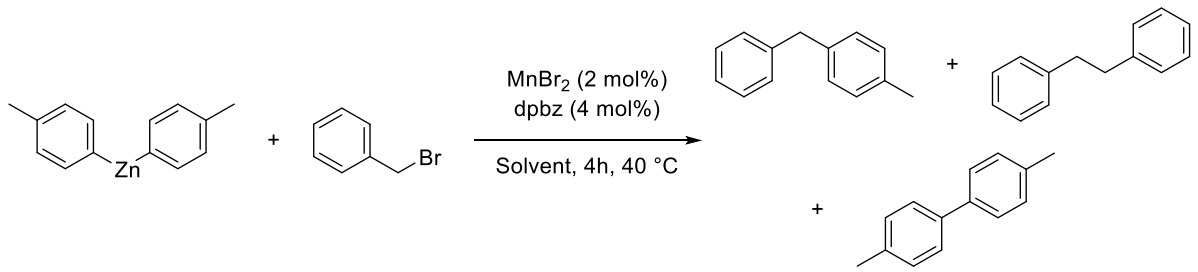

Entry	Ligand	Conversion to Cross-coupling product (%)	Conversion to Homocoupling product of electrophile (%)	Homocoupling nucleophile (%)
1	Toluene	10.7	15.9	18.0
2	PhF	10.6	17.1	19.4
3	DMPU	3.5	4.6	5.6
4	Hexane	8.4	12.7	14.3
5	Acetone	0	0	1.2
6	Diethyl ether	8.4	10.2	11.3
7	DME	6.8	10.5	12.1
8	Dioxane	2.1	1.5	1.8
9	MTBE	6.7	9.4	10.5

4.3 Conclusions and future work

The manganese catalysed Negishi cross-coupling remains a difficult challenge in spite of the range of conditions investigated. In addition to poor conversion, no improvement in selectivity to any one of the possible products was achieved. Additionally, the low selectivity of the products was never improved towards the cross-coupling or the side-products.

Manganese cross-coupling of Grignard reagents has been reported, so it is possible that the zinc reagents used in this investigation were not capable of sufficiently activating the metal. It is predicted that the use of boron compounds would yield an even lower activation using manganese considering that they are even softer nucleophiles.

Another reason for the low conversions obtained is that the manganese could react with one or more of the reagents used in the reaction, and is poisoned, not allowing it to react fully with the substrate.

In this study, only benzyl bromide was tested as the electrophilic partner of the cross-coupling. Aryl halides and alkyl halides could have different reactivity with manganese. Testing of these reagents is unquestionably a step to take

Also in this work, only 4-tolyl zinc was used as the nucleophile. The use of alkyl and vinyl zinc reagents could provide better results for the Negishi Cross-coupling.

Chapter 5. Experimental

5.1. General experimental procedures

Unless otherwise stated, all reactions were carried out under an atmosphere of dry nitrogen using standard Schlenk line techniques or in an argon-filled M. Braun glovebox. All glassware was flame dried with a heat gun and backfilled with nitrogen gas prior to use. Dry solvents were obtained from a Grubbs solvent purification system. Acetone was dried by distillation from boric anhydrite. All solvents were degassed prior use by freeze-pump-thaw cycles.

All chemicals were purchased from common chemical providers and used as received.

UV-Vis spectra were recorded in solution using an Applied Photophysics SX20 Stopped-Flow spectrometer with a xenon arc lamp, monochromator, photomultiplier tube (PMT) detector and a photodiode array. Dip-probe UV-Vis spectra were acquired with an Ocean Optics TP300-UV-VIS Transmission Dip Probe coupled to a DT-MINI-2-GS Deuterium Tungsten Halogen light source and USB2000+UV-VIS-ES detector.

EPR experiments were carried out at Cardiff University under the supervision of Dr Emma Richards, on a Bruker ESP 300E series spectrometer operating at 100 Hz field modulation, 1 mW microwave power and equipped with a standard Bruker TE102 cavity. Spectra simulation was performed by Dr Emma Richards using the Sim32 and EasySpin software packages.

Fe k-edge XAS studies were carried out on the B18 beamline at the Diamond Light Source, Didcot, U.K. All samples were measured in transmission mode. XAS data processing was performed using IFEFFIT with the Horae package (Athena).

5.2 Experimental Details for Chapter 2

5.2.1 Synthesis of $Zn(4\text{-tolyl})_2$

$ZnBr_2$ (5.62g, 24.95 mmol) was loaded in a round bottom flask with Young joint followed by addition of THF (76.8 mL) and (4-tolyl)MgBr (1.04 M, 48 mL, 49.9 mmol) to give a 200 mM solution of Zn reagent. No further purification was done. If a precipitate is present, this can be dissolved easily by warming the mixture at 35 °C.

5.2.2 Synthesis of $FeBr_2(dpbz)_2$

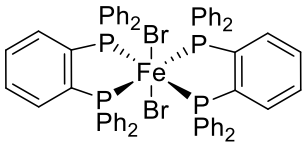

1b

$FeBr_2$ (465 mg, 2.20mmol) was loaded in a Schlenk tube. A suspension was made with 5 mL of THF. The mixture was heated at reflux until a homogeneous solution was obtained and then taken to dryness. The solid was dissolved in dry acetone (25 mL) and dpbz (1.964 g, 4.40 mmol) was added forming a yellow precipitate. The reaction was reflux for 30 min and left stirring overnight. The solvent was vacuum pumped until dryness and re-dissolved in DCM (20 mL), filtered, and layered with hexane (20 mL). Bright yellow crystals were filtrated, dried under reduced pressure yielding a yellow powder (1.60 g). Anal. Found: C, 65.52, H, 4.35. Calcd for $C_{60}H_{4\mathbf{10}}Br_2FeP_{4:C,}$ 65.01: H, 4.36.

5.2.3 Synthesis of $FeBr(dpbz)_2$

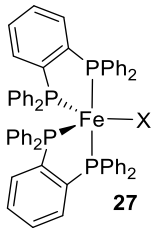

27

$FeBr_2$ (483.1 mg, 2.24 mmol) and dpbz (200 g, 4.48 mmol) followed by addition of THF (10 mL) were loaded in a Schlenk tube. The mixture was reflux until getting a homogeneous solution. KC_8 (7.522 mmol/g, 327.6 mg, 24.64 mmol) was added and the dark red mixture was left stirring at room temperature overnight. The dark red mixture was filtered via cannula and the filtrate was layered with hexane (10 mL) to give a first crop of the target compound. Consecutive crops yielded 62%. Anal. Found C, 69.79, H, 4.75. Calcd for $C_{60}H_{410}BrFeP_4$: C, 70.06, H, 4.70.

5.2.4 Spectroscopic studies of reaction mixtures (Section 2.3)

5.2.4.1 UV-Vis study of the iron catalysed Negishi Cross-coupling

A jacketed Schlenk equipped with an internal cooling coil was flame dried and then taken under vacuum. It was backfilled with dry nitrogen followed by insertion of the dip probe equipped with a rubber stopper to form an air-thigh seal. The Schlenk was evacuated and backfilled with dry nitrogen and the system was taken at the appropriate temperature using a cryostat. THF was added and a THF reference spectrum collected. Subsequently, $Zn(4\text{-tolyl})_2$ was added from a stock solution (250 mM or 200 mM) and the mixture was stirred. Collection of spectra was initiated. Fe complex was subsequently added in the form of a stock solution (40 mM or 20 mM). BnBr was added as a stock solution (2500 mM).

5.2.5 Kinetic studies on the oxidation of Fe(I) (Section 2.4)

5.2.5.1 UV-Vis spectra of Fe complexes

A Schlenk was loaded with **6b** with a stock solution (4.0 mM) diluted as necessary whose UV-Vis spectrum was recorded. The data collected were used to calculate the coefficient of extinction.

5.2.5.2 Stopped-Flow Setup

5.2.5.2.1 General procedure for UV-Vis reaction in the stopped-flow system inside the glovebox

Stock solutions of the reagents were prepared inside the glove box. The stopped-flow light source was set to 742 nm. The thermostat was set at the desired reaction temperature and the system was allowed to reach thermal equilibrium for 30 min. The system was cleaned with THF. Solutions of the pertinent reagents were loaded in the drive syringes. Three drives were conducted before starting data collection. 60 mL were driven and mixed into the reaction cell (20 mL volume). Within the reaction cell, the change in the absorbance with time at 742 nM was recorded by the PMT detector

5.2.5.2.2 $FeBr(dpbz)_2$ + BnBr + additives

A standard solution of BnBr (20mM) and **6b** (1.25mM) were prepared in THF. Standard solutions of LiBr, $MgBr_2$, $AlBr_3$, $ZnBr_2$, $Li[B(Ar_f)_4]$, dpbz.(1.25 mM, 2.5 mM, 5 mM, 10mM, 20mM) were prepared. **6b** was feed in the first drive syringe while BnBr and the additives in the second syringe. Data collection was done at 40 °C.

5.2.5.2.3 $FeBr(dpbz)_2$ + BnBr, Order in Benzyl Bromide

A standard solution of **6b** (2.5 mM) was prepared in THF. Standard solution of BnBr were prepared (0, 1, 2, 4,… equiv) in THF. Absorbance experiment were performed on the reaction mixture and each BnBr solution at 40 °C. **6b** was feed in the first drive syringe and BnBr in the second syringe.

5.2.5.2.4 $FeBr(dpbz)_2$ + BnBr Order in Iron

A standard solution of BnBr (40 mM) was prepared in THF. Standard solution of **6b** was made in the desired concentrations (0.124, 0.25, 0.5 and 1 equiv, with respect to BnBr) in THF. **6b** was feed in the first drive syringe and BnBr in the second syringe. Data collection was done at 40 °C.

5.2.5.2.5 $FeBr(dpbz)_2$ + BnBr +$ZnBr_2$, order in BnBr

A standard solution of **6b** (1.25 mM) and $ZnBr_2$ (20mM) were prepared in THF. Standard solutions of BnBr. (1.25 mM, 2.5 mM, 5 mM, 10mM, 20mM) were prepared in THF Absorbance experiments were carried out to the reaction mixture Data collection was done at 40 °C.

5.2.5.2.6 $FeBr(dpbz)_2$ + BnBr + $ZnBr_2$ order in $ZnBr_2$

A standard solution of **6b** (1.25 mM) and BnBr (20mM) were prepared in THF. Standard solutions of $ZnBr_2$ (1.25 mM, 2.5 mM, 5 mM, 10 mM, 20mM) were prepared in THF. **6b** was feed in the first drive syringe while BnBr and $ZnBr_2$ in the second syringe. Data collection was done at 40 °C. Absorbance experiments were carried out to the reaction mixture. See GP1 at 40 °C

5.2.5.2.7 $FeBr(dpbz)_2$ + BnBr + $ZnBr_2$ order in $FeBr(dpbz)_2$

A standard solution of BnBr (20 mM) and ZnBr (1.25 mM) were prepared in THF. Standard solutions of $FeBr(dpbz)_2$ (0.32 mM, 0.625 mM, 1.25mM, 2.5 mM) were prepared in THF. Data collection was done at 40 °C.

5.2.5.3 Hammett Analysis $FeBr(dpbz)_2$ + RBnBr + $ZnBr_2$

Standard solutions of **6b** (1.25m) and $ZnBr_2$ (20 mM) were prepared in THF. Solution of RBnBr (R= 4-OMe, 4-tBU, 4-Me, 4-iPr, 4-Ph, H, 4-F, 4-Br, 4-Cl, 4-CF3 3-OMe, 3-F, 3-CF3) (1.25 mM, 2.5 mM, 5 mM, 10 mM, 20mM) were prepared in THF . Absorbance experiments were carried out to the reaction mixtures.

5.2.4.4 Eyring Analysis $FeBr(dpbz)_2$ + RBnBr + $ZnBr_2$

Standard solutions of **6b** (1.25m) and $ZnBr_2$ (20 mM) were prepared in THF. Solution of RBnBr (R= 3-MeO, 4-t-Bu, H, 4-Br, 4-F and 4-CF_3) (20 mM) were prepared in THF. Absorbance experiments were carried out to the reaction mixtures at temperatures 10 °C, 20 °C, 30 °C, 40 °C, and 50 °C at 40 °C

5.3 Experimental Details Chapter 3

5.3.1 Stock Solutions of reagents

The XAFS spectra of a range of pertinent species in THF stock solutions were recorded. A standard solution with a concentration of 40 mM was preparade in THF. $Zn(4\text{-tolyl})_2$, BnBr, $FeBr_2$, $FeCl_2$, $FeBr_3$, $FeBr_2(dpbz)_2$, and $FeBr(dpbz)_2$.

5.3.2 Procedure for recording XAF

5.3.2.1 Preparation of sample

Solutions of the reagents were prepared from the stock solutions and transferred inside a globe box into polyimide cylinders which were sealed from the ends. The spectra was collected

5.3.2.2 Preparation of endpoint samples

Mixtures of the reagents to study were prepared from the stock solutions and left to react until the end of the reaction. The solutions were transferred to a cylinder of polyimide and the spectra were collected.

5.4. Experimental details Chapter 4

5.4.1 General procedure for manganese-catalysed coupling

Stock solutions of the pertinent reagents were prepared in THF in the glovebox. Dilutions were done as necessary and mixed in 7mL vials. The reactions were set up according to the variation being studied and heated in a hotplate inside the glovebox. At the end of the reaction the reaction was quenched with HCl 2 M and dodecane was added to the mixture. DCM was added and the organic layer was collected and analysed in a GC apparatus.

Chapter 6. References

1 A. C. Frisch and M. Beller, *Angew. Chemie - Int. Ed.*, 2005, **44**, 674–688.

2 K. C. Nicolaou, P. G. Bulger and D. Sarlah, *Angew. Chemie Int. Ed.*, 2005, **44**, 4442–4489.

3 E. I. Negishi, *J. Organomet. Chem.*, 2002, **653**, 34–40.

4 E. I. Negishi, *Angew. Chemie - Int. Ed.*, 2011, **50**, 6738–6764.

5 M. S. Kharasch and E. K. Fields, *J. Am. Chem. Soc.*, 1941, **63**, 2316–2320.

6 M. TAMURA and J. KOCHI, *Synthesis* , 1971, **1971**, 303–305.

7 M. Kumada, *Pure Appl. Chem.*, 1980, **52**, 669–679.

8 K. Tamao, K. Sumitani and M. Kumada, *J. Am. Chem. Soc.*, 1972, **94**, 4374–4376.

9 R. J. P. Corriu and J. P. Masse, *J. Chem. Soc. Chem. Commun.*, 1972, 144a.

10 R. Jana, T. P. Pathak and M. S. Sigman, *Chem. Rev.*, 2011, **111**, 1417–1492.

11 J. Terao, H. Watanabe, A. Ikumi, H. Kuniyasu and N. Kambe, *J. Am. Chem. Soc.*, 2002, **124**, 4222–4223.

12 J. Terao, A. Ikumi, H. Kuniyasu and N. Kambe, *J. Am. Chem. Soc.*, 2003, **125**, 5646–5647.

13 M. Yamamura, I. Moritani and S.-I. Murahashi, *J. Organomet. Chem.*, 1975, **91**, C39–C42.

14 A. Sekiya and N. Ishikawa, *J. Organomet. Chem.*, 1976, **118**, 349–354.

15 N. A. Sheddan and J. Mulzer, *Org. Lett.*, 2005, **7**, 5115–5118.

16 A. Rivkin, J. T. Njardarson, K. Biswas, T.-C. Chou and S. J. Danishefsky, *J. Org. Chem.*, 2002, **67**, 7737–7740.

17 A. Suzuki, *Angew. Chemie Int. Ed.*, 2011, **50**, 6722–6737.

18 J. K. Stille, *Angew. Chemie*, 1986, **25**, 508–524.

19 Y. Nakao and T. Hiyama, *Chem. Soc. Rev.*, 2011, **40**, 4893.

20 E. Negishi and S. Baba, *J. Chem. Soc., Chem. Commun.*, 1976, 596b–597b.

21 S. Baba and E. Negishi, *J. Am. Chem. Soc.*, 1976, **98**, 6729–6731.

22 N. A. Bumagin, A. B. Ponomaryov and I. P. Beletskaya, *Tetrahedron Lett.*, 1985, **26**, 4819–4822.

23 H. J. Sipe, Jr., D. W. Clary and S. B. White, *Synthesis (Stuttg).*, 1984, **1984**, 283–284.

24 S. Ji, T. Xiao, S. Li, L. Chou, B. Zhang, C. Xu, R. Hou, A. P. E. York and M. L. H. Green, *J. Catal.*, 2003, **220**, 47–56.

25 S. Chatterjee and E. Negishi, *J. Org. Chem.*, 1985, **50**, 3406–3408.

26 H. Gao and P. Knochel, *Synlett*, 2009, **2009**, 1321–1325.

27 E. E. Negishi, *Acc. Chem. Res.*, 1982, **15**, 340–348.

28 S. Bernhardt, G. Manolikakes, T. Kunz and P. Knochel, *Angew. Chemie Int. Ed.*, 2011, **50**, 9205–9209.

29 C. I. Stathakis, S. Bernhardt, V. Quint and P. Knochel, *Angew. Chemie Int. Ed.*, 2012, **51**, 9428–9432.

30 C. E. Tucker and J. G. de Vries, *Top. Catal.*, 2002, **19**, 111–118.

31 R. Giovannini and P. Knochel, *J. Am. Chem. Soc.*, 1998, **120**, 11186–11187.

32 R. Giovannini, T. Stüdemann, G. Dussin and P. Knochel, *Angew. Chemie Int. Ed.*, 1998, **37**, 2387–2390.

33 J. (Steve) Zhou and G. C. Fu, *J. Am. Chem. Soc.*, 2003, **125**, 14726–14727.

34 J. T. Binder, C. J. Cordier and G. C. Fu, *J. Am. Chem. Soc.*, 2012, **134**, 17003–17006.

35 F. Zeng and E. Negishi, *Org. Lett.*, 2001, **3**, 719–722.

36 D. Milstein and J. K. Stiile, *J. Am. Chem. Soc.*, 1978, **100**, 3636–3638.

37 N. Miyaura, K. Yamada and A. Suzuki, *Tetrahedron Lett.*, 1979, **20**, 3437–3440.

38 N. Miyaura, T. Yanagi and A. Suzuki, *Synth. Commun.*, 1981, **11**, 513–519.

39 A. F. Littke and G. C. Fu, *Angew. Chemie - Int. Ed.*, 2002, **41**, 4176–4211.

40 S. Gronowitz, P. Björk, J. Malm and A. B. Hörnfeldt, *J. Organomet. Chem.*, 1993, **460**, 127–129.

41 W. A. Herrmann, C. Brossmer, K. Öfele, C.-P. Reisinger, T. Priermeier, M. Beller and H. Fischer, *Angew. Chemie Int. Ed. English*, 1995, **34**, 1844–1848.

42 D. W. Old, J. P. Wolfe and S. L. Buchwald, *J. Am. Chem. Soc.*, 1998, **120**, 9722–9723.

43 R. B. Bedford and C. S. J. Cazin, *Chem. Commun.*, 2001, 1540–1541.

44 R. B. Bedford, C. S. J. Cazin and S. L. Hazelwood, *Angew. Chemie - Int. Ed.*, 2002, **41**, 4120–4122.

45 M. R. Netherton, C. Dai, K. Neuschütz and G. C. Fu, *J. Am. Chem. Soc.*, 2001, **123**, 10099–10100.

46 B. Saito and G. C. Fu, *J. Am. Chem. Soc.*, 2007, **129**, 9602–9603.

47 J. H. Kirchhoff, M. R. Netherton, I. D. Hills and G. C. Fu, *J. Am. Chem. Soc.*, 2002, **124**, 13662–13663.

48 U. Schmidt, V. Leitenberger, R. Meyer and H. Griesser, *J. Chem. Soc. Chem. Commun.*, 1992, 951.

49 M. Rehahn, A.-D. Schlüter, G. Wegner and W. J. Feast, *Polymer (Guildf).*, 1989, **30**, 1054–1059.

50 EMEA European Medicines Agency, *Guideline on the Specification Limits for Residues of Metal Catalysts or Metal Reagents*, 2008.

51 http://www.infomine.com/investment/metal-prices/palladium/, http://www.infomine.com/investment/metal-prices/palladium/.

52 http://markets.businessinsider.com/commodities/iron-ore-price, http://markets.businessinsider.com/commodities/iron-ore-price.

53 N. G. and A. Earnshaw, *Chemistry of the Elements*, Butterworth-Heinemann, 2nd ed., 1997.

54 J. Emsley, *Nature's Building Blocks: An A-Z Guide to the Elements*, Oxford University Press: Oxford, 2001.

55 E. B. Plietker, *Iron Catalysis in Organic Chemistry*, Wiley VCH: Weinheim., 2008.

56 F. Haber and G. van Oordt, *Zeitschrift für Anorg. Chemie*, 1905, **44**, 341–378.

57 M. Tamura and J. Kochi, *J. Am. Chem. Soc.*, 1971, 93, 1487–1489.

58 G. a. Molander, B. J. Rahn, D. C. Shubert and S. E. Bonde, *Tetrahedron Lett.*, 1983, **24**, 5449–5452.

59 V. Fiandanese, G. Marchese, V. Martina and L. Ronzini, *Tetrahedron Lett.*, 1984, **25**, 4805–4808.

60 V. Fiandanese, G. Miccoli, F. Naso and L. Ronzini, *J. Organomet. Chem.*, 1986, **312**, 343–348.

61 G. Cahiez and S. Marquais, *Tetrahedron Lett.*, 1996, **37**, 1773–1776.

62 G. Cahiez and H. Avedissian, *Synthesis (Stuttg).*, 1998, **1998**, 1199–1205.

63 W. Dohle, F. Kopp, G. Cahiez and P. Knochel, *Synlett*, 2001, **2001**, 1901–1904.

64 M. Sova, R. Frlan, S. Gobec, G. Stavber and Z. Časar, *Appl. Organomet. Chem.*, 2015, **29**, 528–535.

65 B. Hölzer and R. W. Hoffmann, *Chem. Commun.* , 2003, **2**, 732–733.

66 A. Fürstner, D. De Souza, L. Turet, M. D. B. Fenster, L. Parra-Rapado, C. Wirtz, R. Mynott and C. W. Lehmann, *Chem. - A Eur. J.*, 2007, **13**, 115–134.

67 G. Berthon-Gelloz and T. Hayashi, *J. Org. Chem.*, 2006, **71**, 8957–8960.

68 A. Fürstner, A. Leitner, M. Méndez and H. Krause, *J. Am. Chem. Soc.*, 2002, **124**, 13856–13863.

69 A. Fürstner and A. Leitner, *Angew. Chemie - Int. Ed.*, 2002, **41**, 609–612.

70 A. Fürstner and A. Leitner, *Angew. Chemie*, 2002, **114**, 632–635.

71 T. Hatakeyama and M. Nakamura, *J. Am. Chem. Soc.*, 2007, **129**, 9844–9845.

72 Y.-Y. Chua and H. a Duong, *Chem. Commun.* , 2014, **50**, 8424–7.

73 Y.-Y. Chua and H. A. Duong, *Chem. Commun.*, 2016, **52**, 1466–1469.

74 M. H. Chisholm, *J. Organomet. Chem.*, 2014, **751**, 55–59.

75 W. Wu, Q. Teng, Y. Y. Chua, H. V. Huynh and H. A. Duong, *Organometallics*, 2017, **36**, 2293–2297.

76 O. M. Kuzmina, A. K. Steib, J. T. Markiewicz, D. Flubacher and P. Knochel, *Angew. Chemie - Int. Ed.*, 2013, **52**, 4945–4949.

77 A. K. Steib, O. M. Kuzmina, S. Fernandez, S. Malhotra and P. Knochel, *Chem. - A Eur. J.*, 2015, **21**, 1961–1965.

78 D. J. Càrdenas, *Angew. Chemie - Int. Ed.*, 2003, **42**, 384–387.

79 U. H. Brinker and L. König, *Chem. Ber.*, 1983, **116**, 882–893.

80 A. Guérinot, S. Reymond and J. Cossy, *Angew. Chemie - Int. Ed.*, 2007, **46**, 6521–6524.

81 M. Nakamura, K. Matsuo, S. Ito and E. Nakamura, *Communication*, 2004, 0–2.

82 R. B. Bedford, P. B. Brenner, E. Carter, P. M. Cogswell, M. F. Haddow, J. N. Harvey, D. M. Murphy, J. Nunn and C. H. Woodall, *Angew. Chemie - Int. Ed.*, 2014, **53**, 1804–8.

83 T. Nagano and T. Hayashi, *Org. Lett.*, 2004, **6**, 1297–1299.

84 B. D. Sherry and A. Fürstner, *Acc. Chem. Res.*, 2008, **41**, 1500–1511.

85 R. B. Bedford, D. W. Bruce, R. M. Frost, J. W. Goodby and M. Hird, *Chem.Commun.*, 2004, 2822–3.

86 R. B. Bedford, D. W. Bruce, R. M. Frost and M. Hird, *Chem. Commun.* , 2005, 4161–4163.

87 R. B. Bedford, M. Betham, D. W. Bruce, A. a Danopoulos, R. M. Frost and M. Hird, *J. Org. Chem.*, 2006, **71**, 1104–10.

88 R. B. Bedford, M. Betham, D. W. Bruce, S. a Davis, R. M. Frost and M. Hird, *Chem. Commun.* , 2006, **219**, 1398–400.

89 T. Hatakeyama, Y. Fujiwara, Y. Okada, T. Itoh, T. Hashimoto, S. Kawamura, K. Ogata, H. Takaya and M. Nakamura, *Chem. Lett.*, 2011, **40**, 1030–1032.

90 C. L. Sun, H. Krause and A. Fürstner, *Adv. Synth. Catal.*, 2014, **356**, 1281–1291.

91 S. L. Daifuku, M. H. Al-afyouni, B. E. R. Snyder, J. L. Kneebone and M. L. Neidig, *J. Am. Chem. Soc.*, 2014, **136**, 9132–9143.

92 A. Fürstner, R. Martin, H. Krause, G. Seidel, R. Goddard and C. W. Lehmann, *J. Am. Chem. Soc.*, 2008, **130**, 8773–8787.

93 M. Guisán-Ceinos, F. Tato, E. Buñuel, P. Calle and D. J. Cárdenas, *Chem. Sci.*, 2013, **4**, 1098.

94 C. W. Cheung, P. Ren and X. Hu, *Org. Lett.*, 2014, **16**, 2566–2569.

95 M. Nakamura, S. Ito, K. Matsuo and E. Nakamura, *Synlett*, 2005, 1794–1798.

96 S. Ito, Y. I. Fujiwara, E. Nakamura and M. Nakamura, *Org. Lett.*, 2009, **11**, 4306–4309.

97 R. B. Bedford, M. Huwe and M. C. Wilkinson, *Chem. Commun.* , 2009, **12**, 600–2.

98 R. B. Bedford, M. a Hall, G. R. Hodges, M. Huwe and M. C. Wilkinson, *Chem. Commun.* , 2009, **2**, 6430–2.

99 C. J. Adams, R. B. Bedford, E. Carter, N. J. Gower, M. F. Haddow, J. N. Harvey, M. Huwe, M. Á. Cartes, S. M. Mansell, C. Mendoza, D. M. Murphy, E. C. Neeve and J. Nunn, *J. Am. Chem. Soc.*, 2012, **134**, 10333–10336.

100 R. B. Bedford, E. Carter, P. M. Cogswell, N. J. Gower, M. F. Haddow, J. N. Harvey, D. M. Murphy, E. C. Neeve and J. Nunn, *Angew. Chemie*, 2013, **125**, 1323–1326.

101 T. Hatakeyama, Y. Kondo, Y.-I. Fujiwara, H. Takaya, S. Ito, E. Nakamura and M. Nakamura, *Chem. Commun.* , 2009, 1216–1218.

102 X. Lin, F. Zheng and F. L. Qing, *Organometallics*, 2012, **31**, 1578–1582.

103 T. Hatakeyama, T. Hashimoto, Y. Kondo, Y. Fujiwara, H. Seike, H. Takaya, Y. Tamada, T. Ono and M. Nakamura, *J. Am. Chem. Soc.*, 2010, **132**, 10674–6.

104 T. Hashimoto, T. Hatakeyama and M. Nakamura, *J. Org. Chem.*, 2012, **77**, 1168–1173.

105 T. Hatakeyama, T. Hashimoto, K. K. a D. S. Kathriarachchi, T. Zenmyo, H. Seike and M. Nakamura, *Angew. Chemie Int. Ed.*, 2012, **51**, 8834–8837.

106 R. B. Bedford, P. B. Brenner, E. Carter, T. W. Carvell, P. M. Cogswell, T. Gallagher, J. N. Harvey, D. M. Murphy, E. C. Neeve, J. Nunn and D. R. Pye, *Chemistry*, 2014, **20**, 7935–8.

107 E. B. Bauer, *Iron Catalysis II*, Springer International Publishing, Cham, 2015, vol. 50.

108 S. M. Neumann and J. K. Kochi, *J. Org. Chem.*, 1975, **40**, 599.

109 B. Bogdanovi and M. Schwickardi, *Angew. Chemie - Int. Ed.*, 2000, **39**, 4610–4612.

110 J. Kleimark, A. Hedström, P. F. Larsson, C. Johansson and P. O. Norrby, *ChemCatChem*, 2009, **1**, 152–161.

111 A. Hedström, E. Lindstedt and P. O. Norrby, *J. Organomet. Chem.*, 2013, **748**, 51–55.

112 A. Hedström, U. Bollmann, J. Bravidor and P. O. Norrby, *Chem. - A Eur. J.*, 2011, **17**, 11991–11993.

113 A. Bekhradnia and P.-O. Norrby, *Dalt. Trans.*, 2015, **44**, 3959–3962.

114 R. Schoch, W. Desens, T. Werner and M. Bauer, *Chem. - A Eur. J.*, 2013, **19**, 15816–15821.

115 G. Lefèvre and A. Jutand, *Chemistry*, 2014, **20**, 4796–805.

116 M. Nakamura, K. Matsuo, S. Ito and E. Nakamura, *J. Am. Chem. Soc.*, 2004, **126**, 3686–3687.

117 R. Martin and A. Fürstner, *Angew. Chemie - Int. Ed.*, 2004, **43**, 3955–3957.

118 A. Hedström, Z. Izakian, I. Vreto, C.-J. Wallentin and P.-O. Norrby, *Chem. - A Eur. J.*, 2015, n/a-n/a.

119 D. Noda, Y. Sunada, T. Hatakeyama, M. Nakamura and H. Nagashima, *J. Am. Chem. Soc.*, 2009, **131**, 6078–6079.

120 T. J. Colacot and J. Matthey, *Platin. Met. Rev.*, 2011, **55**, 84–90.

121 S. L. Daifuku, J. L. Kneebone, B. E. R. R. Snyder and M. L. Neidig, *J. Am. Chem. Soc.*, 2015, **137**, 11432–11444.

122 Y. Liu, J. Xiao, L. Wang, Y. Song and L. Deng, *Organometallics*, 2015, **34**, 599–605.

123 J. A. Przyojski, K. P. Veggeberg, H. D. Arman and Z. J. Tonzetich, *ACS Catal.*, 2015, **5**, 5938–5946.

124 E. Neeve, University of Bristol, 2013.

125 N. J. Gower, University of Bristol.

126 J. Nunn, 2014.

127 J. L. Kneebone, V. E. Fleischauer, S. L. Daifuku, A. A. Shaps, J. M. Bailey, T. E. Iannuzzi and M. L. Neidig, *Inorg. Chem.*, 2016, **55**, 272–282.

128 V. N. Kondrat'Ev, in *Chemical Kinetics of Gas Reactions*, Elsevier, 1964, p. ii.

129 L. P. Hammett, *J. Am. Chem. Soc.*, 1937, **59**, 96–103.

130 X. Creary, M. E. Mehrsheikh-mohammadi and S. Mcdonald, *J. Org. Chem.*, 1987, **52**, 3254–3263.

131 J. M. Dust and D. R. Arnold, *J. Am. Chem. Soc.*, 1983, **105**, 1221–1227.

132 S. Velmathi, R. Vijayaraghavan, R. P. Pal and A. Vinu, *Catal. Letters*, 2010, **135**, 148–151.

133 J. Streuff, M. Feurer, G. Frey, A. Steffani, S. Kacprzak, J. Weweler, L. H. Leijendekker, D. Kratzert and D. A. Plattner, *J. Am. Chem. Soc.*, 2015, **137**, 14396–14405.

134 R. B. Bedford, *Acc. Chem. Res.*, 2015, **48**, 1485–1493.

135 R. a. Scott, *Compr. Coord. Chem. II*, 2011, 159–186.

136 G. Cahiez, A. Moyeux and J. Cossy, *Adv. Synth. Catal.*, 2015, **357**, 1983–1989.

137 M. B. F. A. Cotton, G. Wilikinson, C. A.Murillo, .

138 G. G. Cahiez, C. Duplais and J. Buendia, *Chem. Rev.*, 2009, **109**, 1434–1476.

139 W. E. Fristad, S. R. Thompson, T. A. Brandvold and J. R. Peterson, *J. Org. Chem.*, 1985, **50**, 3647–3649.

140 X. Sun, X. Li, S. Song, Y. Zhu, Y. F. Liang and N. Jiao, *J. Am. Chem. Soc.*, 2015, **137**, 6059–6066.

141 R. Ren, H. Zhao, L. Huan and C. Zhu, *Angew. Chemie - Int. Ed.*, 2015, **54**, 12692–12696.

142 P. Magnus, A. H. Payne, M. J. Waring, D. A. Scott and V. Lynch, *Tetrahedron Lett.*, 2000, **41**, 9725–9730.

143 K. Iwasaki, K. K. Wan, A. Oppedisano, S. W. M. Crossley and R. A. Shenvi, *J. Am. Chem. Soc.*, 2014, **136**, 1300–1303.

144 J. T. Groves, W. J. Kruper and R. C. Haushalter, *J. Am. Chem. Soc.*, 1980, **102**, 6375–6377.

145 R. V. Ottenbacher, D. G. Samsonenko, E. P. Talsi and K. P. Bryliakov, *Org. Lett.*, 2012, **14**, 4310–4313.

146 L. Ma, Y. Pan, W.-L. Man, H.-K. Kwong, W. W. Y. Lam, G. Chen, K.-C. Lau and T.-C. Lau, *J. Am. Chem. Soc.*, 2014, **136**, 7680–7687.

147 W. Tang, J. Li, X. Jin, J. Sun, J. Huang and R. Li, *Catal. Commun.*, 2014, **43**, 75–78.

148 W. Liu and J. T. Groves, *J. Am. Chem. Soc.*, 2010, **132**, 12847–12849.

149 H. Li, C. L. Sun, M. Yu, D. G. Yu, B. J. Li and Z. J. Shi, *Chem. - A Eur. J.*, 2011, **17**, 3593–3597.

150 B. T. Gregg, P. K. Hanna, E. J. Crawford and A. R. Cutler, *J. Am. Chem. Soc.*, 1991, **113**, 384–385.

151 Z. Mao, B. T. Gregg and A. R. Cutler, *J. Am. Chem. Soc.*, 1995, **117**, 10139–10140.

152 J. Zheng, S. Chevance, C. Darcel and J.-B. Sortais, *Chem. Commun.*, 2013, **49**, 10010.

153 V. K. Chidara and G. Du, *Organometallics*, 2013, **32**, 5034–5037.

154 K. Okada, K. Oshima and K. Utimoto, *J. Am. Chem. Soc.*, 1996, **118**, 6076–6077.

155 Y. Kuninobu, Y. Nishina, T. Takeuchi and K. Takai, *Angew. Chemie - Int. Ed.*, 2007, **46**, 6518–6520.

156 B. Zhou, Y. Hu and C. Wang, *Angew. Chemie - Int. Ed.*, 2015, **54**, 13659–13663.

157 B. Zhou, P. Ma, H. Chen and C. Wang, *Chem. Commun.*, 2014, **50**, 14558–14561.

158 T. Uchida and T. Katsuki, *J. Synth. Org. Chem. Japan*, 2013, **71**, 1126–1135.

159 W. N. Lanzilotta, K. Fisher and L. C. Seefeldt, *J. Biol. Chem.*, 1997, **272**, 4157–4165.

160 S.-K. Kang, J.-S. Kim and S.-C. Choi, *J. Org. Chem.*, 1997, **62**, 4208–4209.

161 G. Cahiez, D. Luart and F. Lecomte, *Org. Lett.*, 2004, **6**, 4395–4398.

162 M. Rueping and W. Ieawsuwan, *Synlett*, 2007, 247–250.

163 G. Cahiez, O. Gager and F. Lecomte, *Org. Lett.*, 2008, **10**, 5255–5256.

164 S. K. Kang, W. Y. Kim, Y. T. Lee, S. K. Ahn and J. C. Kim, *Tetrahedron Lett.*, 1998, **39**, 2131–2132.

165 G. Cahiez, A. Moyeux, J. Buendia and C. Duplais, *J. Am. Chem. Soc.*, 2007, **129**, 13788–13789.

166 Z. Zhou and W. Xue, *J. Organomet. Chem.*, 2009, **694**, 599–603.

167 F. F. Yong and Y. C. Teo, *Tetrahedron Lett.*, 2010, **51**, 3910–3912.

168 T.-J. Liu, C.-L. Yi, C.-C. Chan and C.-F. Lee, *ChemInform*, 2013, **44**, no-no.

169 G. Antonacci, A. Ahlburg, P. Fristrup, P.-O. Norrby and R. Madsen, *European J. Org. Chem.*, 2017, **2017**, 4758–4764.

170 G. Cahiez, F. Lepifre and P. Ramiandrasoa, *Synthesis (Stuttg).*, 1999, **1999**, 2138–2144.

171 G. Cahiez, V. Habiak and O. Gager, *Org. Lett.*, 2008, **10**, 2389–2392.

172 J. Wu, W. Dai, J. H. Farnaby, N. Hazari, J. J. Le Roy, V. Mereacre, M. Murugesu, A. K. Powell and M. K. Takase, *Dalton Trans.*, 2013, **42**, 7404–13.

173 J. Liu and B. Li, *Synth. Commun.*, 2007, **37**, 3273–3278.

174 C. E. I. Knappke, S. Grupe, D. Gärtner, M. Corpet, C. Gosmini and A. Jacobi Von Wangelin, *Chem. - A Eur. J.*, 2014, **20**, 6828–6842.

175 W. D. Miller, A. H. Fray, J. T. Quatroche and C. D. Sturgill, *Org. Process Res. Dev.*, 2007, **11**, 359–364.

176 T. Hatakeyama, S. Hashimoto and K. Ishizuka, 2009, 11949–11963.

177 W. M. Czaplik, M. Mayer, S. Grupe and A. J. von Wangelin, *Pure Appl. Chem.*, 2010, **82**, 1545–1553.

178 A. Joshi-Pangu, M. Ganesh and M. R. Biscoe, *Org. Lett.*, 2011, **13**, 1218–1221.